Cytochrome *c* Oxidase Deficiency:

Study of Aberrant Phenotypes and their Connection to Secondary Functions of Assembly Factors

by

Raffaele Camasta

A thesis

presented to the University of Waterloo

in fulfilment of the

thesis requirement for the degree of

Doctor of Philosophy

in

Biology

Waterloo, Ontario, Canada, 2017

Examining Committee Membership

The following served on the Examining Committee for this thesis. The decision of the Examining Committee is by majority vote.

External Examiner	Robert Cumming PhD
Supervisor(s)	D. Moira Glerum PhD
Internal Member	Mungo Marsden PhD
Other Member(s)	Allison McDonald PhD
Internal-external Member	Guy Guillemette PhD

Author’s Declaration

I hereby declare that I am the sole author of this thesis. This is a true copy of the thesis, including any required final revisions, as accepted by my examiners.

I understand that my thesis may be made electronically available to the public.

Abstract

Mitochondria are double membrane-bound organelles present in all eukaryotic organisms and are involved in myriad cellular pathways. Cytochrome *c* oxidase (COX) is a mitochondrial inner membrane protein complex that is an essential component of the electron transport chain. The assembly of this multi-subunit protein complex is aided by the activities of proteins referred to as COX assembly factors. Mutations in COX assembly factors result in assembly failure and therefore cause COX deficiencies, which are associated with human diseases, such as Leigh syndrome.

In this study, we used the model organism *Saccharomyces cerevisiae* to characterize phenotypes resulting from the loss of any one of a subset of COX assembly factors in cells grown to stationary phase. The vast majority of studies that involve yeast mitochondria have been performed in cells at late exponential phase/early diauxic shift, while the behaviours of mitochondrial mutants at stationary phase are still largely unexplored.

Analyses of cellular functions such as growth, viability and budding index led us to uncover phenotypic differences among the COX assembly mutant strains that were further investigated as a first step towards identifying potential secondary functions of these proteins. Analysis of the cell cycle in a wild-type, respiratory competent strain and in COX assembly mutants led to the novel finding that strains unable to synthesize proteins involved in COX copper metalation, namely Cox17, Sco1 and Cox11, are characterized by a cell cycle progression defect. The same strains also displayed higher sensitivity to hydroxyurea, which is known to increase oxidative stress levels in yeast, leading us to propose that yeast strains defective for these proteins are subject to higher oxidative stress levels than mutants defective for COX assembly factors involved in other assembly pathways. The results of this study represent a major step forward in the phenotypic differentiation of COX deficiencies that arise from the loss of different assembly factors and may be relevant for future studies of human neurodegenerative disorders resulting from faulty COX assembly.

Acknowledgements

First, I would like to thank my supervisor, Dr. D. Moira Glerum, for giving me the opportunity to join her lab and for the incredible support she provided me with throughout the last four years. My skills as a scientist have improved enormously by working under your supervision.

I am also greatly appreciative of my committee members, Dr. Allison McDonald, for her guidance and feedback, and Dr. Bernie Duncker for his willingness to collaborate on my project and share resources across labs. I would also like to thank Dr. Mungo Marsden for volunteering to serve as an impromptu committee member for my defense, for letting me use equipment from his lab as our lab was being set up, and for fixing the X-Ray developer many, many times. Thank you also to Dr. Robert Cumming for agreeing to serve as an external examiner on my committee.

Thank you to the faculty and staff in the Department of Biology at the University of Waterloo for helping me throughout these years, and in particular at the beginning of the program to help me navigate the challenges of being an international student.

Thank you to all my past and present lab mates, in particular Alicia, Seville, Jonathan, Maddie, Amila and Chanele for being a pleasure to work with in the lab, and my fellow QNC inhabitants from the Backhouse lab for making the time in between experiments more enjoyable.

A special thanks to my parents, Lisa and JB for their love and support throughout this period and always.

Table of Contents

List of Abbreviations

DTT	Dithiothreitol
G1	Gap 1
G2	Gap 2
h	Hours
HU	Hydroxyurea
KD	Knockdown
M	Mitosis
mRNA	Messenger RNA
mtDNA	Mitochondrial DNA
PS	Phosphatidylserine
S	Synthesis

List of Acronyms

AMP	Adenosine monophosphate
ATP	Adenosine triphosphate
CFU	Colony forming units
COX	Cytochrome *c* Oxidase
CuL	Copper Ligand
CLS	Chronological lifespan
DNA	Deoxyribonucleic acid
dNTPs	Nucleoside triphosphate
dUTP	Deoxyuridine triphosphate
EDTA	Ethylenediaminetetraacetic acid
EP	Exponential phase
ETC	Electron transport Chain
FACS	Fluorescence activated cell sorting
IMM	Inner mitochondrial membrane
IMS	Intermembrane space
MCF	Mitochondrial carrier family
MELAS	Mitochondrial encephalomyopathy, lactic acidosis, stroke-like episodes
MICOS	Mitochondrial contact site complex
NADH	Nicotinamide adenine dinucleotide
NADPH	Nicotinamide adenine dinucleotide phosphate
NAC	N-Acetyl cysteine
OD_{600}	Optical density measured at 600 nanometers
OMM	Outer mitochondrial membrane
ONPG	ortho-Nitrophenyl-β-galactoside
OXPHOS	Oxidative phosphorylation
PCD	Programmed cell death
PVDF	Polyvinylidene fluoride
PI	Propidium Iodide
PMS	Post-mitochondrial supernatant

PMSF	Phenylmethane sulfonyl fluoride
RLS	Replicative lifespan
RNA	Ribonucleic acid
ROS	Reactive oxygen species
RT	Room temperature
SDS	Sodium dodecyl sulfate
SP	Stationary phase
STE	Sorbitol Tris EDTA buffer
TUNEL	Deoxynucleotidyl transferase dUTP nick end labeling
YPD	Yeast peptone dextrose media

List of Figures

List of Tables

Chapter 1
Introduction and Goals of the Study

1.1 Mitochondria

Mitochondria are subcellular organelles that are present in all eukaryotic cells and are known as “the powerhouse of the cell” due to their roles in energy producing processes such as oxidative phosphorylation (OXPHOS) and Krebs cycle. However, mitochondrial function relates to a variety of other pathways, including fatty acid oxidation, urea cycle and multiple biosynthetic reactions (Scheffler, 2007).

Investigation of mitochondria for over a century has made these organelles well characterized. Structurally, mitochondria contain an outer membrane (OMM) and an inner membrane (IMM); the outer membrane is structured in a way that makes it permeable to molecules of the size of small proteins (Vander Heiden et al., 2000). On the other hand, the inner membrane constitutes an impermeable barrier where the electron transport chain components (ETC) are assembled (Mannella, 2006). Typical of the IMM are its folds, also known as *cristae*, which originate from invaginations of the membrane itself and provide an extended surface area (Mannella, 2006). The portion between the two membranes is called the intermembrane space (IMS), where protons originating from the electron transport pathway accumulate to form a gradient. Another mitochondrial compartment is the protein-rich matrix that is confined by the IMM and that contains the mitochondrial DNA (mtDNA).

1.2 Yeast Mitochondria

Mitochondrial biogenesis and function have been studied using a variety of experimental systems, with the yeast, *Saccharomyces cerevisiae*, being one of the most commonly used model organisms. Pioneering studies were performed by taking advantage of the high degree of conservation between human and yeast mitochondria at both structural and functional levels (Scheffler, 1999). One of the advantages of using yeast to study mitochondrial defects lies in the metabolism of this unicellular eukaryotic organism, as it can rely entirely on fermentation as a source of energy, allowing yeast to survive both mutations

that disrupt oxidative phosphorylation and even those resulting from the complete loss of mtDNA (Lasserre et al., 2015).

Under appropriate environmental conditions, yeast can adopt respiratory metabolism to utilize non-fermentable carbon sources and generate ATP. The electron transport chain is the final step of the respiratory pathway and is composed of multi-subunit complexes embedded in the IMM (Figure 1.1). In most fungi and other eukaryotic organisms, electrons generated from NADH and $FADH_2$ are sequentially transferred between four complexes (I-IV); Complex IV catalyzes the last step of this process, which is the transfer of electrons to molecular oxygen (Joseph-Horne et al., 2001; Stuart, 2008). Among the multi-subunit complexes of the ETC, NADH:ubiquinone oxidoreductase (Complex I), ubiquinol:cytochrome *c* oxidoreductase, also known as cytochrome bc_1 (Complex III) and cytochrome *c* oxidase (Complex IV) couple the transfer of electrons to proton pumping from the mitochondrial matrix into the IMS (Saraste, 1999); the succinate dehydrogenase complex (Complex II) mediates electron transfer from succinate to ubiquinone without the associated movement of protons (Joseph-Horne et al., 2001). The mobile electron carriers that play a role in the ETC are ubiquinone, localized within the IMM, and cytochrome *c*, localized in the IMS (Stuart, 2008). The electrochemical gradient established by the ETC is essential for the production of ATP through the F_1F_0 ATP synthase, also known as Complex V (Joseph-Horne et al., 2001). One distinctive feature of the *S. cerevisiae* ETC is the absence of the traditional Complex I, found in all higher eukaryotes, replaced in its function by three NADH dehydrogenases, namely Nde1, Nde2 and Ndi1 (Joseph-Horne et al., 2001).

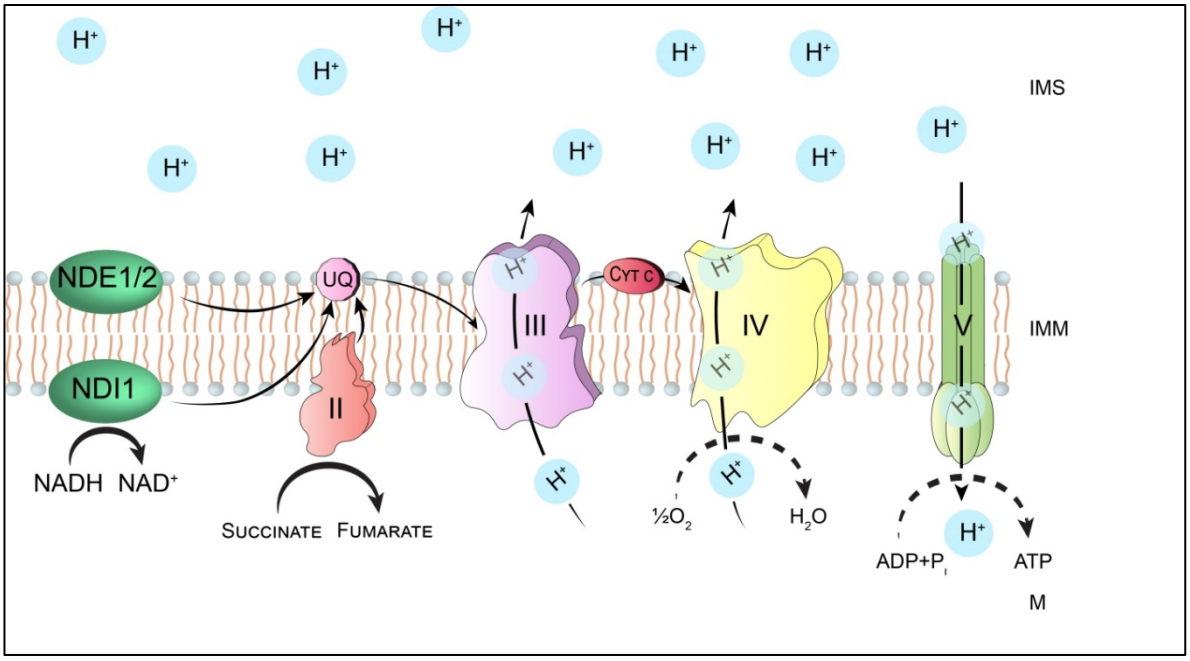

Figure 1.1 Schematic of *Saccharomyces cerevisiae* electron transport chain showing the different molecules and protein complexes involved. IMM, inner mitochondrial membrane; OMM, outer mitochondrial membrane; IMS, mitochondrial intermembrane space; M, Matrix; Nde1/2, external NADH dehydrogenases; NDI1, external NADH dehydrogenases; II, succinate dehydrogenase complex; III, ubiquinol:cytochrome *c* oxidoreductase; IV, cytochrome *c* oxidase; V, F_1F_0 ATP synthase; UQ, ubiquinone; cyt c, cytochrome *c*; H^+, proton gradient generated by the activity of some complexes of the electron transport chain.

1.3 Cytochrome *c* Oxidase

Cytochrome *c* oxidase (COX) is a multi-subunit protein complex of the IMM that plays a fundamental role during aerobic respiration by transferring electrons to molecular oxygen, which is the final electron acceptor of the ETC (Rich & Marechal, 2010). Investigation of COX started early in the 20th century and remains the subject of great interest for researchers worldwide today (Soto et al., 2012). Isolation of intact and functional COX by Fowler et al., (1962) was a breakthrough in the study of this enzyme, allowing subsequent characterization of its subunits (Rubin & Tzagoloff, 1973a). Another pioneering study, performed by Clark-Walker & Linnane, (1966), led to the conclusion that synthesis of yeast respiratory complexes is carried out by two distinct protein synthesis machineries. Later, it was found that the core subunits (subunits 1, 2 and 3) of Complex IV are synthesized by mitochondrial ribosomes and have different chemical and structural properties when compared to the subunits synthesized by cytosolic ribosomes (Poyton & Schatz, 1975; Rubin & Tzagoloff, 1973b).

Another crucial achievement in COX research was the determination of the bovine COX crystal structure in the 1990s (Tsukihara et al., 1995, 1996; Yoshikawa et al., 1998), allowing the study of interface contacts between the various subunits. The knowledge obtained from the crystal structure was instrumental in discovering the presence of zinc, magnesium and sodium atoms within the protein complex; however, the roles played by these metals in COX are still unclear (Fontanesi et al., 2008).

1.4 Assembly of Yeast Cytochrome *c* Oxidase

Thirteen COX subunits have been characterized in humans while eleven are known in yeast. Among the structural subunits, COX1, COX2 and COX3 are large, hydrophobic trans-membrane proteins that form the catalytic core of the complex and are encoded by mitochondrial DNA. The enzyme core is also known to contain two copper centers, namely Cu_A and Cu_B, and two heme groups, namely heme A and heme a_3. The Cu_A copper center is located in subunit 2, while Cu_B and the two heme groups are found in subunit 1. All other subunits are encoded by nuclear DNA. Their roles vary from assembly and stabilization of the complex to determination of the dimeric active form of the enzyme and to formation of a protective shield around the core (Fontanesi et al., 2008).

The assembly of this essential enzyme has been investigated extensively and most of what is known is due to work performed in mammalian systems and, to a lesser extent, in yeast (McStay et al., 2013). A first model was proposed in the 1980s following an experimental approach that included insertion of radiolabeled subunits into the nascent complex in rat liver mitochondria. It was also hypothesized that the insertion of the various subunits into the assembling complex would happen in a sequential, ordered manner (Wielburski & Nelson, 1983). This model was confirmed by a study of human COX assembly intermediates by Blue-Native gel electrophoresis. From this study it was concluded that COX assembly likely initiates around a seed formed by one of the three core subunits, COX1, and then proceeds with the insertion of the other subunits through formation of intermediates (Nijtmans et al., 1998). Subassemblies similar to those found in human cells were identified in yeast mutants for the core subunit *cox2* and for the assembly chaperone *pet100* (Church et al., 2005; Horan et al., 2005), indicating that this pathway is conserved among eukaryotes. After formation of the first assembly intermediate, S1, composed of COX1 alone, COX4-I and COX5a subunits (Cox5a

and Cox6 in yeast) are inserted, marking the progression towards assembly of the second intermediate, S2 (Fontanesi et al., 2008). However, a necessary step between the first two assembly intermediates is the insertion of heme into COX1. It has been hypothesized that introduction of heme A into subunit 1 might have a role in stabilizing the COX1-COX4-COX5a intermediate (Fontanesi et al., 2008).

After formation of S2, all other subunits are inserted into the forming complex with the exceptions of COX6a and COX7a/b (yeast subunits 13 and 7, respectively), which are added to the holoenzyme at the end (Nijtmans et al., 1998; Williams et al., 2003) (Figure 1.2).

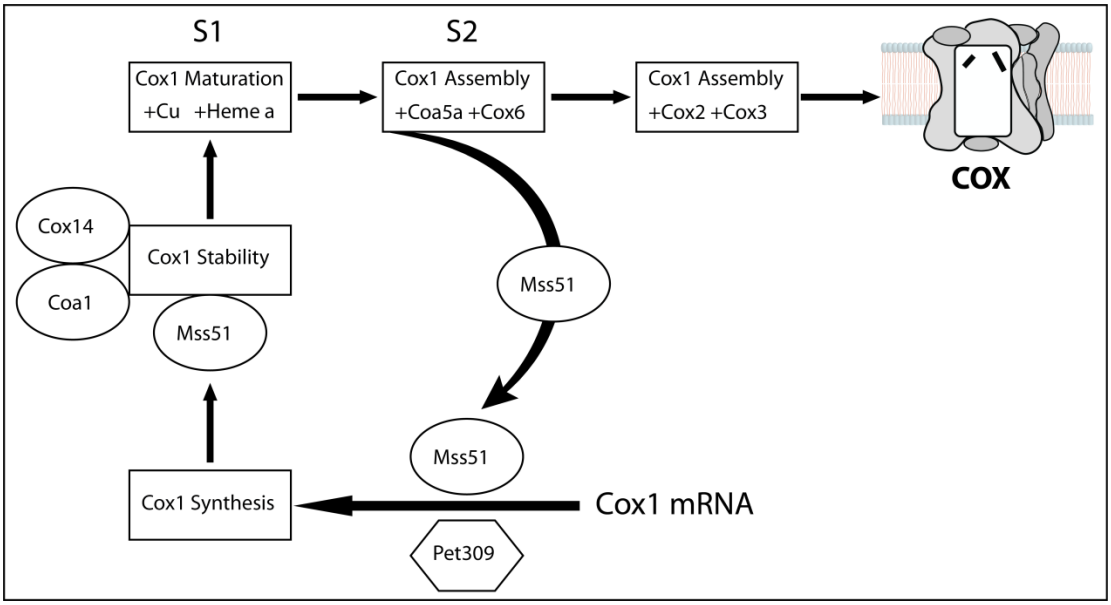

Figure 1.2 Schematic of the initial phases of COX biogenesis. Cox1 is synthesized from mRNA through the functions of translational regulators such as Mss51 and Pet309. The first COX assembly intermediate, S1, is composed by Cox1 alone. The insertion of copper and iron redox centers marks progression to the second assembly intermediate, S2, which consists of the Cox1-Coa5a-Cox6 complex. COX assembly is then completed by the addition of all of the other subunits. COX, cytochrome *c* oxidase. Modified after Fontanesi et al., (2008).

1.4.1 Cytochrome *c* Oxidase Assembly Factors

Besides the structural subunits, a large number of COX assembly factors have been discovered and characterized. Yeast strains carrying mutations affecting COX assembly have provided a powerful tool for identifying genes encoding proteins that play a role in this process (Soto et al., 2012). The functions of assembly factors are multiple and include

activation/regulation of translation, membrane insertion, copper transport and heme biosynthesis (Zee & Glerum, 2006). However, none of the COX assembly factors characterized so far is known to associate with the assembled, functional enzyme. Although thorough research to identify and characterize factors involved in COX assembly has been conducted, functions of some of these proteins are still unknown. Yeast COX assembly factors, their human homologs and their functions are reported in Table 1.1.

Table 1.1 Yeast assembly factors sorted by their roles in cytochrome *c* oxidase biogenesis (modified after Zee & Glerum, 2006) [1].

Protein	Reference	Function	Localization	Human Homolog
Translational activators or regulators				
Pet309	(Manthey & McEwen, 1995)	Cox1 translation	Matrix	LRPPRC
Mss51	(Barrientos et al., 2004)	Regulation of Cox1 translation	Matrix	
Cox14	(Barrientos et al., 2004)	Regulation of Cox1 translation	IMM	
Coa3	(Mick et al., 2010)	Regulation of Cox1 expression	IMM	CCDC56
Pet111	(Mulero & Fox, 1993)	Cox2 translation	Matrix	
Pet54	(Brown et al., 1994)	Cox3 translation	Matrix	
Pet122	(Brown et al., 1994)	Cox3 translation	Matrix	
Pet494	(Brown et al., 1994)	Cox3 translation	Matrix	
Membrane Insertion				
Oxa1	(Hell et al., 1998)	Insertion of charged domains	IMM	OXA1
Mba1	(Ott et al., 2006)	Insertion of uncharged domains	IMM	
Cox18	(Saracco & Fox, 2002)	Cox2 C-terminus insertion	IMM	
Mss2	(Saracco & Fox, 2002)	Cox2 C-terminus insertion	IMM	
Pnt1	(Saracco & Fox, 2002)	Cox2 C-terminus insertion	IMM	
Subunit-specific chaperones				
Cox20	(Hell et al., 2000)	Cox2 chaperone	IMM	COX20
Copper insertion				
Cox17	(Glerum et al., 1996a)	Copper chaperone	Cytosol/IMS	COX17
Cox11	(Carr et al., 2005)	Copper insertion into Cox1	IMM	COX11
Sco1	(Dickinson et al., 2000)	Copper insertion into Cox2	IMM	SCO1/SCO2
Heme biosynthesis				
Cox10	(Tzagoloff et al., 1993)	Heme b to heme O conversion	IMM	COX10
Cox15	(Barros et al., 2001)	Heme O to heme A conversion	IMM	COX15
Pet117	(Taylor et al., 2017)	Heme A synthesis	Matrix	
Assembly chaperones				
Shy1	(Mashkevich et al., 1997)	Subcomplex assembly	IMM	SURF1
Pet100	(Church et al., 2005)	Nuclear-encoded subunit assembly		
Unknown/Recently Characterized				
Cmc1	(Horn et al., 2008)	Mitochondrial copper metabolism	IMM	CMC1
Coa1	(Pierrel et al., 2007)	Cofactor Insertion	IMM	
Cox19	(Bode et al., 2015)	Folding modulator in the IMS	Cytosol/IMS	COX19
Cox23	(Barros et al., 2004)	Copper chaperone	Cytosol/IMS	COX23
Fmp32	(Paupe et al., 2015)	Unknown	Unknown	CDC90A
Pet191	(Khalimonchuk et al., 2008)	Complex Maturation	IMM	PET191
Cox16	(Carlson et al., 2003)	Unknown	IMM	COX16

[1] Imp1, Imp2 and Som1 are not included in this list as their specificity is not limited to COX assembly.

1.4.2 Assembly Factors in Heme A Biosynthesis

As mentioned above, COX is the terminal enzyme of the mitochondrial electron transport chain where it catalyzes the oxidation of cytochrome *c* and the reduction of molecular oxygen to water. Essential to this function are heme A and a_3 groups, which allow binding of oxygen to the complex. At least three ancillary factors are thought to be involved in the biogenesis of heme A molecules in yeast, namely Shy1, which is the yeast homolog of human SURF1, Cox10 and Cox15 (Barros et al., 2001; Smith et al., 2005; Tzagoloff et al., 1993). A model for heme A assembly involves Cox10, a heme O synthase, which generates a hydroxyethyl farnesyl heme by transferring a farnesyl diphosphate to protoheme. The heme O intermediate is then substrate of heme A synthase, Cox15, which oxidizes the heme O intermediate to generate heme A (Hederstedt, 2012; Moraes et al., 2004). Shy1, the yeast homolog of SURF1, is a protein thought to function in the early steps of COX assembly. The exact role played by Shy1 has not been completely defined. A study performed in *Rhodobacter sphaeroides* suggested a role for Shy1 in either formation or stabilization of heme a_3 (Smith et al., 2005). Another hypothesis is that Shy1 might play a role in incorporating COX subunits into early subassemblies (Fontanesi, Jin, et al., 2008; Pierrel et al., 2007).

Another study, by Bareth et al., (2013) identified a protein complex in yeast that includes Cox15 and Shy1, suggesting a functional link between these two factors (Bareth et al., 2013). In the same study, association of Cox15 and Cox1 in the absence of Shy1 was also found, possibly explaining the residual COX activity detected in patients affected by Leigh syndrome caused by mutations of SURF1 (Coenen et al., 1999; Tiranti et al., 1998; Zhu et al., 1998). Moreover, in the absence of Cox1, Cox15 still associated with early assembly intermediates while Shy1 did not. This led to the hypothesis that Shy1 might interact with Cox1 to prevent progression of COX assembly until the insertion of heme A by Cox15 is complete (Bareth et al., 2013).

Adding to the knowledge provided by investigations of Shy1, Cox10 and Cox15, a recent study shed light on the function of a still uncharacterized assembly factor, Pet117, in yeast. This protein appears to localize in the mitochondrial matrix where it associates with the IMM and was found to interact with Cox15, possibly playing a role in Cox15 oligomerization, a necessary step for its function as a heme A synthase (Taylor et al., 2017).

1.4.3 Assembly Factors in Cytochrome *c* Oxidase Copper Metalation

The insertion of redox centers is fundamental to the assembly of functional COX. In yeast, insertion of copper into Cu_A and Cu_B centers is facilitated by the activity of proteins capable of binding these ions. Cox17 is a small, natively unfolded (Abajian et al., 2004; Punter & Glerum, 2003), cysteine-rich protein that plays an essential role in COX assembly. Yeast *cox17* null mutants fail to assemble a functional COX complex; however, this phenotype is rescued by the addition of copper to the growth media (Glerum et al., 1996a). The discovery of Cox17 dual localization to the cytoplasm and mitochondria led to the hypothesis of a copper-shuttling function between the two cellular compartments for this protein (Beers et al., 1997). Once in the IMS, Cox17 is responsible for delivering copper ions to two other cuproproteins, namely Cox11 and Sco1 (Horng et al., 2004). Sco1 is a metallochaperone responsible for the transfer of copper to the copper center Cu_A in Cox2 (Dickinson et al., 2000; Lode et al., 2000). Sco1 is essential for COX assembly in yeast and its overexpression can rescue the phenotype of a *cox17* null mutant, likely by increasing the efficiency of copper intake from alternate sources of cellular copper (Glerum et al., 1996b). In yeast, as well as in humans, a Sco1 homolog, called Sco2 is present (Smits et al., 1994). However, it is believed that genes encoding yeast Sco1 and Sco2 resulted from a duplication event that occurred independently (paralogs) from the eponymous respective human genes (Papadopoulou et al., 1999). Interestingly, yeast strains depleted of Sco2 still succeed in assembling functional COX. Conversely, overexpression of this protein can rescue the phenotype resulting from point mutations of Sco1 but cannot compensate for the complete lack of Sco1; Sco2 overexpression can also rescue the respiratory deficiency of a strain lacking Cox17 (Glerum et al., 1996b). Another essential assembly factor in COX metalation is Cox11, a metallochaperone that receives copper ions from Cox17 and is responsible for the formation of the copper center, Cu_B, in Cox1 (Horng et al., 2004).

The model for COX copper metalation based on Cox17 functioning as a shuttle between cytoplasm and mitochondria has been challenged. A study provided evidence that the Cox17-copper complex exists as a dimer in the cytosol and as a tetramer in the IMS (Heaton et al., 2001); therefore, the free passage of such a complex through the OMM would be unlikely (Banci et al., 2009). Reinforcing this theory, results of another study showed that when Cox17

is tethered to the inner mitochondrial membrane, the assembly of COX is not adversely affected (Cobine et al., 2004; Maxfield et al., 2004). Adding to the complexity of this pathway, a study by Cobine et al., (2004), demonstrated the existence of a copper pool in the mitochondrial matrix. Further investigations led to the identification of a low molecular weight complex formed by copper ions and a copper ligand (CuL). The copper ligand has not been fully characterized yet but it appears to be an anionic, fluorescent, non-proteinaceous molecule (Vest et al., 2013). CuL has been proposed to bind and transport copper ions from the cytosol to the IMS. Here, copper ions would be imported into the mitochondrial matrix with the aid of Pic2, a member of the mitochondrial carrier family (MCF) (Vest et al., 2013). The current model for copper provision to Sco1 and Cox11 is that Cox17 would enter the IMS in an unfolded state. Cox17 then becomes a substrate of Mia40, resulting in the formation of two disulfide bonds in Cox17 (Banci et al., 2009), allowing it to bind one copper molecule and subsequently transfer it to Sco1 and Cox11 (Figure 1.3).

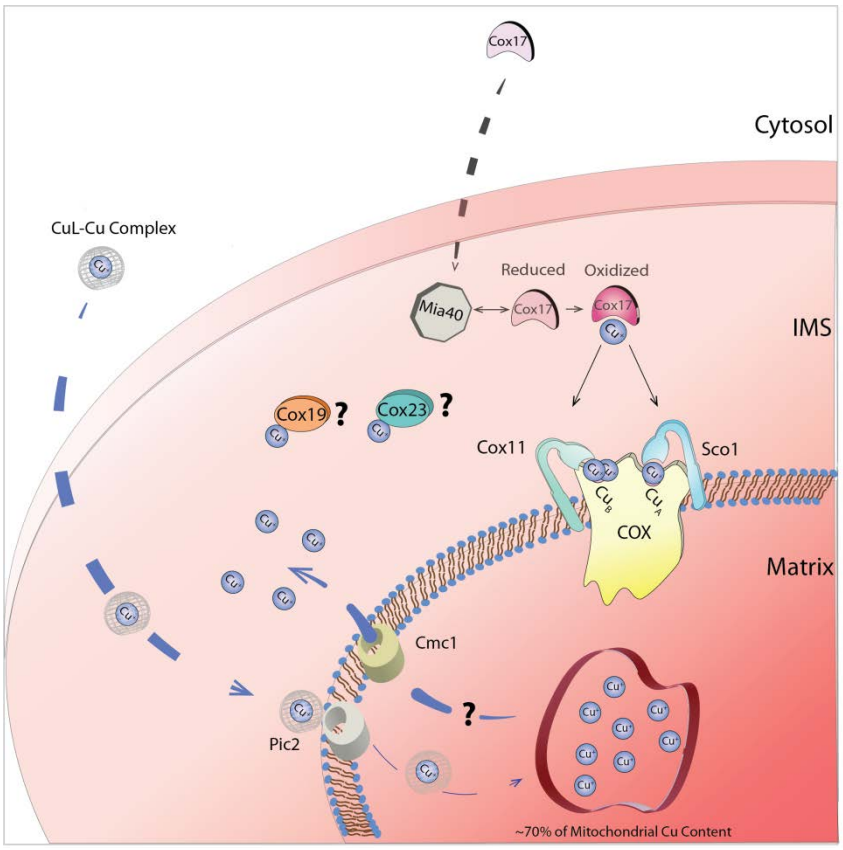

Figure 1.3 Schematic of COX copper metalation pathway. Cox17 enters the IMS in a reduced state and becomes substrate of Mia40. Upon interaction with Mia40, Cox17 transitions to its oxidized state and becomes capable of binding copper ions that are then delivered to another two cuproproteins, Sco1 and Cox11, and ultimately to COX. How copper reaches Cox17, however, is unknown and matter of debate. A model has been proposed suggesting copper is shuttled from cytoplasm to the intermembrane space (IMS) with the aid of a non-proteinaceous copper ligand (CuL). Once in the IMS, ions would be transferred to the mitochondrial matrix through Pic2. The efflux of copper from the pool in the matrix, however, is still poorly understood and subject of investigation. Another two proteins, namely Cox19 and Cox23, are thought to play a yet unknown role in COX assembly. According to this model, an unknown transporter would be playing a role in the efflux of copper ions from the copper pool in the matrix to the IMS (Leary et al., 2009). Modified after Banci & Bertini, (2013).

1.5. Mitochondrial Disease

Decades of research devoted to the study of mitochondria and their functions have identified a number of mitochondria-related disorders and their underpinning mechanisms. The study of COX alone, as an example, has helped the understanding of a number of aberrant phenotypes caused by COX deficiencies.

The first mitochondrial disorder was observed by Luft et al., (1962) in a 30 year old woman who presented with symptoms that arose at a young age. Symptoms included extensive perspiration, a very high caloric intake and muscle weakness. At a cellular level, abnormal accumulation of variably sized mitochondria in muscle cells was observed. Moreover, electron microscopy of the organelles revealed the presence of paracrystalline inclusions (Luft, 1995). Over the years, an increasing number of mitochondrial disorders have been described. Interestingly, in spite of the fact that mitochondria are actively involved in several metabolic pathways, all the cases initially investigated were related to dysfunctions of the mitochondrial respiratory chain (Koenig, 2008). Sequencing and elucidation of the mitochondrial genome organization in the early 1980s (Anderson et al., 1981) represented a step forward in the identification of mitochondrial disorders. By 1989, the first deletion in the mtDNA that was associated with disease in humans was described (Holt et al., 1989). In the intervening years, over 200 mutations in the mtDNA associated with disease have been identified. These mutations are associated with mitochondrial disorders such as mitochondrial encephalomyopathy, lactic acidosis, stroke-like episodes (MELAS), and a host of other (McFarland et al., 2002, 2010) mitochondrial disorders that are caused by dysfunctions affecting the metabolic pathways in which mitochondria play a role (DiMauro et al., 2013).

1.5.1 Leigh Syndrome and Respiratory Deficiency

Leigh syndrome, also known as necrotizing encephalomyopathy, was first described by Denis Leigh in 1951 while studying the cause of death of an infant presenting symptoms that included, among others, blindness, deafness and spasticity of the limbs. Following autopsy, no abnormalities were recorded with the exception of the nervous system of the patient, which had necrotic lesions associated with demyelination, vascular proliferation and other aberrations (Finsterer et al., 2008; Leigh, 1951). Leigh syndrome is nowadays considered the most common mitochondrial disease in infants (Munaro et al., 1997), with an estimated frequency of 1:40,000 births (Rahman et al., 1996). Typical manifestations of this disorder include developmental delay, lactic acidosis, necrotic lesions that affect the nervous system, and psychomotor regression (Leigh, 1951).

The outcome of diagnosed Leigh syndrome is generally poor (Piao et al., 2006). In most cases, the disease is fatal and patients die during childhood (before age 5) (Bénit et al.,

2004). The low frequency of this disorder and its lethality at a young age are some of the reasons why a curative treatment is not available yet. The onset of Leigh disease is often due to defects affecting mitochondrial enzymes. For example, deficiencies at the level of pyruvate dehydrogenase, coenzyme-Q and defects in mitochondrial respiratory chain complexes I, II, IV and V, have been shown to be associated with Leigh syndrome (Cooper et al., 2006; Horváth et al., 2006; Rahman et al., 1996). In the majority of Leigh disease cases that are related to respiratory chain deficiencies, mutations affect the subunits of the complexes (i.e. SDHA), or other factors involved in the assembly of the complexes (Debray et al., 2007). However, Leigh disease is not exclusively caused by mutations in nuclear encoded genes, as certain mutations of the mtDNA are a known determinants of Leigh disease (Rahman et al., 1996).

1.5.2 Assembly Factors in Mitochondrial Disease

The importance of COX assembly factors is underlined by the severity of phenotypes resulting from their aberrations. As mentioned above, Leigh syndrome is one of the most common mitochondrial diseases, especially among infants (Munaro et al., 1997). Mutations of *SURF1* have been found in the majority of patients affected by this mitochondrial disorder (Brown & Brown, 1996; Munaro et al., 1997).

Mutations of SCO1 and SCO2 result in diseases that occur as a consequence of COX deficiency. Interestingly, in spite of the cooperative functions of these proteins, their mutations result in very different clinical manifestations. Defects in both SCO1 and SCO2 can cause encephalopathy. However, mutations affecting SCO1 often associate with hepatopathy, while those affecting SCO2 result in cardiomyopathy. Similarly to what was observed for SCO2, aberrant versions of COX10, COX15 and COA5 were also found to associate with cardiomyopathy (Dimauro et al., 2012). While no diseases in humans are known to originate from mutations affecting the cuproprotein COX11, a single-nucleotide polymorphism found in the human *COX11* gene has been identified as a significant risk factor in breast cancer (Ahmed et al., 2009; Fasching et al., 2012).

1.6. Secondary Functions of Cytochrome *c* Oxidase Assembly Factors

A common belief that developed from studies performed in yeast is that mutations affecting COX assembly factors would result in very similar biochemical phenotypes in spite of the variety of functions performed by this multitude of proteins (Zee & Glerum, 2006). However, recent studies have provided evidence supporting the hypothesis that ancillary factors involved in the assembly of COX might have secondary functions not necessarily tied to the electron transport chain.

Cox17, Cox11 and Sco1 are the three cuproproteins that, among the assembly factors, are proposed to carry out novel functions. As mentioned above, these proteins are all involved in delivering copper ions to COX during formation of the prosthetic centers in Cox1 and Cox2, a process in which Sco1 and Cox11 act downstream of Cox17. However, the steps of the pathway that precede interactions between Cox17 with both Cox11 and Sco1 are still partially unknown and a matter of debate. An open question, for example, is how Cox17 receives copper ions in the IMS, since a non-proteinaceous copper ligand that would replace Cox17 as a copper shuttle was identified (Vest et al., 2013). The hypothesis that Cox17 is not involved in shuttling copper ions to the IMS opens up the possibility that the cytosolic pool of the protein might be tied to a different function of the protein.

1.6.1 Function of Cox17 in maintenance of Inner Membrane Integrity

A recent study by Chojnacka et al., (2015), unveiled a novel function of Cox17, namely as a regulator of the assembly of the mitochondrial contact site complex (MICOS).

MICOS is a six-subunit protein complex that was recently characterized. Localized to the cristae junction (Rabl et al., 2009), MICOS is essential in establishing and maintaining the mitochondrial inner membrane architecture and integrity. Among its six subunits, Mic60 and Mic10 constitute the core of the complex and their deficiency results in detachment of the cristae from the IM (John et al., 2005; Rabl et al., 2009). Both core components of the MICOS complex have been found interacting with proteins believed to function as stability and or biogenesis regulators. One regulator is the IMM protein Aim24, which interacts with Mic10 (Harner et al., 2014), and the other one is Cox17, which was found to associate with Mic60.

The interaction between Cox17 and Mic60 seems to be independent of the Cox17-Sco1 interaction that occurs during COX assembly (Chojnacka et al., 2015). Based on experimental evidence, two hypotheses were formulated with regards to Cox17's novel role. One is that the small metallochaperone is necessary for assembly and stability of MICOS in a way that depends on its capability of binding copper ions. Alternatively, Cox17 activity could be limited to delivering copper ions to the complex, which might regulate the levels of mature MICOS (Chojnacka et al., 2015).

1.6.2 Cox11 and Sco1 in Redox Metabolism

The recently discovered connection of Cox17 to a pathway that regulates the architecture of the mitochondrial inner membrane was not the first time COX assembly factors have been proposed to carry out secondary functions. Sco1 and Cox11 were proposed to be involved in cellular processes related to redox metabolism (Banting & Glerum, 2006; Williams et al., 2005). Reactive oxygen species (ROS) are highly reactive molecules that can induce cellular damage through the modification of DNA and proteins. A variety of enzymes such as superoxide dismutases, catalases and peroxidases are utilized by the cells to prevent ROS-induced damage (Figure 1.4) (Herrero et al., 2008).

As mentioned above, Sco1 is a metallochaperone that receives copper ions from Cox17 and delivers them to the copper center Cu_A in subunit 2. Nonetheless, studies performed over the past decade indicate that the activity of this protein might not be limited to formation of COX prosthetic centers. A Sco1 homolog in *Neisseria* has been shown to function in the protection of cells from oxidative stress (Seib et al., 2003). PrrC, a Sco1 homolog in *Rhodobacter sphaeroides* is a component of a signal transduction pathway involved in sensing changes to the oxygen tension and it was proposed to function as a copper binding protein as well as a thiol-disulfide oxidoreductase (McEwan et al., 2002). Interestingly, no copper ions were found in either human or *Bacillus subtilis* Sco1 crystal structures (Williams et al., 2005; Ye et al., 2005). Furthermore, similarities between SCO1 and the structures of peroxiredoxins and thioredoxins were found, suggesting that perhaps SCO1 could be involved in redox metabolism (Williams et al., 2005). This theory found support in the finding that a yeast *sco1* null mutant strain displayed hypersensitivity to concentrations of hydrogen peroxide in the millimolar range (Banting & Glerum, 2006). Another study investigated the effects of *scox*

knockdown (KD) in *Drosophila*. In this experimental system, scox is a single ortholog of the Sco proteins (Porcelli et al., 2010) and *scox* KD resulted in flies developing a severe cardiomyopathy. Affected cells displayed a metabolic switch from respiration to glycolysis and an increased amount of ROS. Ultimately, *scox* KD triggered p53-dependent apoptosis as a consequence of the increased oxidative stress. However, the disruption of either the p53 or of the apoptotic pathways rescued the effects of *scox* KD, reinforcing the theory that Sco1 might have a role in redox regulation (Martinez-Morentin et al., 2015; Williams et al., 2005).

Cox11, another key component of the COX copper provision pathway has also been proposed to carry out a secondary function. Similarly to what was described for Sco1, yeast *cox11* null mutant cells also displayed hypersensitivity to peroxide concentrations in the millimolar range (Banting & Glerum, 2006). Further investigation led to finding that hypersensitivity of *sco1* mutants can be partially suppressed by overexpression of *SCO2* or *COX11*, perhaps due to partially overlapping functions of Sco1 and Cox11 under oxidative stress conditions. On the other hand, overexpression of *SCO1* or *SCO2* cannot rescue peroxide sensitivity of a *cox11* null mutant (Veniamin et al., 2011). Consolidating the theory of assembly factors being involved in redox metabolism was the finding that *sco1* and *cox11* null mutants clear exogenous peroxide to a lesser extent than a wild type strain (Veniamin et al., 2011).

In spite of the accumulating evidence in support of the notion that Cox11 and Sco1 might be involved in redox metabolism, their precise roles remain unknown. Further investigation is therefore required, especially in the case of Sco1, where contradictory findings and hypotheses have been formulated.

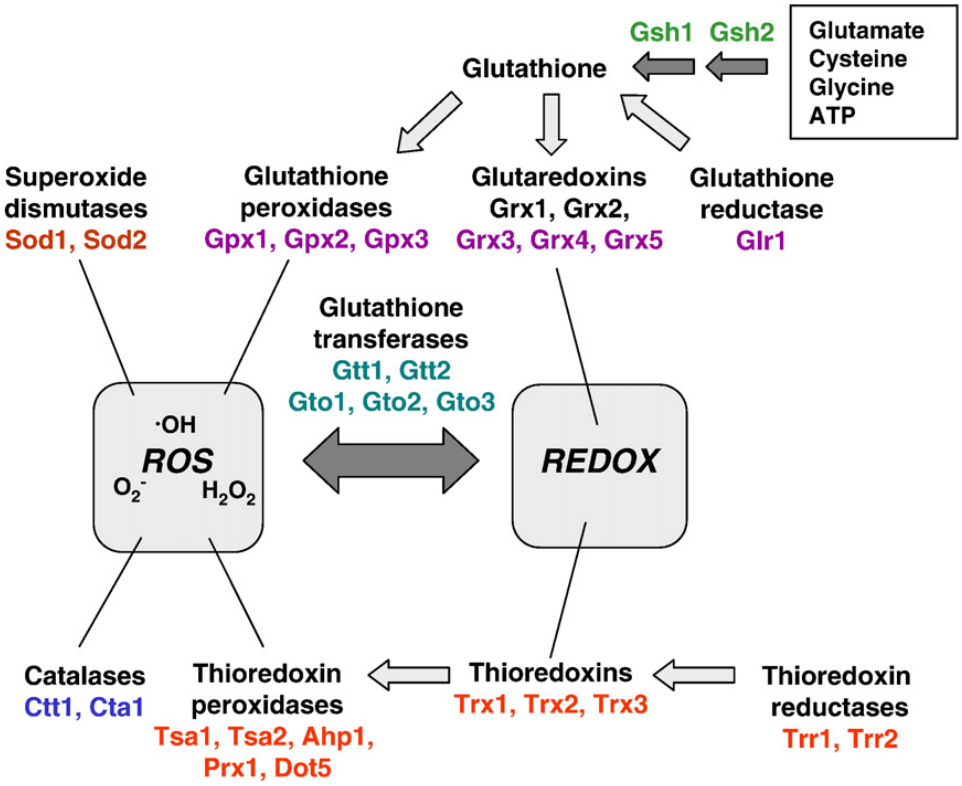

Figure 1.4 Schematic of yeast redox metabolism. Cellular processes such as the oxidative phosphorylation can generate reactive oxygen species, namely oxygen superoxide, hydrogen peroxide and the hydroxyl radical. Activities of catalases, glutathione/thioredoxin peroxidases and superoxide dismutases are fundamental in counteracting the presence of highly reactive molecules within a cell. A reducing intracellular environment, which plays an important role in the defense against oxidative stress is ensured by proteins such as thioredoxins and glutaredoxins. REDOX, oxidation/reduction reactions that neutralize ROS and control the state of sulphydril groups. According to Herrero et al., (2008).

1.7. Cellular Processes Linked to Mitochondrial Defects

1.7.1 Yeast Apoptosis

Mitochondria, as mentioned above, host numerous essential cellular processes, such as the electron transport chain. At the same time, these organelles are a known source of intracellular ROS. Increased ROS levels as a consequence of mitochondrial dysfunction have been associated with mechanisms involved in neurodegenerative disorders such as Parkinson's disease (Sherer et al., 2003). Oxidative stress resulting from ROS accumulation beyond the

capacity of the cellular scavenging mechanisms has also been associated with cell death through the apoptotic pathway (Kannan et al., 2000).

Apoptosis, also known as programmed cell death (PCD) is a process that allows removal of damaged cells within a population without negative impacts to the surrounding cells. Necrosis, in contrast, is a form of cell death that may occur in heavily damaged cells and that culminates in cell lysis with consequent release of cytoplasmic content in a manner that can have negative effects on other cells. In humans, apoptosis is an important factor in homeostasis and it is known to play a role in pathways linked to tumor suppression, neurodegenerative diseases and viral infections (Steller, 1995).

In yeast, the existence of a PCD pathway had been uncertain for a long time. In fact, no protein homologous to human apoptotic regulators were found in either *Schizosaccharomyces pombe* or *Saccharomyces cerevisiae*. This uncertainty was removed by the pioneering work of Madeo et al., (1997), which demonstrated that deletion of cell cycle gene *CDC48* resulted in *Saccharomyces cerevisiae* cells presenting with the hallmarks of apoptosis (Madeo et al., 1997). Signs of activation of the PCD pathway are the presence of DNA cleavage, chromatin condensation, externalization of phosphatidylserine to the outer leaflet of the plasma membrane and the release of cytochrome *c* from mitochondria into the cytosol (Ludovico et al., 2002; Madeo et al., 1997; Manon et al., 1997).

To explain the debated “need” for a unicellular organism to undergo programmed cell death, it has been suggested that yeast apoptosis should be considered in the context of a cell population rather than focusing on individual cells. A study of yeast grown for prolonged lengths of time showed that chronological aging correlates with death by activation of the apoptotic pathway. Interestingly, it was found that yeast lacking Yca1, a yeast ortholog of mammalian caspases (Madeo et al., 2002), did not survive longer than wild-type cells with a functional apoptotic response pathway. Apoptosis might therefore benefit a population by safely removing less adapted cells, whose degradation releases simple nutrients that become available to other cells (Herker et al., 2004).

A large body of knowledge has accumulated since the first evidence of apoptosis in yeast was provided. The many biochemical and morphological similarities between *S. cerevisiae* and human PCD uncovered by years of research make yeast a good model for the study of this cellular process. All the same, despite the similarities, yeast and human apoptosis

mechanisms also display some divergent characteristics (Guaragnella et al., 2012). The execution of mammalian apoptosis typically occurs through accumulation of Bcl2 homology 3 (BH3) proteins on the OMM. An example of a BH3 containing protein that is involved in promoting apoptosis in humans is Bax, which acts to form pores on the OMM, in turn causing the release of cytochrome *c* to the cytoplasm (Danial et al., 2004). Cytochrome *c* then binds the adaptor protein Apaf1 causing it to oligomerize into a heptamer, called the apoptosome, which is responsible for the subsequent recruitment of caspase-9 proteins. Finally, caspase-9 proteins activate downstream caspases resulting in apoptotic induction. In yeast, on the other hand, only one gene homolog of caspases has been found to date, *YCA1*, which encodes a metacaspase that is characterized by substrate specificity different from that of the mammalian caspases (Wilkinson & Ramsdale, 2011). Similarly, only one BH3 protein was discovered in yeast, Ybh3, which was shown to translocate to mitochondria and induce programmed cell death by functioning in membrane depolarization upon treatment with acetic acid and hydrogen peroxide (Büttner et al., 2011).

Intriguingly, yeast apoptosis has been shown to occur in a caspase-dependent, as well as a caspase-independent, fashion (reviewed by Madeo et al., 2009). However, some of the mechanisms underlying these pathways, as well as some of the factors involved, are not understood and remain the subject of investigation. A striking feature of yeast PCD is that its modes of activation and execution in response to stimuli seem to depend on the status of a cell. Phase of growth, metabolic state and environmental conditions are all factors that seem to have a role in determining the apoptotic route followed by cells (Guaragnella et al., 2012). For example, acetic acid treatment of cells with increased respiratory activity triggers a Nuc1-dependent PCD (Büttner et al., 2007). On the other hand, cells at the stationary phase of growth were shown to be less sensitive to acetic acid treatment (Ludovico et al., 2002) and to become highly resistant to the presence of acetic acid after adaptation to acid stress (Guaragnella et al., 2008; Ždralević et al., 2012).

1.7.1.1 Roles of Mitochondria in Yeast Apoptosis

A link between mitochondria and apoptosis is known in both yeast and mammalian systems. In fact, these organelles are thought to be one of the major players in determining the

fate of a cell with respect to either a pro-survival or pro-apoptotic route. Evidence of a mitochondrial-dependent PCD in yeast was obtained after cytochrome *c* release in cells treated with acetic acid was observed. Reinforcing this theory, cells lacking mtDNA or the ATP synthase and cells unable to synthesize cytochrome *c* showed higher resistance to PCD induction upon exposure to acetic acid (Ludovico et al., 2002).

A clear discriminant between the caspase-dependent and caspase-independent PCD pathways is the release of cytochrome *c*. In yeast, an equivalent of the human apoptosome has not been identified and yeast cytochrome *c* has been shown incapable of activating metazoan caspases (Bender et al., 2012; Hüttemann et al., 2011; Kluck et al., 2000). However, central questions regarding the exact function of cytochrome *c* in yeast apoptosis remain unanswered. For instance, the specific mechanisms and factors triggering cytochrome *c* release and the exact mode of function of this protein in this process are still unknown (Guaragnella et al., 2012).

Despite evident gaps in knowledge, several studies have contributed to define a chronological model of the events occurring during a typical PCD response of yeast cells induced with acetic acid (Figure 1.5). Exposure to acetic acid shows its effect on cellular homeostasis, starting about 15 minutes after induction, through accumulation of ROS. Cytochrome *c* release has been shown to initiate approximately one hour post-induction and it continues for up to two and half hours. Afterwards, released cytochrome *c* is degraded, likely by the action of proteases whose identity remains unknown. Lastly, about three and a half hours after induction, cell death occurs through caspase-like activation (Giannattasio et al., 2008, 2005, Guaragnella et al., 2008, 2006; Guaragnella, et al., 2010; Guaragnella et al, 2007; Pereira et al., 2007; Ribeiro et al., 2006). The pro-apoptotic roles of cytochrome *c* and Yca1 are known, as it was found that defects in these two factors reduce the death rate. On the other hand, this also means that, even though at a lower rate, cells lacking cytochrome *c* and Yca1 are still able to undergo PCD. Such evidence clearly indicates the presence of a caspase-independent apoptotic pathway that is not characterized by cytochrome *c* release. Another notable feature of the Yca1-independent pathway is its insensitivity to the antioxidant N-acetyl cysteine, whose presence would prevent ROS formation, cytochrome *c* release and therefore disrupt the caspase-dependent PCD (Guaragnella et al., 2010; Guaragnella et al., 2011; Guaragnella, Passarella, et al., 2010; Pereira et al., 2007).

1.7.1.2 Other Mitochondrial Factors in Programmed Cell Death

Besides the mechanisms and their components described above, other mitochondrial-related factors have been implicated in yeast PCD.

Considering the electron transport chain as a possible cell death trigger upon production of ROS through electron slippage, for instance, would be logical. In keeping with this this idea, investigations led to the identification of NDI1, a NADH dehydrogenase that is a homolog of AMID, a metazoan apoptotic inducing factor. Overexpression of NDI1 resulted in induction of apoptosis, perhaps due to ROS accumulation, in cells grown in glucose-rich media (Li et al., 2006).

In a discussion of yeast PCD, two other mitochondrial proteins, namely Nuc1 and Aif1, have been identified as players in this pathway. Aif1 is the yeast homolog of human AIF, a key player in caspase-independent apoptosis (Hangen et al., 2010). In yeast, as in humans, Aif1 translocates from mitochondria to the nucleus upon apoptotic induction (Wissing et al., 2004). Interestingly, it appears that Aif1 might be especially involved in PCD associated with oxygen stress and aging (Xu et al., 2010).

Similarly, Nuc1 is the yeast homolog of EndoG, a metazoan endonuclease G characterized by DNase/RNase activity, which is necessary for DNA degradation during apoptosis (Li et al., 2001). Like Aif1, Nuc1 also translocates to the nuclear compartment after apoptosis has been triggered. However, when overexpressed, Nuc1 promotes PCD in a way that is independent of Aif1 and Yca1 (Büttner et al., 2007), indicating that PCD might be regulated by multiple, redundant pathways (Guaragnella et al., 2012).

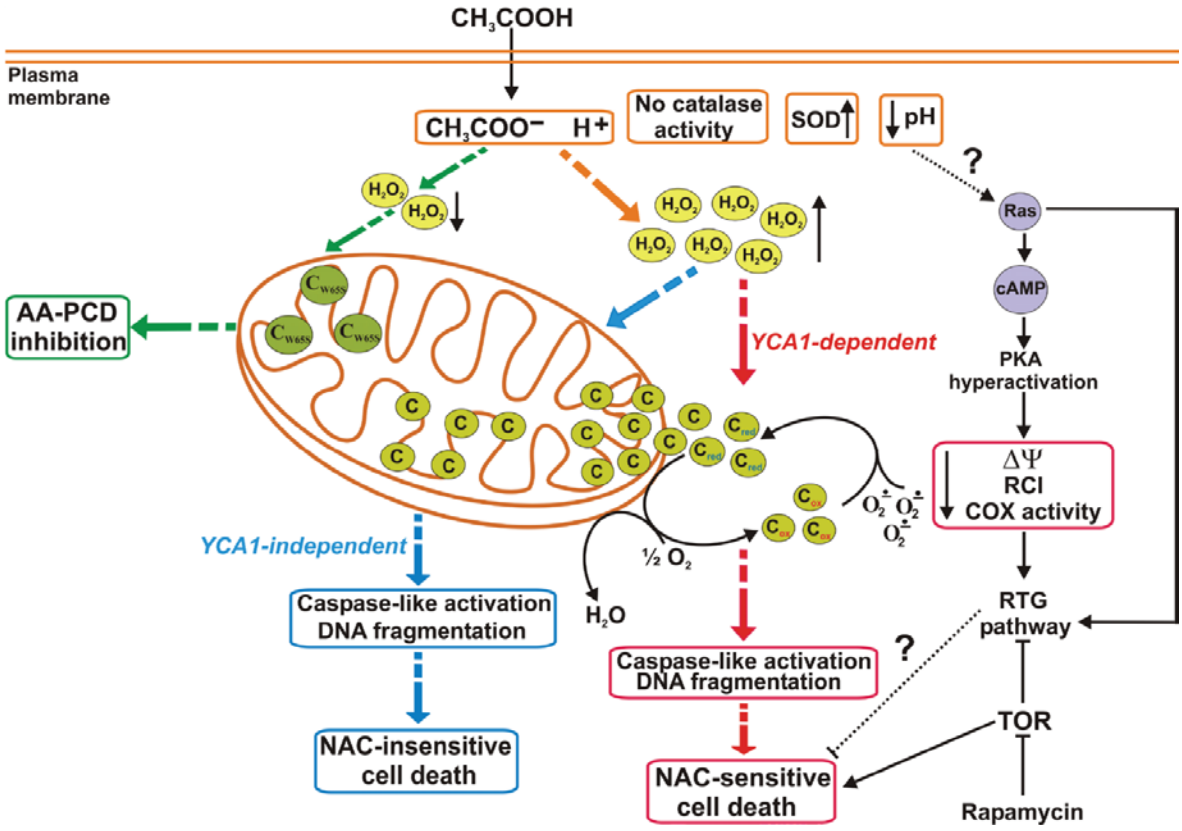

Figure 1.5 Yeast caspase-dependent and caspase-independent apoptotic pathways (according to Guaragnella et al., 2012). The caspase-dependent pathway relies on the function of the yeast caspase Yca1 and on the release of cytochrome *c* to the cytosol following a burst in ROS generation. Disruption of the caspase-dependent route reduces but does not stop apoptotic activation, which can proceed in a caspase-independent manner and that is insensitive to the presence of a strong anti-oxidant such as N-Acetyl cysteine (NAC). Findings from numerous studies have generated a significant body of knowledge since yeast PCD was first described. Nevertheless, numerous questions are still unanswered and molecular mechanisms remain poorly understood and require further investigation.

1.8. Yeast Stationary Phase

Until about 30 years ago, common belief among the scientific community was that glucose depletion by growing yeast cells would result in growth arrest with “cell shut down” followed by death within a few days. This concept was later challenged by a series of studies that started a new chapter of yeast research. This work led to the discovery that, not only do cells not die after glucose depletion, they are capable of undergoing at least another cell division, allowing the whole growth cycle to be divided into three distinct phases. Exploration of this new scenario was stimulated by the thinking that, after all, most of the known cell types

exist in a non-dividing state and that yeasts survived for millennia under growth conditions far different from those provided in a typical research laboratory (Werner-Washburne et al., 2015).

A common method used to grow yeast cells for research purposes involves incubation of this unicellular organism in glucose-rich media. This experimental set-up allows cells to rapidly grow and multiply exponentially by adopting fermentative metabolism based on the consumption of available simple sugars. This initial stage is known as the logarithmic phase of growth and it ends upon the exhaustion of the glucose in the media. The time required to reach this phase of growth may vary depending on the yeast strain used; however, as a general rule, cells will reach the end of logarithmic phase after growing for at least 24 hours. At this point, a switch from fermentative to respiratory metabolism is necessary to initiate the consumption of the non-fermentable carbon sources present in the media that are a by-product of fermentation. This phase is also referred to as the diauxic shift and is characterized by a slower growth rate, in comparison to the logarithmic phase. It can take several days for a yeast culture to deplete the carbon sources (Figure 1.6), whereupon, once resources to support cellular growth are no longer available, the culture reaches saturation and the cell density plateaus. This stage, which is usually reached after about a week, is known as stationary phase (Gray et al., 2004; Werner-Washburne et al., 1993).

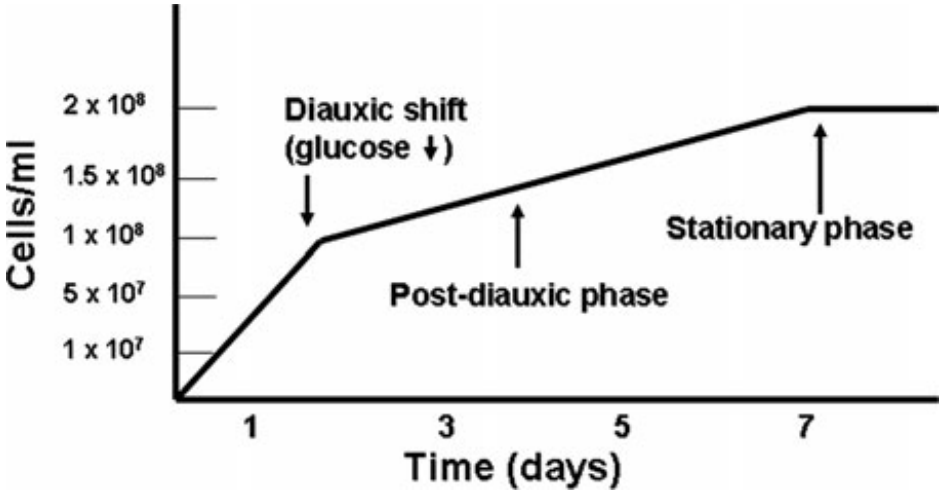

Figure 1.6 Growth curve of yeast grown in glucose-containing media. Typically, a yeast culture will deplete glucose after about one day and enter the diauxic shift. Once the non-fermentable carbon source are also exhausted, growth rate reaches a plateau determining the shift to the stationary phase of growth (According to Werner-Washburne et al., 2015).

1.8.1 Characteristics of Cells in Stationary Phase Cultures

In considering cells in stationary phase cultures, it is important to distinguish between the terms “stationary phase” and “quiescence”. The “stationary phase” refers specifically to the state of a culture that has reached saturation, while the term quiescence relates to the state of a cell in such a culture (Gray et al., 2004). In the past, stationary phase cultures were seen as homogenous cell populations composed of individual cells characterized by an identical intrinsic status. This assumption was recently proved wrong by the identification of two distinct cell types within a saturated culture: quiescent and non-quiescent cells (Allen et al., 2012).

Upon density gradient separation of cell populations in a stationary phase culture, it was found that quiescent cells appeared more refractile by phase contrast microscopy and were more thermotolerant. These cells were also shown to retain high level of viability, to maintain reproductive capability for at least three weeks, to be genomically stable and to contain low amounts of ROS (Allen et al., 2012; Aragon et al., 2007). Synchronization is another feature typical of cells at this phase of growth. It is worth pointing out that synchronous, aging cells make an ideal candidate for the study of other processes such as aging and the cell cycle (Laun et al., 2006; Moore & Miller, 2007).

In contrast, non-quiescent cells differ from quiescent cells in many substantive ways. While non-quiescent cells also show high levels of viability for up to three weeks, they do not seem to be able to retain their reproductive capability in a way that is independent of the replicative age. Interestingly, non-quiescent cells do not stop proliferating after glucose exhaustion and show significant accumulation of ROS after 7 days and apoptotic induction at 14 days of incubation (Allen et al., 2012). Another significant difference between quiescent and non-quiescent cells comes from the analysis of mRNA content. Quiescent cells, in fact, displayed mRNA profiles that would fit cells that are preparing to face conditions of stress and therefore require mRNA encoding proteins involved in vesicle-mediated transport and ROS metabolism. Non-quiescent cells, instead, showed abundance of mRNA encoding proteins involved in DNA repair, recombination and rearrangement, consistent with a high proportion of these cells undergoing apoptosis or necrosis (Allen et al., 2012).

1.8.2 Mitochondrial Function in Stationary Phase Cultures

Mitochondria have been proposed to exert an essential role in cell survival, especially after glucose depletion when cells switch from fermentative to respiratory metabolism. In stationary phase cultures, mitochondrial function seems to differ depending on the cell population. Cells in a quiescent state were found to contain intact and fully functional mitochondria characterized by high respiratory rate. On the contrary, mitochondria of cells that do not enter quiescence and keep dividing instead, seem to have no detectable respiratory function after seven days (Davidson et al., 2011). Moreover, it was found that a portion of non-quiescent cells produce petite mutants at a high rate, a sign of increased mutations affecting mitochondrial function (Davidson et al., 2011). Trying to explain the heterogeneity of stationary cultures in a functional context, Werner-Washburne et al., (2015), hypothesized that non-quiescent cells in stationary phase cultures are the yeast equivalent of the "hypermutable" sub-population described in the microbial literature (Gonzalez et al., 2008; Sniegowski, 1995; Sundin & Weigand, 2007). In such a scenario, the predictable mutability would be triggered by stress conditions and would contribute to yeast evolution (Werner-Washburne et al., 2015).

1.8.3 Yeast Stationary Phase Cultures as a Model for the Study of Higher Eukaryotes

The intrinsic status of yeast cells in stationary phase cultures makes them suitable for the study of aging processes that could subsequently be inferred in higher eukaryotes. For instance, synchronization, which is a hallmark of quiescence (Laun et al., 2006; Moore & Miller, 2007), could be exploited for studies that could provide insights about cell cycle-related processes during aging.

Programmed cell death pathways represent another relevant area of research involving stationary phase cells. Apoptotic pathways have already been proposed to play a role in the physiology of aging yeast populations (Herker et al., 2004). In higher eukaryotes, such as *Drosophila* and humans, aging of stem cell niches is the subject of extensive research (Drummond-Barbosa, 2008; Rossi et al., 2008; Wallenfang, 2007). Although many hypotheses for models of aging have been made, whether aging causes a decline in stem cell function or stem cells decline is responsible for aging remains unclear (Drummond-Barbosa, 2008).

Quiescent yeast cells share a number of physiological tracts with certain human cell types such as eggs, stem cells and neurons. Biochemical properties common to these cell types include high abundance of mRNAs associated with protein-mRNA complexes, low ROS levels, low apoptotic rate and the retention of reproductive capability (Allen et al., 2012; Aragon et al., 2007).

1.9. Roles of Mitochondria in Yeast Cell Cycle

1.9.1 Yeast Cell Cycle

The cell cycle consists of a set of events that occur in a specific order and that are necessary to ensure cell growth and division. Cell cycle progression and its control systems within a cell have been investigated for a long time and studies performed using *S. cerevisiae* have contributed greatly to the understanding of this process in higher eukaryotes (Nasmyth, 1996).

As a fundamental element in the life cycle of a cell, proper execution of cell division requires tight control. Cell cycle phases and their control systems were found to be strongly conserved among eukaryotes from unicellular organisms, such as yeast, to humans. Given the nature of cell cycle control networks, it is possible to approximate cell cycle events as an alternation between two self-maintaining stable steady states (G1 and S/G2/M) (Nasmyth, 1996). Work performed in the 1970s by Hartwell and co-workers has built the foundation of our current understanding of cell cycle events. A series of experiments led to the isolation and characterization of 150 temperature-sensitive *Saccharomyces cerevisiae* mutant strains. These cells were capable of reproducing at the permissive temperature of 23 °C but not at the restrictive temperature of 36 °C, allowing for the identifications of 32 genes encoding proteins that are essential for completing cell division (Hartwell et al, 1973). Cells defective for essential cell cycle proteins displayed growth arrest at specific stages and allowed the building of models that defined the order of cell cycle events based on the phenotypes observed. For example, *cdc28* mutant cells did not display any of the typical cell cycle events, leading to the conclusion that the encoded protein was involved in one of the early steps, later defined as START (Hartwell et al, 1973). Research conducted in the following years has revealed that Cdc28 belongs to a group of cyclin-dependent protein kinases (CDKs), which are fundamental

in regulating cell cycle progression. These proteins, upon interaction with certain cyclins, are responsible for phosphorylation of target proteins needed to initiate processes such as DNA replication, breakdown of the nuclear envelope, chromosome condensation and spindle assembly (Morgan, 1995; Murray, 2004).

1.9.1.1 Cell Cycle Phases

A growing cell initially undergoes a Gap1 phase, G1, the longest of the Gap periods, and it will then face three different choices. First, a cell might decide to proceed with DNA replication and division. Alternatively, if conditions are unfavourable, a cell might exit the cell cycle and enter a G_0 or quiescent state. Ultimately, haploid yeast strains might undergo mating with cells of the opposite mating type; the response to release of mating hormones is arrest of the cell cycle in G1 (Forsburg & Nurse, 1991).

A cell is committed to completing division once it has reached a sufficient size and has passed the START point (Figure 1.8). At this stage, increased cyclin-CDK activity induces activation of G1-S transcription factors. Among the first cyclins to be transcribed are yeast Cln1 and Cln2 (Eser et al., 2011).Through a positive feedback mechanism, G1 cyclins are capable of increasing their own transcription. This sequence of events culminates with increased CDK-cyclin activity which commits a cell to complete division (Bertoli et al., 2013). Hence, a cell that passes the START must complete the processes that eventually lead to division, starting with replication of the genomic content during the synthesis (S) phase. DNA synthesis takes approximately 25 % of the time required for a cell to proliferate (Hartwell, 1974). Generally, DNA replication also corresponds to the emergence of a bud from the mother cell. In cell cycle research, morphological changes associated with progression are an important feature that can be used to estimate the phase a certain cell is at by visual observation. Duplication of the DNA content is a multi-step process that starts with unwinding of the double helix and proceeds through the action of DNA polymerases (reviewed in Labib, (2010)).

When DNA replication is complete, cells will transition through a Gap2 (G2) phase before initiating nuclear and cellular division. G2 phase is generally shorter than G1 and allows

mother and daughter cells to grow in size before entering mitosis. Also, at this stage the nucleus starts to migrate towards the bud neck (Hartwell, 1974).

The events that come after G2 and that conclude cellular reproduction, are nuclear and cellular division. Prophase is the first step of mitosis and is characterized by attaching of microtubules to sister kinetochores. Chromosome alignment follows during metaphase and sister chromatids are separated during anaphase. Lastly, spindle disassembly and nuclear membrane constriction during telophase are some of the events associated with the conclusion of mitosis (Winey & O'Toole, 2001). The execution of the cell cycle leads to a mother cell from which a small bud has emerged (Figure 1.7). At this point, separation of the bud from the mother will happen following constriction of an actomyosin ring, septum formation and subsequent destruction. The separation of the bud from a mother cell is also characterized by the formation of a chitin bud scar that will remain on the mother cell (Hartwell, 1974).

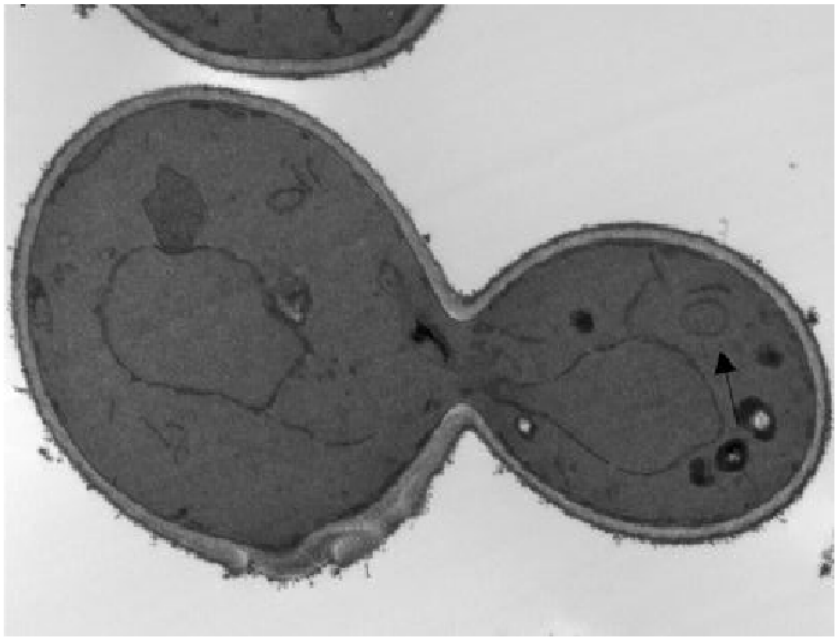

Figure 1.7 Photograph of wild-type yeast budding cell. Arrowhead highlights a mitochondrion. According to Srikumar et al., (2013). Morphological changes, such as the emergence of a bud when cells enter the S phase can be used to monitor cell cycle progression.

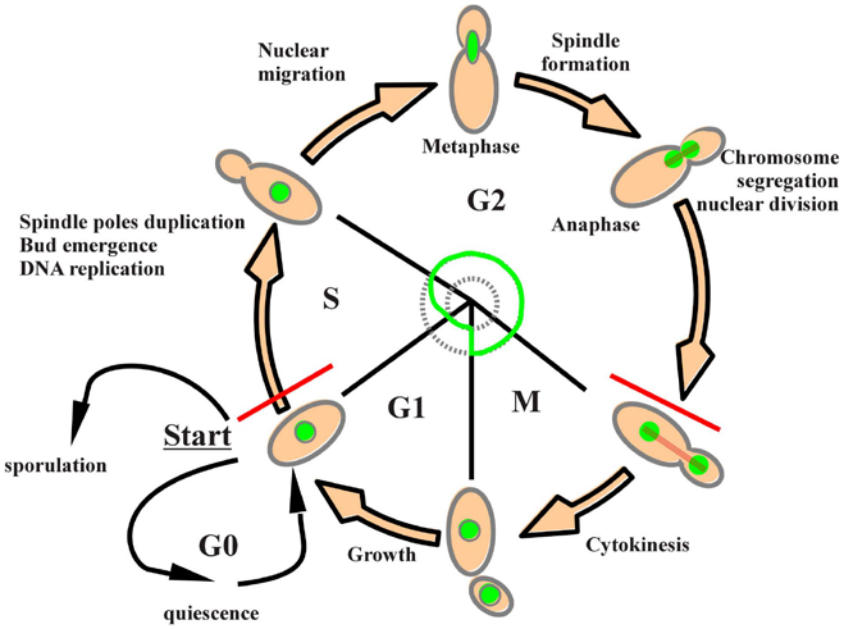

Figure 1.8 Typical yeast cell cycle progression (according to Delobel & Tesnière, (2014)). A cell will initially grow during a Gap1 (G1) phase until a critical size is reached. Once the START checkpoint is passed, a cell will initiate the DNA replication phase (S). A Gap2 (G2) phase, where chromosome segregations occurs, precedes the mitosis phase (M) and the cytokinesis.

1.9.1.2 Mitochondrial Involvement in Regulation of Cell Cycle Events

The involvement of mitochondria in myriad pathways makes these organelles a crucial factor in cell homeostasis, particularly given their multiple functions in cellular metabolism. In the recent past, the hypothesis of a connection between metabolic processes and cell cycle has received support from growing experimental evidence. Being fundamental in many biochemical pathways, mitochondria have also been the subject of investigation in this area.

Studies in human cells have shown that the use of serum deprived media stops DNA replication, while removal of glucose or certain amino acids results in arrest at G0/G1 phase (Holley & Kiernan, 1974; Lee & Finkel, 2013).

One pathway associated with growth arrest in the absence of glucose was found to be mediated by p53 and dependent on AMP-activated protein kinase activity. Other energetic stresses such as ETC disruption were also found to trigger p53-mediated cell cycle arrest (Mandal et al., 2005). Two pathways have been linked to cell cycle arrest induced by mitochondrial dysfunction in *Drosophila*. Growth arrest can occur through p53-mediated degradation of

cyclin E (Mandal et al., 2010, 2005) or via ROS-dependent induction of Dacapo, which is the *Drosophila* homolog of human p27 (Owusu-Ansah et al., 2008).

Evidence of mitochondrial influence on cell cycle events in yeast is also emerging. A study in *S. cerevisiae* showed that cells lacking mtDNA are characterized by a slower G1-S progression in comparison to wild-type. The same study demonstrated that the lack of mtDNA per se, and not the lack of mtDNA-encoded gene products, determines G1 arrest. Interestingly, it was also demonstrated that this G1 arrest is mediated by Rad53, the yeast ortholog of the CHK2 kinase. This finding is a first indication that proteins involved in response to DNA damage might also function in mtDNA maintenance and checkpoint (Lee & Finkel, 2013).

A connection between oxidative stress and cell cycle defects has also been established. When synchronized yeast cells were treated with a known reactive oxygen species, such as hydrogen peroxide, a delayed S phase was initially detected, followed later by arrest at G2/M (Shapira et al., 2004). Such a defect was attributed to hydrogen peroxide effects on gene regulation associated with the G2/M transcriptional complex Mcm1-Fkh2-Ndd1 (Shapira et al., 2004). It was also proposed that this distinct cell cycle response could be due to the modification of protein cysteines or methionines by the peroxide treatment. Another, more recent study, reported that *S. pombe* cells carrying a mutated version of a gene involved in heme biosynthesis were hypersensitive to hydroxyurea treatment (HU). The authors suggested that the mitochondrial defect caused by heme deficiency, combined with HU treatment, might increase ROS production to levels that exceed the capability of cellular ROS scavenging mechanisms (Singh & Xu, 2017).

1.10. Goals of the Study

Cytochrome *c* Oxidase is a mitochondrial inner membrane protein complex that plays a fundamental role in the electron transport chain. The importance of this complex is underlined by human diseases caused by defects in COX function and assembly. Extensive research in mammals and other model organisms has led to an improved understanding of COX function and assembly; however, there remain many open questions and molecular mechanisms not yet understood. In the recent past, evidence has emerged that certain COX assembly factors may have secondary functions unrelated to their roles in the assembly of a functional electron transport chain.

The majority of studies performed in yeast, and involving the COX complex, have utilized cells grown to late exponential phase/early diauxic shift. However, preliminary experiments for the study presented here suggested a differential expression of Cox17 at different phases of growth, namely exponential and stationary phases. Detection of increased Cox17 protein levels in whole cell lysates at stationary phase led us to hypothesize that Cox17 might have a novel, secondary function in the yeast stationary phase.

Chapter 2

Materials and Methods

2.1 Yeast Strains

Table 2.1 Yeast strains used in this study

Strain	Genotype	Source
W303	MAT**a**, *ade2-1 his3-1,15 leu2-3,112 trp1-1 ura3-1*	Glerum Lab
W303	MAT**α**, *ade2-1 his3-1,15 leu2-3,112 trp1-1 ura3-1*	Glerum Lab
W303 ρ^0	MAT**a**, *ade2-1 his3-1,15 leu2-3,112 trp1-1 ura3-1*	Glerum Lab
W303 ρ^0	MAT**α**, *ade2-1 his3-1,15 leu2-3,112 trp1-1 ura3-1*	Glerum Lab
W303ΔCOX17	MAT**a**, *ade2-1 his3-1,15 leu2-3,112 trp1-1 ura3-1 COX17::TRP1*	This Study
W303ΔCOX17	MAT**α**, *ade2-1 his3-1,15 leu2-3,112 trp1-1 ura3-1 COX17::TRP1*	Glerum Lab
W303ΔSCO1	MAT**a**, *ade2-1 his3-1,15 leu2-3,112 trp1-1 ura3-1 SCO1*::*URA3*	Glerum Lab
W303ΔCOX11	MAT**a**, *ade2-1 his3-1,15 leu2-3,112 trp1-1 ura3-1 COX11*::*HIS3*	Glerum Lab
W303ΔCOX4	MAT**a**, *ade2-1 his3-1,15 leu2-3,112 trp1-1 ura3-1 COX4*::*URA3*	This Study
W30Δ3COX4	MAT**α**, *ade2-1 his3-1,15 leu2-3,112 trp1-1 ura3-1 COX4*::*URA3*	Glerum Lab
W30Δ3COX15	MAT**a**, *ade2–1 his3–1,15 leu2–3,112 trp1–1 ura3–1 cox15::HIS3*	Glerum Lab
KL14	MAT**α** met-6	Glerum Lab
CB11	MAT**a** ade-1	Glerum Lab
	Strains Used for LacZ Assay	
W303plNEG	MAT **a** ade2-1 his3-11, 15 leu2-3,112 trp1-1 ura3-1 + YEp 351 - LacZ	Glerum Lab
W303plCOX17	MAT **a** ade2-1 his3-11, 15 leu2-3,112 trp1-1 ura3-1 + 5'- COX17 UTR + LacZ	Glerum Lab
W303plSCO1	MAT **a** ade2-1 his3-11, 15 leu2-3,112 trp1-1 ura3-1 + 5'- SCO1 UTR + LacZ	Glerum Lab
W303plCOX11	MAT **a** ade2-1 his3-11, 15 leu2-3,112 trp1-1 ura3-1 + 5'- COX11 UTR + LacZ	Glerum Lab

2.2 Yeast Growth Curve

Yeast growth curves were obtained by measuring the optical density of a wild-type and mitochondrial mutant strains at 600 nm (OD_{600}). Cells were incubated overnight at 30 °C and 230 rpm in YPD media (2 % glucose, 2 % peptone, 1 % yeast extract). The following day, cultures were normalized to an OD_{600} = 0.1 (t = 0 h) and incubated under the same conditions. The time of incubation represents the starting point (t = 0 h) of the growth curve. To determine

transitions through different phases of yeast growth, OD_{600} was measured and the values plotted against time to obtain the growth curve.

2.3 Mating and Sporulation

Mating and subsequent sporulation of diploid strains were used to obtain MAT a W303ΔCOX17 and MAT a W303ΔCOX4. These strains were used to perform synchronization experiments using the mating hormone α-factor.

Diploid patches were made on YPD agar by mating the respiratory competent, parent strain W303 (MAT a) with W303ΔCOX17 and W303ΔCOX4 (MAT α). Following overnight incubation at 30 ºC, patches were replica-plated onto minimal agar media WO (2 % glucose, 0.67 % nitrogen base without amino acids but with ammonium sulfate, 2 % agar) to which the strain-specific supplements were added to complement auxotrophies (see Table 2.1). After an overnight incubation, the patches were replica-plated onto plates containing sporulation media (1 % potassium acetate, 0.05 % glucose, 2 % agar). Plates were incubated for approximately a week at room temperature and sporulation verified using a light microscope. Glusulase treatment (15 μL of glusulase added to a loopful of tetrads suspended in H_2O, incubated 15 minutes at RT) was used to isolate spores which were then plated on WO plates with the addition of the strain-specific supplements. Following growth, approximately 150 colonies per strain were re-patched on fresh WO added with supplements. Colonies were then replica-plated onto ethanol-glycerol plates (1 % yeast extract, 2 % peptone, 2 % glycerol, 2 % ethanol) containing plated cells of rho^0 strains of the opposite mating types. Colonies capable of growing on non-fermentable carbon sources after mating with a MAT α rho^0 strain were selected, re-streaked and their genotype further verified.

2.4. Determination of Cell Viability

Cellular viability was assessed by the capability of the cells to form colonies. Cultures were started as described above and aliquots were taken at determinate time points (24, 48, 144 and 192 hours), serially diluted, plated on YPD media in triplicate and incubated 48 hours at 30°C. Afterwards, the number of colony-forming units (CFU) was determined by counting colonies and viability calculated as number of viable cells per millilitre of culture.

2.5 Determination of Yeast Replicative Lifespan

Yeast replicative lifespan analysis (RLS) was carried out as described by Steffen et al., (2009). RLS defines the number of times a cell can replicate during its lifetime. Growth of the yeast cultures started from aliquots stored at -80 °C by plating on YPD agar (2 % Glucose, 2 % Peptone, 1 % Yeast Extract, 2 % Agar) and incubated at 30 ºC for 48 hours. Single colonies were then used to re-patch strains on fresh YPD agar plates, which were incubated overnight at 30 ºC. The following day, for each strain, a light patch was streaked onto a new YPD plate and incubated overnight at RT. These plates were then used to carry out the RLS analysis.

Approximately 50 cells from each strain were selected and, among these, a minimum of 20 cells were arrayed vertically and incubated for approximately two hours at 30 ºC. Once each cell completed division, newly-formed virgin daughter cells were separated from the mother cells and the generation of the bud represents one replicative cycle. From this point forward, cells were incubated for intervals of time necessary to complete replication (approximately two hours for young cells, three or more hours for older cells) and the buds separated with the aid of a micro-dissecting needle and counted.

Strains were considered to have reached the end of their replicative lifespan when an individual cell did not complete division for four consecutive time points. The plates were kept at 4 °C overnight between successive days of RLS testing. A non-parametric, Wilcoxon Rank-Sum test was performed to determine whether or not the differences in lifespan among the strains were significant. A wild-type strain was included in each experiment as a reference.

2.6 Determination of Yeast Budding Index

The budding index of the strains used in this study was determined as the percentage of cells presenting with a bud at 24, 48, 144 and 192 hours of incubations in YPD media. A minimum of 600 cells were counted at each time point for each strain. Visual observation of the cells was performed with the use of a microscope (100x magnification) connected to a camera and the images used for counting purposes.

2.7 Analysis of DNA Content with Fluorescence-Activated Cell Sorting

To analyze cell cycle progression of wild-type and mitochondrial mutant cells, standard approaches require synchronization. For these experiments, MAT a strains were used and synchronized by treatment with 10 μg/mL α-factor for approximately 3 hours, which causes cells to arrest in G1 phase and to acquire the typical "schmoo" morphology. Synchronized cells were washed twice with pre-warmed YPD media and centrifuged at 4,000 x g for 5 minutes at RT to remove the extra α-factor. $5*10^6$ cells/mL were released by re-suspension into pre-warmed medium and incubated at 30ºC and 230 rpm. When diluted in fresh medium, cells will re-enter the cell cycle in a synchronous fashion. To monitor progression through the cell cycle, 1 mL aliquots were taken from synchronous cultures every 20 minutes until up to 140 minutes (2 hours and 20 minutes) past release. At the end of each time point cells were spun down at 14,000 x g for a few seconds, washed with 1 mL dH_2O and fixed by re-suspension in 1 mL of absolute ethanol. Fixed cells were stored at 4 ºC. After fixation, approximately $5*10^6$ cells were spun for 30 seconds at 16,000 x g, re-suspended in 500 μL of dH_2O and spun down once more. Samples were then re-suspended in 500 μL of 50 mM Tris-HCl pH 8.0, treated with DNase-free RNase A (80 μg/mL) and incubated at 37 ºC for three hours. Following RNase treatment, samples were spun under the conditions described above and re-suspended in 500 μL of 50 mM Tris-HCl pH 7.5. Proteinase K was added to each sample (0.25 mg/mL) and incubated for one hour at 50 ºC. Finally, cells were spun down and re-suspended in 100 μL 200 mM Tris-HCl pH 7.5, 200 mM NaCl, 78 mM $MgCl_2$. SYTOX Green stain was then added to a final concentration of 1 mM. Prior to loading onto a BD FACSAria Fusion flow cytometer, cells were briefly sonicated. The fluorescence of 20,000 cells was measured and data analyzed with a FACSDiva 8.0.1 software. An unstained sample was used as a negative control.

Cell fixation and subsequent preparation for flow cytometric analysis of asynchronous cultures was carried out as described by Zhang & Siede, (2004). Briefly, overnight cultures were started and normalized to OD_{600} = 1 the following day. Aliquots (approximately $1*10^7$ cells approximately) were taken at 24 and 192 hours after normalization, respectively. Cells were centrifuged at 14,000 x g five seconds, re-suspended in dH_2O and centrifuged once more. Pellets were re-suspended in the remaining traces of water by vortexing and fixed by adding 1 mL of absolute ethanol to the re-suspended yeast cells. Once fixed, samples were stored at 4

ºC. Prior to flow cytometry, cells were re-suspended, centrifuged at 14,000 x g for a few seconds, washed with dH_2O and pelleted once again.

At this point, cells were re-suspended in 50 mM Sodium citrate and treated with a DNase-free RNase A (80 µg/mL) for 1 hour at 50 ºC. This step was followed by another hour of incubation at 50 ºC after addition of Proteinase K (0.25 mg/mL). Afterwards, 1 mL of Propidium Iodide (PI, 16 µg/mL in 50 mM sodium citrate pH 7.0) was added to each cell suspension. Lastly, cells were briefly vortexed and the fluorescence of 20,000 cells measured with a BD FACSAria Fusion flow cytometer. An unstained sample served as a negative control. Raw data were processed using the FACSDiva 8.0.1 software.

2.8 Preparation of Cell Extracts

Crude protein extracts were generated from yeast cultures grown overnight and subsequently normalized to OD_{600} = 0.1 in 100 mL of YPD media. For each strain, 45 mL aliquots were taken after 24 and 192 hours incubation, respectively. Cells were harvested by centrifugation at 4,500 x g for 10 min at 4ºC, re-suspended in 20 mL of dH_2O and centrifuged again under the same conditions. The supernatant was discarded and cells were re-suspended in 10 mL of 1.2 M Sorbitol. Following another centrifugation at 4,500 x g, cell wet weight was determined and cell walls digested through the addition of 3 mL per gram of pellet of a buffer containing Zymolyase 20T (1.2 M Sorbitol, 75 mM Na_2HPO_4/NaH_2PO_4, pH 7.5, 1 mM EDTA, 1 % (v/v) 2-mercaptoethanol, 9.9 Units/mL of Zymolyase). The wild-type strain was incubated at 30ºC for 2h and 40 minutes while 2 hours was sufficient to obtain spheroplasts from mutant strains. Spheroplasts were then harvested by centrifugation at 4,500 x g for 5 minutes, washed twice with 1.2 M Sorbitol and re-suspended in a 2-fold volume of STE Buffer (0.5 M Sorbitol, 20mM Tris-HCl pH 7.5, 0.5 mM EDTA pH 8.0). A protease inhibitor cocktail was added to the suspension prior to manual homogenization with a Dounce homogenizer kept on ice. Cell homogenates were then spun at 7,000 x g for 10 min and the supernatants saved and stored at -80 ºC for further analysis. Protein determination was carried out according to Lowry et al., (1951).

2.9 Isolation of Mitochondria

Mitochondria from cells at late exponential phase and stationary phase of growth were isolated as described previously (Banting & Glerum, 2006).

Briefly, overnight yeast cultures were prepared and normalized to an OD_{600} = 0.1 in 800 mL of YPD media the following day. Cells were harvested by centrifugation after 24 and 192 hours incubation at 30 ºC and 230 rpm shaking. After washing step with dH_2O and 1.2 M Sorbitol, wet weights of pellets were determined and 3 mL per gram of pellet of digestion buffer containing Zymolyase 20T (1.2 M Sorbitol, 75 mM Na_2HPO_4/NaH_2PO_4, pH 7.5, 1 mM EDTA, 1 % (v/v) 2-mercaptoethanol, 9.9 Units/mL of Zymolyase) added to the cells. Cells were incubated in digestion buffer as for cell extracts described above. The resulting spheroplasts were harvested by centrifugation, washed with 1.2 M Sorbitol and re-suspended in STE buffer. A Waring® blender was used to generate a cell homogenate that was subsequently spun down twice at low speed (1,500 x g for 10 minutes at 4 ºC). The supernatant from each centrifugation was saved and later centrifuged at 17,000 x g for 15 minutes at 4 ºC to isolate mitochondria. An aliquot of the post-mitochondrial supernatant (PMS) fraction was saved for further analysis. The mitochondrial pellet was then re-suspended in STE and centrifuged at 20,000 x g for 15 minutes at 4 ºC. The washing step was repeated once more prior to re-suspension of mitochondria in 200 µL of STE buffer. Phenylmethane sulfonyl fluoride (PMSF, 1 mM) was added to inhibit protease activity.

2.10 SDS-PAGE and Western Blotting

Protein extracts were separated by electrophoresis through SDS-polyacrylamide gels. Prior to electrophoresis, proteins were mixed with an appropriate amount of 4 x loading buffer (200 mM Tris-HCl, pH 6.8, 4 % SDS, 40 % Glycerol, 4 % β-Mercaptoethanol, 0.4 % Bromophenol blue). When blotting for small, hydrophobic proteins such as certain COX subunits, protein samples were not boiled to prevent aggregation; otherwise, samples were boiled at 95 °C for five minutes prior to loading. For the experiments presented here, 5 or 6 % polyacrylamide stacking gels and 6, 7, 10, or 12 % separating gels were used, depending on the molecular weight of the proteins of interest. Electrophoresis was generally carried out for one hour at 150 V. Following SDS-PAGE, proteins were transferred onto a nitrocellulose

membrane. PVDF was the membrane used when transferring larger proteins. Transfer of proteins from gel to the membrane was carried out at 100 V for 30 minutes in a cooled unit filled with transfer buffer (192 mM Glycine, 25 mM Tris, 20 % Methanol with the addition of 0.05 % SDS when the size of proteins of interest was over 100 kDa). Equal loading and transfer efficiency was determined by staining with Ponceau S (0.2 % Ponceau S, 3 % TCA, 3 % Sulfosalicylic acid). Membranes were incubated for an hour at RT in blocking solution first and for another hour with a primary antibody appropriately diluted in blocking solution (10 mM Tris – HCl, pH 8.0, 1 mM EDTA, 150 mM NaCl, 0.1 % Triton X-100, 1.5 % milk). TEN-T buffer (10 mM Tris – HCl, pH 8.0, 1 mM EDTA, 100 mM NaCl, 0.1 % Tween 20, 1.5 % milk) was used as blocking solution when blotting for Mcm2, while a TBS-T buffer (20 mM Tris, 150 mM NaCl, 0.1 % Tween 20, 4 % milk, pH 7.6) was used for Western blotting of Rad53. In between primary and secondary antibodies incubations, membranes were washed three times for 10 minutes at RT with blocking solution without milk. Incubation with a secondary antibody conjugated to horse radish peroxidase was carried out under the same conditions used for the primary and was followed by another three washing steps. 500 µL of Clarity ECL substrate were spread over the membrane surface and chemiluminescence detected using a ChemiDoc MP system. Raw images were processed using BIO-RAD “Image Lab 5.2” software. Densitometric analysis was performed using ImageJ 1.50i software. A list of the antibodies used and the respective dilutions are reported below.

Table 2.2 List of the antibodies used in this study and their respective dilution factors.

Primary	Dilution	Source	Secondary	Dilution	Source
α-Cox17	1:200 (mito); 1:500 (WCL)	Glerum Lab	α-Rabbit IgG	1:10,000	Abcam
α-Aco1	1:1,000	Bulteau Lab	α-Rabbit IgG	1:10,000	Abcam
α-Act1	1:10,000	Thermo Fisher	α-Rabbit IgG	1:25,000	Abcam
α-Cox11	1: 1,000	Glerum Lab	α-Rabbit IgG	1:10,000	Abcam
α-Cox4	1: 1,000	Sigma-Aldrich	α-Mouse IgG	1:5,000	Thermo Fisher
α-Mcm2	1: 500	Santa Cruz	α-Goat IgG	1:5,000	Promega
α-Por1	1:10,000	Molecular Probes	α-Mouse IgG	1:10,000	Thermo Fisher
α-Rad53	1: 1,000	Abcam	α-Rabbit IgG	1:10,000	Abcam
α-Sco1	1: 500	Glerum Lab	α-Rabbit IgG	1:10,000	Abcam
α-Sod1	1: 500	Online Antibodies	α-Rabbit IgG	1:10,000	Abcam

N.B. Mito = mitochondrial isolations, WCL = whole cell lysates

2.11 Phosphatidyl Serine Externalization Assay

Externalization of phosphatidylserine (PS) on the outer leaflet of the plasma membrane is one of the early hallmarks of apoptosis. A commonly used method to detect apoptosis consists of staining cells with Annexin V-FITC, which specifically binds to PS.

In this study, yeast cultures were grown for 24 and 192 hours. At each time point, cultures were normalized to $1*10^7$ cells/mL in YPD for late exponential phase and PBS for stationary phase cells and incubated in the presence of 3 mM hydrogen peroxide for exponential phase

cells or 90 mM in the case of stationary phase cultures. Incubation in the presence of peroxide was used to induce the apoptotic response in cells. After peroxide treatment, cells were harvested by centrifugation, re-suspended in wash buffer (1.2 M Sorbitol, 0.1 M potassium phosphate pH 6.5 1 % β-Mercaptoethanol) and treated with Zymolyase 20T (46.1 mg/mL) for 10 minutes at 30°C and 150 rpm. For stationary phase cultures, cell wall digestion required a longer incubation (20 minutes). Spheroplasts were harvested by centrifugation, washed in wash buffer without β-Mercaptoethanol, re-suspended and diluted in binding buffer (10 mM Hepes-NaOH, pH 7.4, 140 mM NaCl, 2.5 mM $CaCl_2$, 1.2 M sorbitol) to obtain $1*10^6$ cells/mL. Staining was performed with Annexin V-FITC/PI using a commercially available kit (Biotool, Houston, TX, USA). PI staining was included as a way to assess the integrity of the cells. Each run included an unstained sample (negative control), samples stained with either only FICT or only PI (positive controls) and double stained samples. The fluorescence intensity of at least 30,000 cells was analyzed using a BD FACSAria Fusion flow cytometer. Data were analyzed using the FACSDiva 8.0.1 software. Analysis of unstained samples revealed a significant presence of background fluorescence, which was particularly pronounced in the wild-type strain. For this reason, sets of samples from each strain were run with an unstained control specific for that strain.

2.12 LacZ Assay

LacZ assays were used to determine whether the promoters of several COX assembly factors genes were sensitive to hydrogen peroxide. This method quantitates LacZ expression in constructs containing the promoter region of the genes *COX17*, *SCO1* and *COX11*. LacZ expression was quantified spectrophotometrically following incubation with the substrate ortho-Nitrophenyl-β-galactoside (ONPG).

Overnight cultures were incubated in YPD at 30 ºC and 230 rpm. The following day, cultures were normalized to an OD_{600} = 0.1 and treated with different concentrations of hydrogen peroxide (0 mM, 0.02 mM, 0.2 mM, 0.5mM) for two hours at 30 ºC and 230 rpm. Afterwards, the samples were centrifuged at 2,500 rpm for 10 minutes, re-suspended in 10 mL of Z-Buffer (60 mM Na_2HPO_4, 40 mM NaH_2PO_4 * H_2O, 10 mM KCl, 1.0 mM Mg_2SO_4 * 7 H_2O, 0.27 % β-mercaptoethanol) and centrifuged once more. Cells were re-suspended in 1 mL of Z-Buffer in glass tubes and lysed by the addition of three drops of chloroform and two drops of 0.1 % SDS.

ONPG substrate was added (0.2 mL of a 4 mg/mL stock solution) and samples were incubated for 5 minutes at 37 ºC. The reaction stopped by adding sodium carbonate (100 mg/mL). Absorbance at 420 nm was measured and LacZ expression quantified. The absorbance of a W303plNEG strain was subtracted from those of the strains containing the plasmid with the promoter regions of the genes *COX17, SCO1* and *COX11* to eliminate any background expression as the plasmid of W303plNEG contains only the LacZ gene but no upstream promoters. A plasmid loss assay was also performed to determine the percentage of cells that retained the plasmid. This data was then accounted for when calculating LacZ expression.

2.13 Yeast Spot Assay

Standard spot assay were used to assess sensitivity of cells to hydroxyurea (HU). Yeast cultures were grown overnight in YPD and normalized to OD_{600} = 1 in sterile water the following day. For each strain, serial dilutions were prepared (10^0 - 10^{-5}) and 5 µL of each dilution were spotted on YPD and YPD containing 240 mM hydroxyurea plates. Once dry, plates were incubated for six days at 30 °C and growth scored.

2.14 Statistical Analyses

Error bars reported in figures indicate the standard error of the mean (S.E.M). To appreciate significance of the difference between the replicative lifespan of wild type and mitochondrial mutant strains (Figure 3.10), a non-parametric Wilcoxon Rank-Sum test was performed. Differences between experimental groups were significant for $p \leq 0.01$.

Where indicated, a one way ANOVA statistical analysis was performed to determine whether differences between the means of multiple data groups were significant ($p < 0.05$). To compare the means of individual groups further, a Games-Howell post hoc test was utilized. Differences were considered significant for $p < 0.05$.

Chapter 3

Results

3.1 Identifying a Role for Mitochondrial Cuproproteins in Peroxide Metabolism

Mutations affecting COX ancillary factors were historically thought to yield virtually identical respiration deficient phenotypes as a consequence of faulty COX assembly (Zee & Glerum, 2006). In the recent past, however, this common belief has been challenged by growing experimental evidence in support of the idea that assembly factors might be involved in secondary functions. A scenario in which activities of assembly factors are not exclusively limited to the ETC might lead to the identification of as-yet unknown phenotypes and link mutations in mitochondrial proteins with different cellular pathways.

As described previously, some studies have already linked COX assembly factors with novel functions. Cox11 and Sco1 have been associated with an uncharacterized role in redox metabolism, as shown by studies that demonstrated hydrogen peroxide hypersensitivity of yeast cells lacking these cuproproteins (Banting & Glerum, 2006; Veniamin et al., 2011). Cox17, another key player in the COX copper metalation pathway, was found to play a role in the maintenance of the mitochondrial inner membrane architecture by interacting with Mic60, a core component of the MICOS complex (Chojnacka et al., 2015). A yeast *cox17* knockout strain fails to clear concentrations of hydrogen peroxide in the micromolar range (Glerum lab, unpublished results). This finding suggested a potential role for Cox17 as a peroxide sensor. Given the hypersensitivity of cells lacking Sco1 or Cox11, it was hypothesized that these proteins might function as peroxidases. Alternatively, if not acting as peroxidases themselves, Sco1 and Cox11 might regulate the activity of other peroxidases.

As a first approach to determining whether these cuproproteins might respond to hydrogen peroxide, the existence of peroxide-responsive elements in the promoter region of the genes encoding these proteins was investigated. For this purpose, yeast strains transformed with plasmids containing the promoter regions of the genes *COX17*, *SCO1* and *COX11* fused with the LacZ gene were used. A W303plNEG was used as a negative control, as this strain

was transformed with a plasmid that contains the LacZ gene without an upstream promoter. The plasmids used for this experiment were prepared by Dr. Graham Banting and Andrea Pellegrino (University of Alberta).

As displayed in Figure 3.1, no relationship appears to exist between the expression of the proteins tested and exposure to hydrogen peroxide as none of the strains showed a significant change in target gene expression upon peroxide treatment. While expression levels did not seem related to changes in peroxide concentrations, they seemed to differ based on the strain. More specifically, expression levels from the COX17 promoter were consistently higher than for all other promoters. Because these experiments were conducted using cells grown to late exponential/early diauxic shift, we then wondered whether expression of Cox17 could vary based on the yeast growth phase.

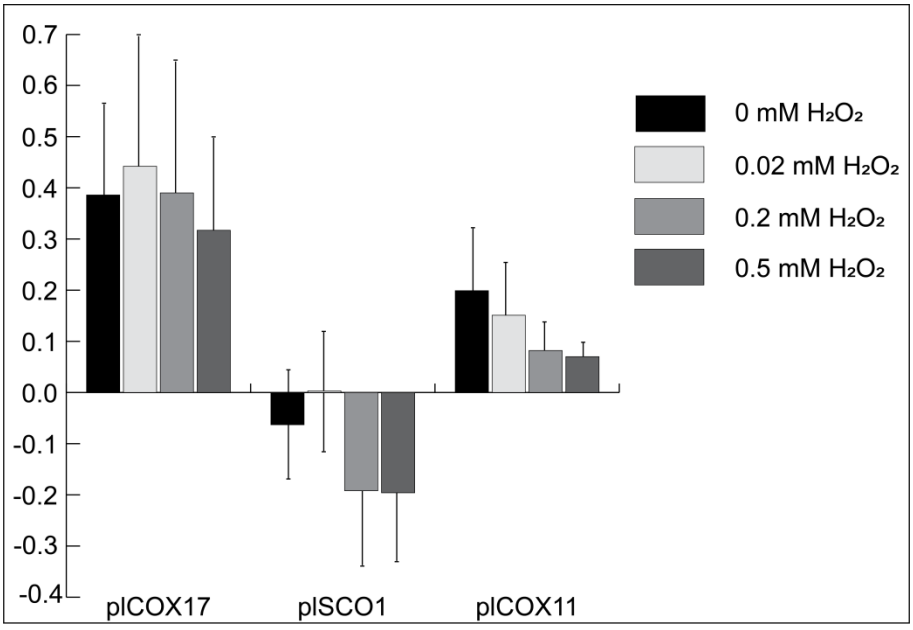

Figure 3.1 LacZ assay of *S. cerevisiae* W303plCOX17, W303plSCO1 and W303plCOX11. These strains have been transformed with plasmids that contain the promoter region of the genes *COX17*, *SCO1* and *COX11* respectively, fused with the LacZ gene. The W303plNEG (the plasmid does not contain upstream promoter) was used as a negative control and its absorbance values were used to normalize the absorbance values of the other strains. Absorbance values reported here account for plasmid loss. A_{420}, absorbance measured at 420 nm. Error bars indicate the standard error of the mean. Each assay was repeated at least twice for each hydrogen peroxide concentration. A one-way ANOVA, followed by Games-Howell post hoc test, failed to reveal significant differences (i.e. $p<0.05$) in LacZ expression levels after treatment with different peroxide concentrations (see Supplementary Table 1)

3.2 Mitochondrial Aberrations Cause Reduced Growth and Viability at Stationary Phase

Preliminary experiments aimed at identifying potential peroxide-responsive elements in the genes encoding Cox17, Sco1 and Cox11 revealed a higher expression of the reporter gene when associated with the promoter of COX17 than with the promoters of the other two genes. An initial step towards verifying this hypothesis consisted of estimating the growth kinetics of our strains and identifying the different growth phases, namely exponential phase, diauxic shift, post-diauxic shift and stationary phase. The viability of each strain was also determined at the different growth phases, allowing us to assess phenotypic variability among the mitochondrial mutants.

A variety of mitochondrial mutant strains was investigated, including null mutants for genes encoding the cuproproteins Cox17, Cox11 and Sco1, which are involved in COX copper metalation and are thereby necessary for the assembly of functional COX. Depletion of either Cox15 or Cox4 results in similar COX-deficient phenotypes, although these mutants are functionally different. Cells defective for the heme A synthase Cox15 are heme deficient and fail to assemble a functional COX. Cox4-deficient cells are also characterized by defective COX assembly, but the assembly failure is due to the lack of the structural subunit Cox4. Rho^0 cells, which lack mtDNA, cannot synthesize any of the three COX core subunits (Cox1, Cox2 and Cox3), or subunits of Complex III and the ATP synthase.

The optical density at 600 nm (OD_{600}) over a 192 hour period served as a measure of cell growth. Yeast strains were cultured in YPD media, which provides a fermentable carbon source (glucose), and allows the growth of respiratory deficient strains that would otherwise be incapable of growing if provided with non-fermentable carbon sources such as ethanol and glycerol.

As expected, a wild-type respiratory competent strain, W303, showed the most robust growth throughout the incubation period reaching the highest OD_{600} among the strains tested. The growth of all of the mutants was negatively impacted as shown by a lower OD_{600} in comparison to the wild-type strain (Figure 3.2). Interestingly, the *cox11* null mutant was characterized by having the lowest growth rate among all strains. Moreover, the growth curve for this strain shows a decline in the optical density from 24 to 192 hours incubation,

suggesting that cells lacking Cox11 might undergo cell death at a higher rate than the other mitochondrial mutants at stationary phase. The rho^0 strain and those lacking Sco1 or Cox4 grew to OD_{600} between 3 and 4, while a *cox17* null mutant reached a slightly higher value, between 4 and 5.

Other than allowing a comparison among the strains in terms of growth, these experiments also gave an estimation of growth kinetics. Within the first 24 hours of incubation, cells grew exponentially. Afterwards, yeast growth slows down and once all the non-fermentable carbon sources are depleted, cultures reach saturation. As seen in Figure 3.2, after exponential growth and the diauxic shift, yeast growth arrests or increases just minimally, with OD_{600} reaching a plateau. Generally, yeast cultures are believed to reach stationary phase after five to seven days of incubation. Given that our strains showed little to no change in optical density between 48, 144 and 192 hours of incubation, it was decided that eight days was an appropriate length of time for incubation.

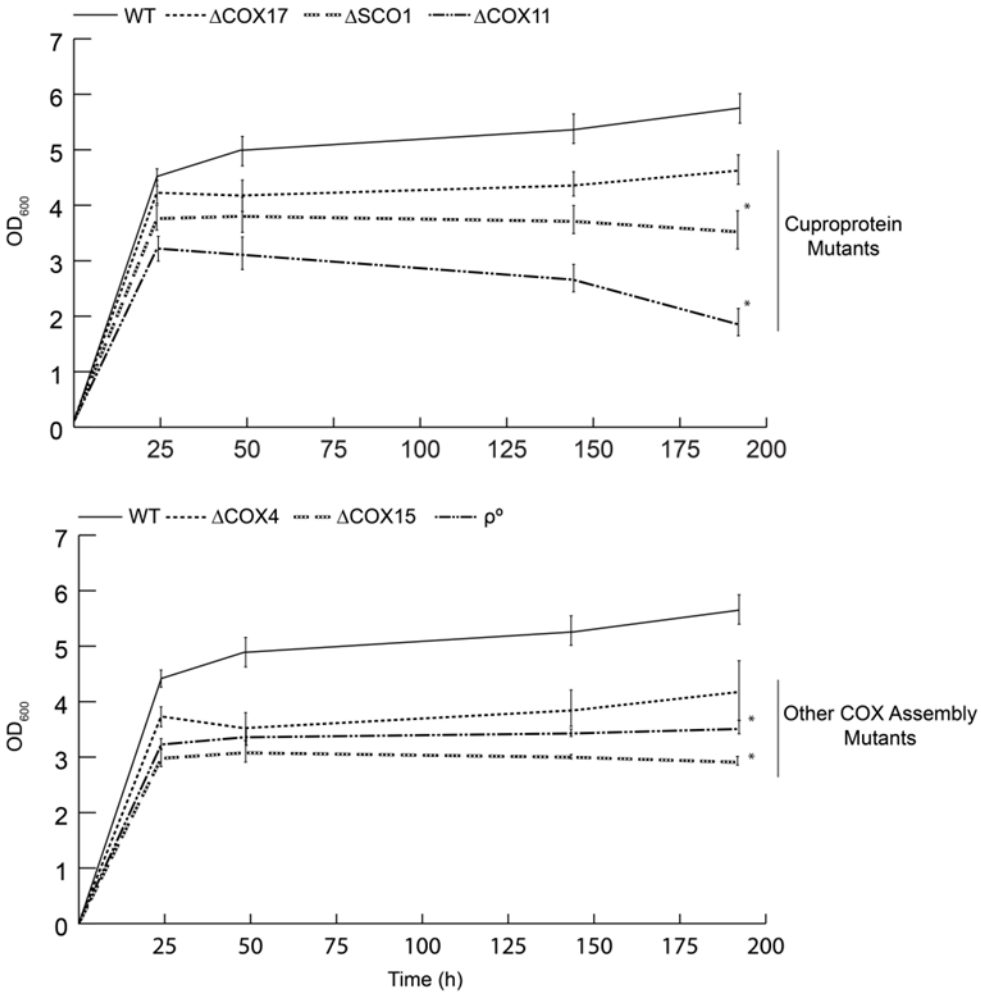

Figure 3.2 Growth curves of a wild-type W303 strain and selected mitochondrial mutants. Cells were grown in YPD media at 30 ºC for 192 hours. At t = 0 h, OD_{600} was normalized to 0.1 from overnight cultures. Growth curves were performed a minimum of three times for each strain. As expected, wild-type, respiratory competent cells could grow to higher density levels than respiratory deficient mutant strains. Among the mitochondrial mutant strains, a *cox11* null mutant was characterized by the lowest growth levels. Error bars indicate the standard error of the mean. Asterisks denote a statistically significant difference ($p < 0.05$: ΔSCO1 SP, 1.2E-03; ΔCOX11 SP, 2.0E-11; ΔCOX15 SP, 3.2E-08; ρ^0 SP, 3.6E-06) between the OD_{600} of wild type and mitochondrial mutant strains at 192 h incubation. Statistical significance was determined by performing a one-way ANOVA followed by Games-Howell post hoc test (see Supplementary Table 2).

To gain further insight into the cell physiology of the mutants, especially at stationary phase, the viability of the strains was determined at different time points. Cultures were prepared as described for growth curve experiments and viability was determined by serial dilution followed by plating on YPD and incubation for 48 hours at 30 °C. At a density of $30*10^6$

cells/mL, a wild-type strain was more viable than mutants defective for COX assembly factors (17-26*10^6 cells/mL) (Figure 3.3). Consistent with the lower growth state, a *cox11* null mutant was also the least viable strain, barely reaching 50 % of the wild-type viability levels at exponential phase. Surprisingly, the viability of mtDNA-less cells was found to be slightly higher than that of wild-type cells at 24 hours. The same rho^0 strain however, showed the most significant difference between the two phases of growth, with a 70 % reduction in viability levels from exponential to stationary phase. Viability of all of the other mitochondrial mutants tested also showed a more robust decrease at stationary phase than wild-type cells. While the lower viability of respiratory deficient cells at stationary phase could be predicted, the differences between some of the mutants were unexpected. Cox11, Sco1 and Cox17 are all proteins involved in copper delivery to COX. Nevertheless, the survival rates of these mutants were found to be different, with *cox17* and *sco1* mutants displaying viability levels corresponding to 30-40 % of those of the wild-type at stationary phase. In contrast, the survival rate of a *cox11* mutant was more than ten times lower than that of respiratory competent cells. Strains defective for Cox4 and Cox15 and mtDNA-less cells, on the other hand, displayed survival rates at stationary phase similar to that of the *cox17* and *sco1* knockout strains.

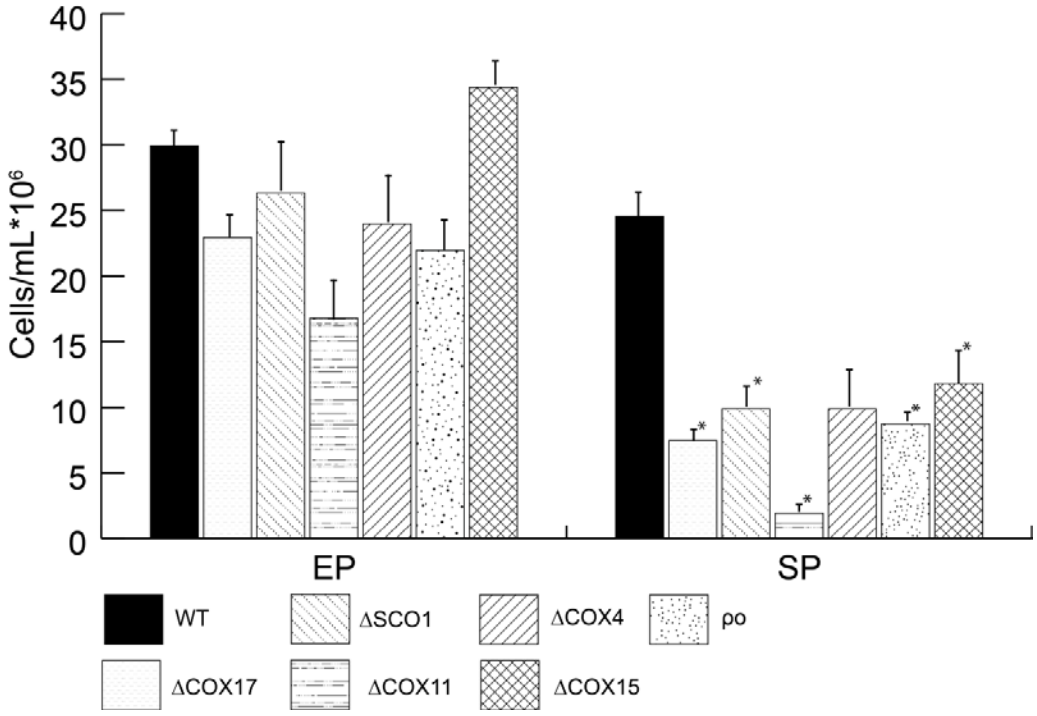

Figure 3.3 Viability of wild-type (WT) and mutant strains at late exponential (24 hours, EP) and stationary phases (192 hours, SP). Viability was determined in at least three biological replicates by serial dilution of cultures and plating on YPD media for 48 hours at 30 °C. Colony forming units (CFU) were counted and viability expressed as number of cells per mL. A minimum of 200 colonies were counted for yeast grown for 24 and 48 hours samples while 100 colonies were counted in plates inoculated with cultures after 144 and 192 hours of incubation. Error bars indicate standard error of the mean. Experiments were carried out in collaboration with Polina Myrox and Manisha Bhojwani. Asterisks denote a statistically significant difference ($p < 0.05$: ΔCOX17 SP, 2.3E-07; ΔSCO1 SP, 3.0E-04; ΔCOX11 SP, 5.0E-09; ΔCOX15 SP, 1.3E-06; ρ^0 SP, 5.0E-02) between viability levels of wild-type and mitochondrial mutants at a given time point. Statistical significance was determined by performing a one-way ANOVA followed by Games-Howell post hoc test (see Supplementary Table 3).

3.3 Protein Abundance at Different Phases of Growth

Results of initial experiments aimed at identifying peroxide-responsive elements in the promoter regions of *COX17*, *COX11* and *SCO1* genes suggested that expression of Cox17 was higher in cells grown to late exponential/early diauxic shift phases (Figure 3.1), leading us to ask whether Cox17 expression would increase over time through the various growth phases.

To test this hypothesis, yeast cells were grown in rich YPD media (2 % glucose, 2 % peptone, 1 % yeast extract) for eight days. Cells were harvested at different stages of growth and whole

cell lysates generated. Protein abundance was determined via Western Blotting and, as shown in Figure 3.4, the abundance of Cox17 increased at stationary phase of growth in respiratory competent, W303, wild-type cells. A densitometric analysis established that Cox17 abundance at stationary phase is almost double that at exponential phase. Superoxide dismutase 1 (Sod1) protein levels also increased at stationary phase, with a band intensity at stationary phase approximately 6-fold higher than at exponential phase in the wild-type strain and 2.5 times higher in the *cox17* mutant. However, increased Sod1 steady state protein levels at stationary phase were expected as this protein has shown to be essential for cell survival at stationary phase (Longo et al., 1996). As a loading control, Act1 levels showed no change in abundance at different phases.

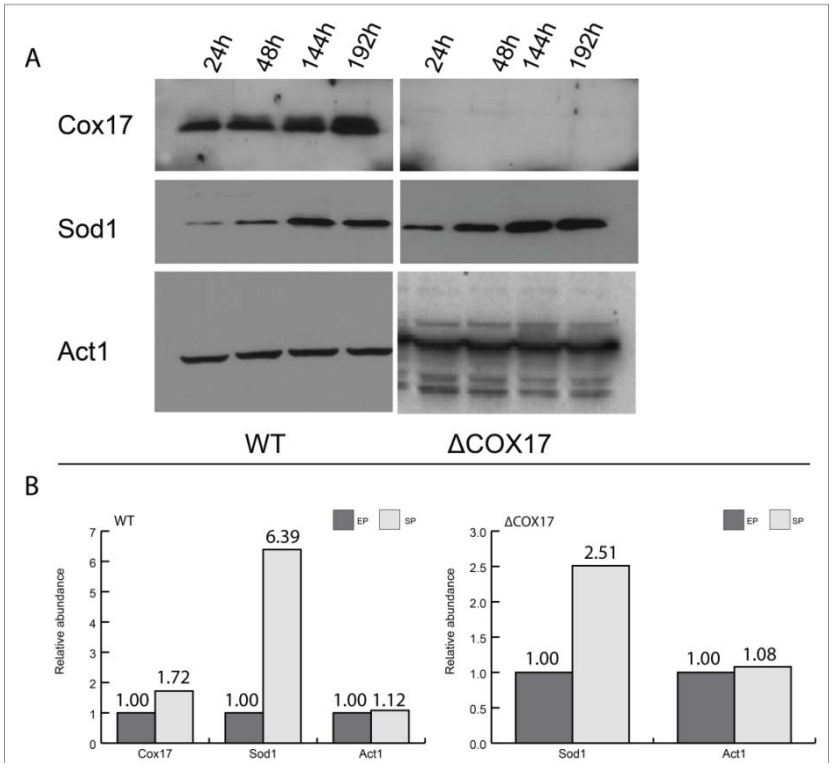

Figure 3.4 (A) Western Blot analysis of Cox17, Sod1 and Act1. Abundance of Cox17, Sod1 and Act1 at different phases of growth was assessed via Western Blotting of whole cell lysates generated from cells grown for 24, 48, 144 and 192 hours in YPD media. 15 µg of protein were loaded in each lane. (B) Comparative densitometric analysis of protein abundance in whole cell lysates generated from wild-type and *cox17* null mutant strains. The intensity of the cross-reacting band in stationary phase samples was normalized to the protein intensity of cell lysates obtained at exponential phase. EP, exponential phase (24 h); SP, stationary phase (192 h). The blots shown here are best representatives of three biological replicates.

Mitochondria are believed to play an important role in the survival of yeast cells at stationary phase. Therefore, an increased abundance of certain mitochondrial proteins at this stage of growth could be related to roles that such proteins might play in cell survival. Evidence that Cox17 steady-state levels in whole cell lysates increased at stationary phase led us to investigate how this protein is distributed between the cytoplasm and mitochondrial inner membrane space at different phases of yeast growth.

To observe the distribution of Cox17, as well as that of other mitochondrial proteins, at different time points, cell fractionation and Western blotting of mitochondria and post-mitochondrial supernatant fractions were performed. The strains used for these experiments were the *cox17* null mutant and the wild-type parent strain.

As shown in Figure 3.5-A, Cox17 abundance decreased in mitochondria at stationary phase while it slightly increased in the post-mitochondrial supernatant fraction. It would be tempting to speculate that increased cytosolic steady-state levels at stationary phase might be indicative of a secondary function of this protein at this phase of growth. Alternatively, increased cytosolic Cox17 steady-state levels at stationary phase might result from a re-distribution of the protein upon reduction of the disulfide bonds, as demonstrated by Bragoszewski et al., (2015). Mitochondrial fractions were also blotted to detect cuproproteins Cox11 and Sco1, along with Cox4. Steady-state levels of these proteins did not seem to change based on the yeast growth phase in wild-type cells, while they decreased in stationary phase *cox17* mutant cells (Figure 3.5-B). Porin, Por1, is commonly used as loading control when immunoblotting mitochondrial preparations. However, since Por1 levels declined in Cox17 deficient cells at 192 hours, as confirmed by densitometric analysis, Ponceau S general protein stain was used to ensure equal amounts of mitochondrial protein were loaded in each lane. A decrease in the abundance of the loading control, Por1, as well as of the other proteins tested in the mutant strain at stationary phase suggests that a generalized reduction of steady-state protein levels might be a consequence of other cellular processes such as mitophagy. Experiments aimed at investigating mitophagy were not performed in this study. Nevertheless, an analysis of steady-state protein levels of markers for autophagy, such as Atg8, would be a good starting point to evaluate the involvement of this cellular process to explain the low mitochondrial protein abundance in our respiratory mutants at stationary phase.

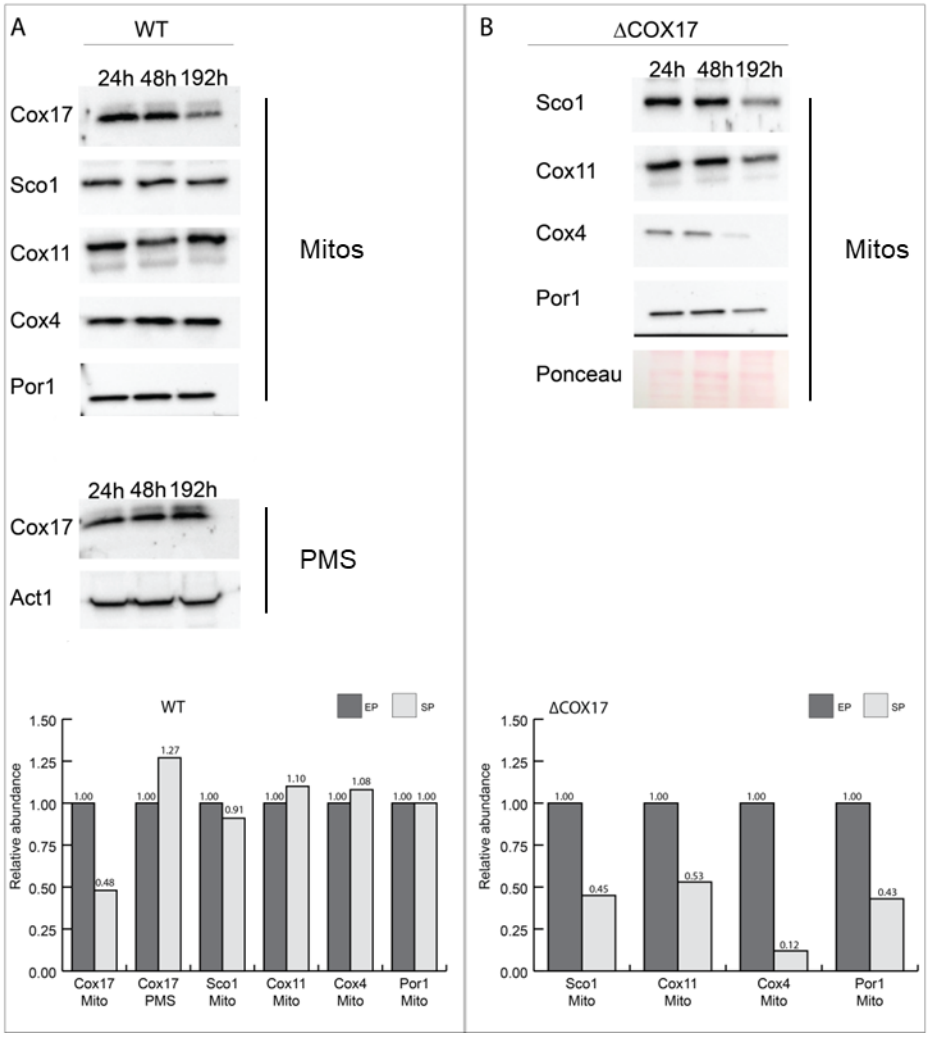

Figure 3.5 Western Blotting of mitochondrial fractions (Mitos) and post-mitochondrial supernatant fractions (PMS) to assess steady state levels of mitochondrial proteins at different growth phases in a wild-type (A) and *cox17* mutant strains (B). Antibodies specific for Cox17, Sco1, Cox11 and Por1 were used to determine abundance of these proteins in mitochondrial preparation of wild-type (WT) and *cox17* mutant cells. For blotting of mitochondrial proteins, 10 μg of protein were loaded in each lane while for western blotting of post-mitochondrial supernatant (PMS) 20 μg of protein were loaded. Because we found that the abundance of Por1, which is used as a marker for mitochondrial proteins, decreased in our respiration deficient mutant strain, we have included the Ponceau S general protein stain to show that equal amounts of mitochondrial protein have been loaded into each well of the gel. A comparative densitometric analysis of protein abundance in mitochondrial and post-mitochondrial fractions from wild-type and *cox17* null mutant strains was performed. The intensity of the cross-reacting band in stationary phase samples was normalized to the protein intensity of samples collected at exponential phase. EP, exponential phase (24 h); SP, stationary phase (192 h). The blots shown here are best representatives of three biological replicates.

3.4 COX Assembly Mutations Alter Budding Index at Stationary Phase

Visualization of cells with a phase-contrast microscope during growth curve experiments revealed that some respiratory deficient strains appeared to have a higher proportion of budded cells when compared to a respiratory competent strain at stationary phase of growth. This was surprising since synchronization in a non-budded state is considered to be a hallmark of stationary phase cells. Thus, budding indices of mitochondrial mutants and respiratory competent strains were determined to verify this initial observation. Cells were grown under the same conditions used to generate growth curves, in YPD media and starting at an OD_{600} = 0.1. Cells were applied to microscope slides and imaged with a phase-contrast microscope connected to a camera. Budding indices were determined as the percentage of budding cells of at least 600 cells per strain after 24, 48, 144 and 192 hours of incubation. As shown in Figure 3.6, all of the strains showed a decreasing budding index from late exponential phase (24 hours) to stationary phase (192 hours). At exponential phase, all strains had budding indices between 50 and 60 %, with the exception of the rho^0 strain, which had a budding index significantly lower, around 30 %. Once glucose becomes depleted in a culture, cells will switch to respiratory metabolism and then, once all sources of energy in the media are exhausted, cultures become saturated and enter stationary phase with OD_{600} values reaching a plateau. All of the mitochondrial mutants tested are respiratory deficient and therefore cannot grow if provided only with non-fermentable carbon sources. Under these circumstances, budding indices of mutant strains would be expected to be lower than that of a wild-type strain at stationary phase. Surprisingly, only the rho^0 strain was characterized by a budding index lower than that of the wild-type. At stationary phase, c*ox11* and *sco1* null mutants had budding indices at stationary phase very close to that of the wild-type, which was approximately 30 %. Budding indices of the other mutant strains were found to be higher than that of the wild-type, especially in the case of a *cox17* null mutant, which displayed a number of cells with buds at stationary phase accounting for approximately 50% of the number of cells counted. Budding indices of each strain at different growth phases are reported in Table 3.1. The strains with a high percentage of budding cells at stationary phase are all defective for COX activity and lack proteins that play independent roles in the assembly of the COX complex. Therefore, it seemed unlikely that the phenotypes observed could be linked to the

known functions of these proteins. Rather, anomalies in the budding indices suggested the possibility of cell cycle defects for these mutants. It is also clear from these results that strains lacking different COX assembly factors can display divergent phenotypes when assessed for functions seemingly unrelated to the mitochondrial respiratory chain.

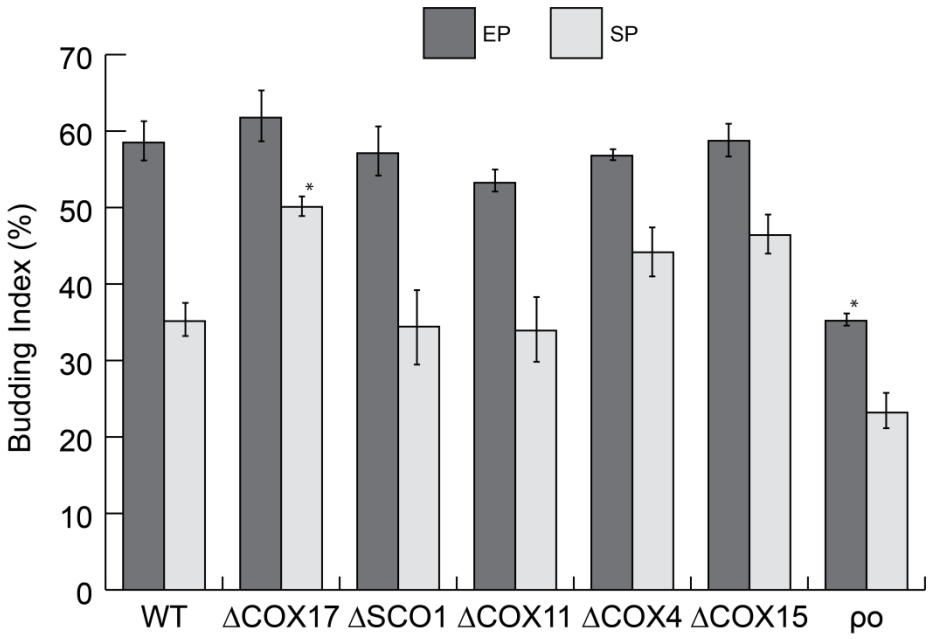

Figure 3.6 Budding indices of wild-type (WT) and mitochondrial mutants at late exponential and stationary phases. Budding indices were plotted based on the data reported in Table 3.1. EP, exponential phase measured after 24 hours incubation; SP, stationary phase, measured after 192 hours incubation. Error bars represent the standard error of the mean. Asterisks denote a statistically significant difference ($p < 0.05$: ΔCOX17, 7.6E-04; ρ^0, 4.0E-05) between the budding indices of wild-type and mitochondrial mutants at a given time point. Statistical significance was determined by performing a one-way ANOVA followed by Games-Howell post hoc test (see Supplementary Table 4). Determination of the budding index at different growth phases was performed at least three times for each strain.

Table 3.1 Budding Indices of wild-type and mitochondrial mutants at exponential (EP) and stationary phases (SP). Each budding index was calculated as the percentage of cells with buds after counting 600 cells for each strain per time point. Budding indices are the results of at least three biological replicates. p values indicate the significance at 0.05 level of the difference between the means of wild-type and each mitochondrial mutants at exponential and stationary phases. Significance levels were determined by a one-way ANOVA followed by Games-Howell post hoc test.

Strain	Growth Phase	Budding Index	p value
WT	EP	55 ± 3	
	SP	35 ± 2	
ΔCOX17	EP	62 ±3	0.921
	SP	50 ± 1	**0.001**
ΔSCO1	EP	57 ± 3	1.000
	SP	34 ± 5	1.000
ΔCOX11	EP	53± 1	0.997
	SP	34± 4	1.000
ΔCOX4	EP	57± 1	1.000
	SP	44± 3	0.558
ΔCOX15	EP	59 ± 2	0.996
	SP	46 ± 3	0.258
ρ^0	EP	35± 1	**3.953E-05**
	SP	23± 2	0.168

3.5 COX Assembly Defects Correlate with Accumulation of Cells at G2/M Phase in Non-Synchronous Cultures

To explore a connection between mutants with respiratory chain deficiencies and cell cycle defects, a flow cytometry-based approach was adopted. Non-synchronous cultures were analyzed to infer the proportion of cells with different DNA content at both late exponential and stationary phases. Culture aliquots taken at 24 and 192 hours were stained with propidium iodide (PI) and the fluorescence of 20,000 events assessed. As seen in Figure 3.7, most of the mitochondrial mutants displayed a higher proportion of cells in G2/M than that of the wild-type strain at both late exponential and stationary phases. The ratio between the “area under the curve” of the peak corresponding to cells at G1 and the “area under the curve” of the peak corresponding to cells at the G2/M phase was then calculated for each strain. High G1/G2 ratios correspond to cultures with higher numbers of cells in G1 rather than G2/M phase at harvesting.

As shown in Figure 3.8, at the late exponential phase of growth, rho^0 cells showed a G1/G2-M ratio between 4 and 5, the highest among all strains. This result is in accordance with a study that reported a G1-S transition defect in rho^0 cells (Crider et al., 2012). In contrast, the respiratory competent strain revealed a G1/G2 ratio of 3. In spite of the fact that the budding indices of all of the other mutants were similar to wild-type at exponential phase, their G1/G2 ratios were found to be approximately half of that of wild-type, indicating a significantly higher proportion of cells in G2/M phase.

When cultures reached stationary phase, analysis of DNA content showed that, as expected, G1/G2 ratios increased in all strains as nutrient depletion corresponds to growth arrest. However, the proportion of the increase seemed to vary depending on the strain. A c*ox11* null mutant displayed the biggest difference between the two phases of growth and *cox4* displayed the smallest. Rho^0 cells were once again characterized by having the highest number of cells in G1, with a G1/G2 ratio higher than 5. Strains that could not express *COX11*, *COX17*, *SCO1*, *COX4* and *COX15*, on the other hand, had ratios significantly lower than that of wild-type at stationary phase. Interestingly, as shown previously (Figure 3.6), *cox17*, *cox4* and *cox15* mutants were also the strains with the highest budding indices at 192 hours incubation. These results in part confirm observations made of budding indices and reinforce the hypothesis that mutations affecting COX assembly mutants have repercussions for cell cycle mechanisms.

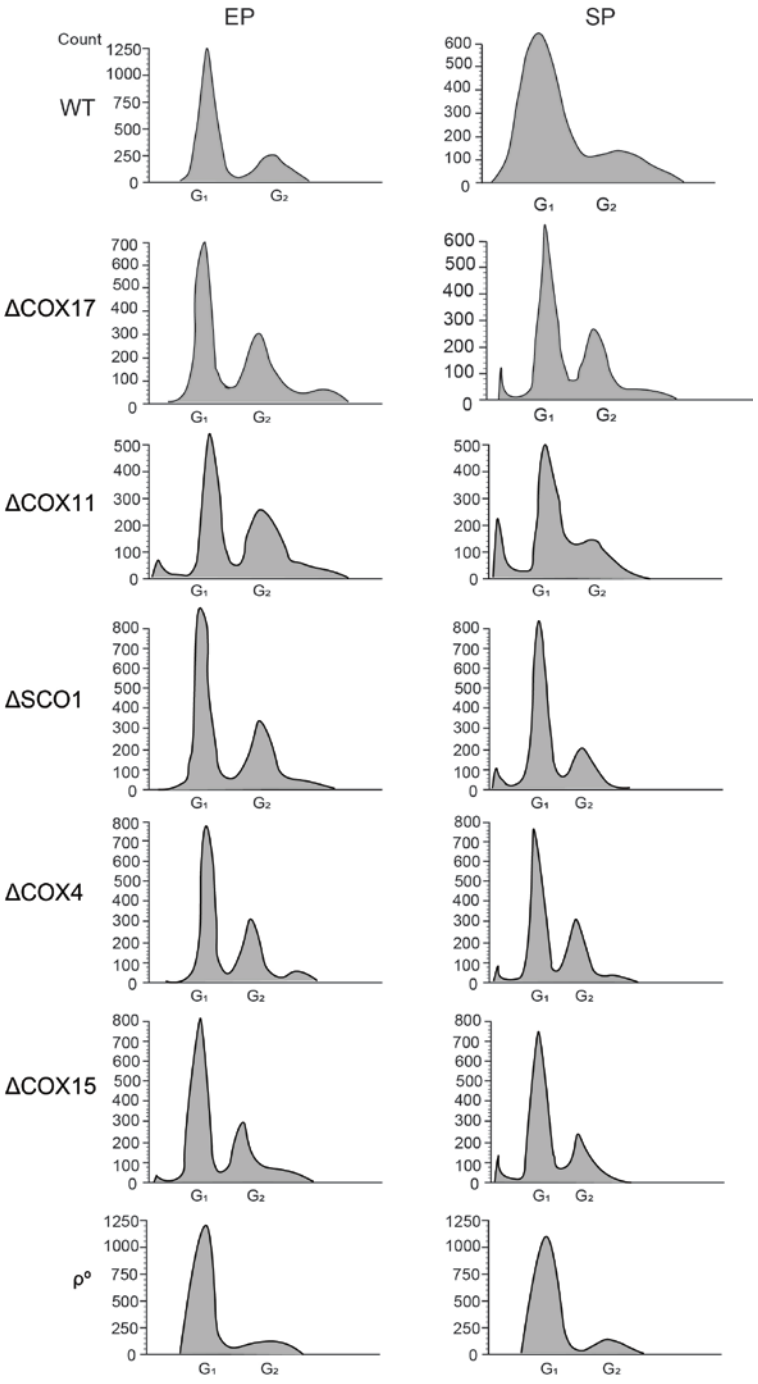

Figure 3.7 DNA content analysis of non-synchronous cultures grown in YPD and harvested at exponential (EP) and stationary (SP) phases. Fluorescence of 20,000 cells was analyzed and data analyzed with a FACSDiva 8.0.1 software. An unstained sample was used as a negative control. This figure is the best representative of experiments conducted at least three times for each strain.

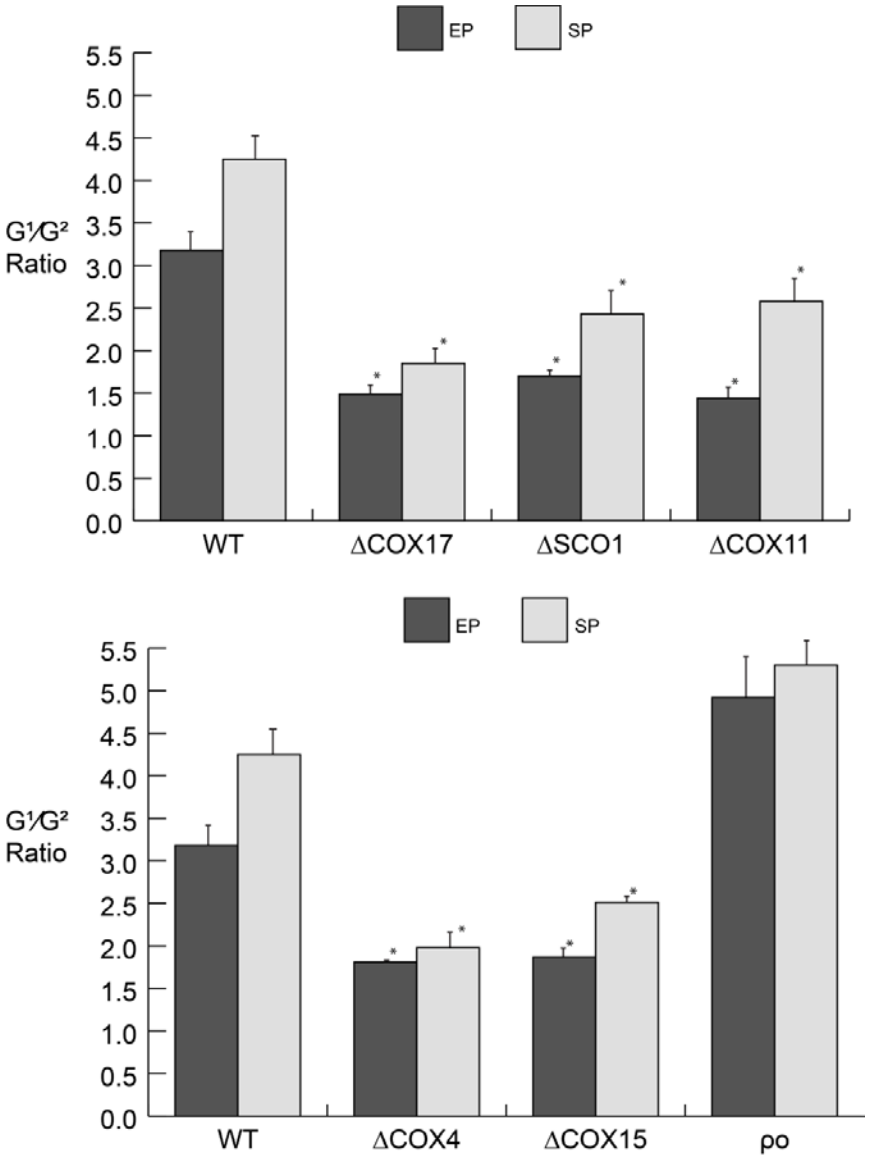

Figure 3.8 DNA content analysis of wild-type (WT) and mitochondrial mutants non-synchronous cultures. Cells were grown in YPD starting from an OD_{600} = 0.1 and incubated at 30 ºC for up to 192 hours. Aliquots were collected at 24 and 192 hours and processed for PI staining. Data was analyzed with FACSDiva 8.0.1 software. The area under the curve was calculated for each fluorescence peak and the ratio between G1/G2 peaks calculated. Error bars indicate the standard error of the mean. EP, Exponential phase; SP, stationary phase. Asterisks denote a statistically significant difference ($p < 0.05$: ΔCOX17 EP, 3.2E-03; ΔCOX17 SP, 1.1E-03; ΔSCO1 EP, 8.0E-03; ΔSCO1 SP, 3.6E-02; ΔCOX11 EP, 1.0E-02; ΔCOX11 SP, 4.6E-02; ΔCOX4 EP, 1.4E-02; ΔCOX4 SP, 2.1E-03; ΔCOX15 EP, 1.4E-02; ΔCOX15 SP, 7.7E-03) between G1/G2 ratios of wild type and mitochondrial mutants at a given time point. Statistical significance was determined by performing a one-way ANOVA followed by Games-Howell post hoc test. Measurement of DNA content at different growth phases was performed at least three times for each strain (see Supplementary Table 5).

3.6 COX Assembly Defects Result in Divergent Cell-Cycle Aberrations

As previously mentioned, it has been shown that the lack of mtDNA triggers a checkpoint that blocks G1-S transition. It is also known that this cell cycle block is not caused by loss of mitochondrial function, but rather that it is specifically due to the lack of mtDNA (Crider et al., 2012).

The rho^0 strain used in this study displayed a lower budding index than any other strain and non-synchronous rho^0 cells revealed the highest G1/G2 ratio at exponential and stationary phases. However, other mitochondrial mutants were phenotypically different from rho^0 cells. This led us to hypothesize that other factors might be involved in the impacts on the cell cycle and that this response might be triggered only by certain mutations. A flow cytometry-based analysis of cell cycle progression using synchronous cultures was initiated. Cultures were synchronized at G1 phase by exposure to the mating hormone α-factor and subsequently released by re-suspension in fresh media. Aliquots were taken every 20 minutes for up to 140 minutes and analyzed by fluorescent activated cell sorting (FACS) using SYTOX Green. The choice of a fluorophore, other than PI, was driven by the higher accuracy and reproducibility that is provided by SYTOX Green.

As depicted in Figure 3.9, a rho^0 strain shows almost no G2/M cells, when compared to the wild-type, at 80 minutes after release, further confirming the mtDNA-dependent cell cycle defect. *cox4* and *cox15* null mutants display a DNA content as a function of time very similar to that of wild-type, consolidating the hypothesis that loss of mitochondrial function per se does not trigger a checkpoint response, as both mutants are characterized by a complete lack of COX activity (Banting & Glerum, 2006; Glerum et al., 1996a). While loss of COX activity in the mutants was described already, activity assays performed by other members of the lab confirmed the lack of COX activity in these strains. In contrast with *cox4* and *cox15* mutants, strains lacking the cuproproteins Cox17, Sco1 and Cox11 displayed DNA content distributions over time that more closely resembled that of rho^0 cells rather than wild-type cells or *cox15* and *cox4* mutants.

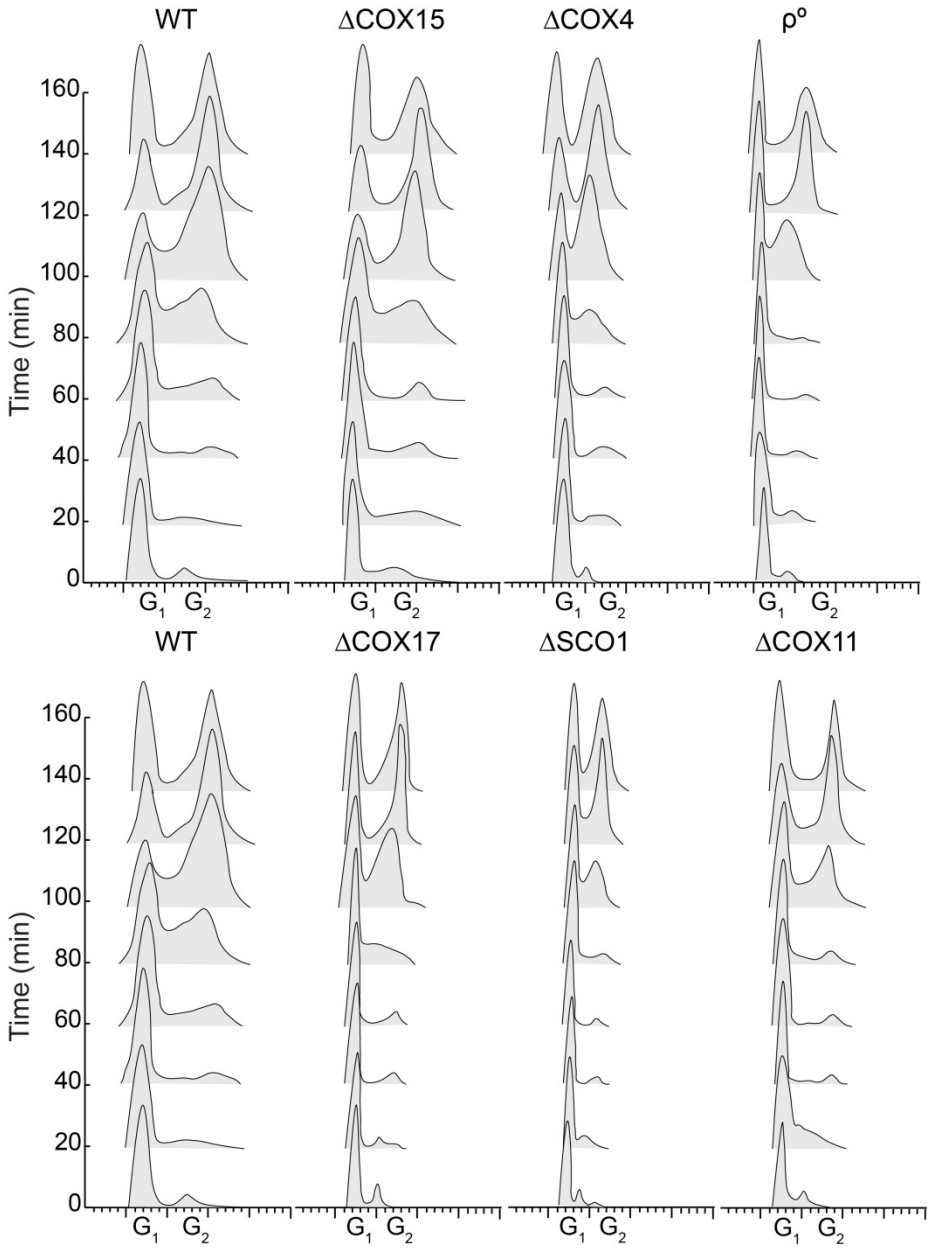

Figure 3.9 Analysis of DNA content of wild-type (WT) and mitochondrial mutant strains. Cells were synchronized with α-factor and incubated in YPD for three hours at 30 ºC. Release in fresh YPD media represented the start of cell cycle progression (t = 0 min). Samples were collected every 20 minutes up to 140 minutes. Cells were fixed and later prepared for staining with SYTOX Green followed by flow cytometry to determine DNA content. At least three replicates of each strain were performed.

3.7 Yeast Replicative Lifespan Is Not Affected by Respiratory Deficiency

At first glance, the experimental data reported above might seem contradictory. In fact, DNA content of cells in non-synchronous cultures indicated that some mitochondrial mutants had significantly lower G1/G2 ratios than wild-type. This finding was supported by the budding index of some mutants being higher than wild-type at stationary phase. On the basis of these results, it would be tempting to speculate that some mitochondrial mutants are still capable of undergoing cell division after 192 hours incubation. On the other hand, it should to be noted that a respiratory competent strain still reaches the highest OD_{600} throughout the whole growth period and that it is characterized by higher viability than all of the mitochondrial mutants tested at stationary phase.

Taken together, these show a situation in which, as one would expect, wild-type cells grow more and are more viable than respiratory deficient cells; at the same time, however, certain mitochondrial mutations appear to yield cells with a budding index higher than wild-type and populations with a higher proportion of cells having DNA content typical of G2/M phase.

To determine whether respiratory deficient cells possess a higher replicative capability than wild-type cells, which could explain the anomalous budding indices of the mutants, the replicative lifespan (RLS) of wild-type and mitochondrial mutants was examined. RLS is a measure of how many times a cell can divide prior to becoming senescent, and differs from the chronological life span (CLS), which is a measure of how long a cell can survive before death. RLS was determined by following a well-established protocol (Steffen et al., 2009). Cells were grown on YPD agar plates, virgin cells isolated and incubated for the time necessary to complete one division. Newly formed buds were counted, removed from mother cells and the process repeated until cells could no longer divide.

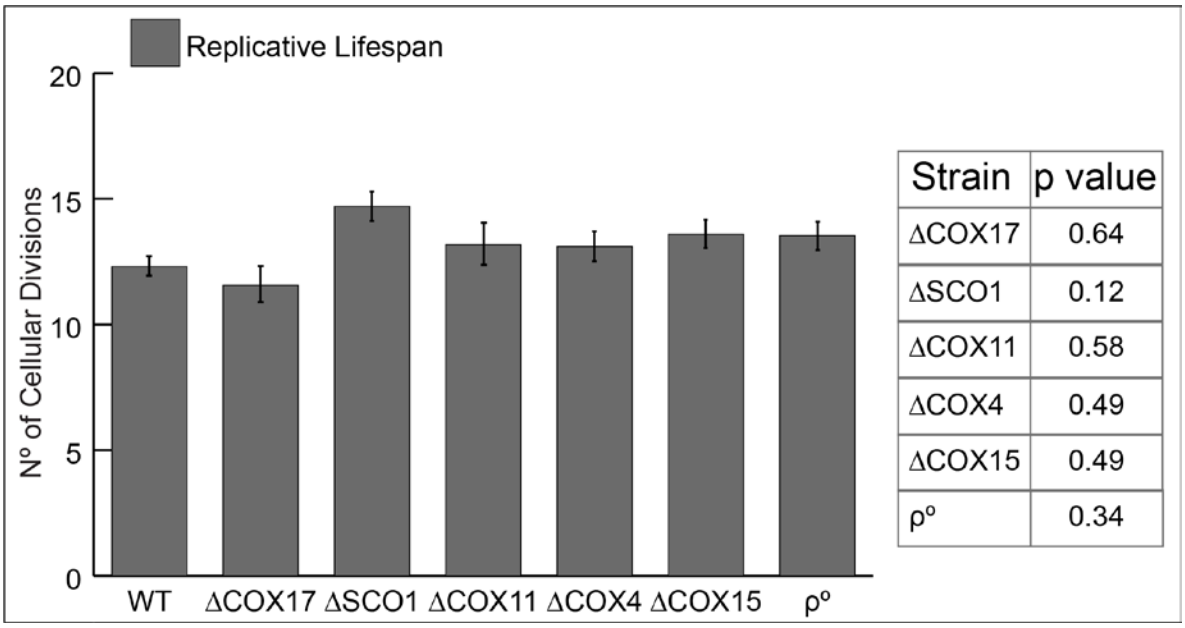

Strain	p value
ΔCOX17	0.64
ΔSCO1	0.12
ΔCOX11	0.58
ΔCOX4	0.49
ΔCOX15	0.49
ρ°	0.34

Figure 3.10 Replicative lifespan of wild-type and mitochondrial mutant cells. Yeast strains were retrieved from frozen aliquots (stored at -80 °C) prior to each experiment, grown on YPD for two days at 30°C, re-patched on fresh YPD plates and grown overnight at 30°C. Finally, cells were lightly patched onto fresh YPD plates and incubated overnight at room temperature. The following day, virgin cells were isolated from the patches and incubated for the time required to complete one division. Daughter cells were counted and removed from mother cells and the process repeated until all cells stopped dividing. Plates were sealed and stored at 4ºC overnight. For each strain, 20-25 cells were selected to carry out the assay. Error bars represent standard error of the mean. To determine whether differences between experimental groups were significant ($p \leq 0.01$), a non-parametric Wilcoxon Rank-Sum test was performed. RLS of each strain was determined a minimum of three times for each strain.

As shown in Figure 3.10, no significant differences in RLS between wild-type and mitochondrial mutants were found. These results seem to exclude reproductive capability as a factor in determining the unexpected phenotypes described for a subset of the mutants.

Western blotting of whole cell lysates to assess Mcm2 steady-state protein levels was performed to verify further whether mitochondrial mutants still undergo cell replication in stationary phase cultures. Mcm2 is a component of the Mcm2-7 hexameric helicase complex, and it is consitutively expressed in cells that are replicating their genomic material (Young & Tye, 1997). As shown in Figure 3.11, Mcm2 steady-state levels do not appear to change in the wild-type strain from exponential to stationary phases. On the other hand, Mcm2 abundance was below detection limits at stationary phase in all of the mitochondrial mutants and because

this protein is necessary for DNA replication, it seems unlikely that the mutants could still undergo cell division at this stage of growth.

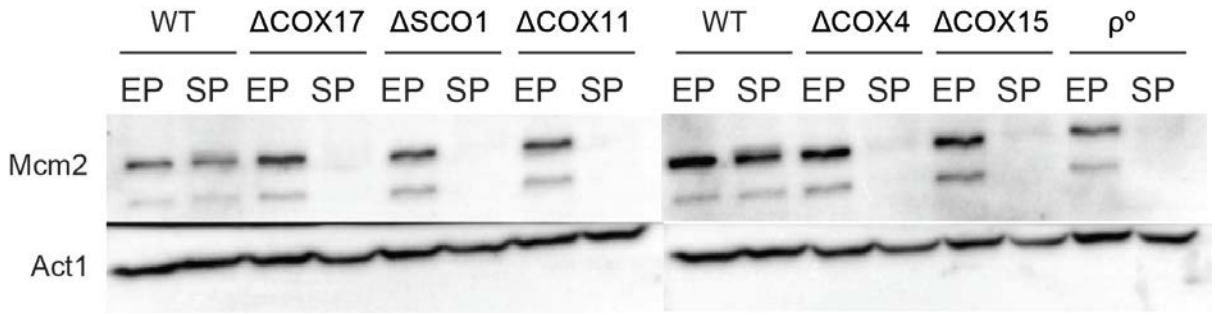

Figure 3.11 Western Blotting of whole cell lysates generated from cultures harvested at exponential and stationary phases were performed to assess Mcm2 steady state levels. Act1 steady-state levels were also determined and served as a loading control. 55µg of protein were loaded in each lane. EP, Exponential phase; SP, stationary phase.

As it appears that mutant cells are not different from the wild-type in terms of replicative ability, it is possible that high budding indices and low G1/G2 ratios of certain mutants at stationary phase could be a consequence of G2/M arrest. Cell cycle checkpoints have been investigated extensively from yeast model systems such as *S. cerevisiae* and *S. pombe* to humans. DNA damage occurring during cell replication generally results in the production of an intermediate composed of single-stranded DNA coated by a Replication Protein A (RPA). In *S. cerevisiae,* the kinase Rad53 is considered the main effector in response to DNA damage, which determines cell cycle arrest between metaphase and anaphase. Dun1, another protein kinase, is also activated in the response to DNA damage and is capable of mediating transcriptional responses that include the activation of the enzyme necessary for dNTP production, ribonucleotide reductase (Barnum & O'Connell, 2014). Another factor that plays a role in cell cycle checkpoint activation is cell size. In *S. cerevisiae*, a cell size control at the G1-S transition is well characterized. On the other hand, definitive proof of the existence of a similar checkpoint at the G2/M transition has not been obtained yet and conflicting theories exist (Turner et al., 2012).

The DNA content analysis of synchronized cells performed in this study revealed that strains lacking the cuproproteins involved in COX copper metalation are characterized by a delayed S phase, resembling the defect caused by treatment with hydrogen peroxide described by Shapira et al., 2004. In non-synchronous cultures, with the exception of the rho^0 strain, all of the

mitochondrial mutants showed a lower G1/G2 ratio than wild-type at late exponential and stationary phases, potentially resulting from a G-M arrest, which could be caused by increased oxidative stress due to the COX assembly defect. In contrast, a rho^0 strain was characterized by the highest G1/G2 ratio at late exponential and stationary phases and showed a delayed G1/S transition in synchronized cells. Accordingly, the budding index of this strain was the lowest among all strains at both phases of growth. The budding index of the COX assembly mutants, on the other hand, is similar to wild-type at late exponential phase. Once cultures reach stationary phase, a subset of the mutants, namely *cox17*, *cox15* and *cox4*, display a higher budding index than the wild-type, while *sco1* and *cox11* null mutants do not show any differences from the respiratory competent strain. A possible explanation for why only certain mitochondrial mutants show a delayed S phase could be that an oxidative stress threshold is reached earlier by cells defective for proteins involved in copper delivery to COX such as Cox17, Cox11 and Sco1. *cox4* and *cox15* null mutants, on the other end, might reach the threshold at a later time point as cultures approach stationary phase and their oxidative stress levels increase. It should be noted that according to this model, *cox11* and *sco1* mutants would also be expected to display budding indices higher than that of the wild-type, similar to the other COX assembly mutants. However, anomalous budding indices at stationary phases in *cox11* and *sco1* mutants were not observed in the experiment described in this study and possible explanations for this phenotype are further discussed below (Discussion, 4.2).

Western blotting to assess Rad53 steady-state protein levels in whole cell lysates prepared from cultures harvested at different growth phases was performed to observe any differences between mitochondrial mutants and the wild-type strain that could have been related to the cell cycle phenotypes described above. As seen in Figure 3.12, no changes in Rad53 steady-state protein levels were detected in the wild-type strain from exponential to stationary phase. Interestingly, Rad53 protein levels were below detection limits in all of the mitochondrial mutant strains at stationary phase while in exponentially growing cultures the abundance of this protein did not differ from that of the wild-type strain.

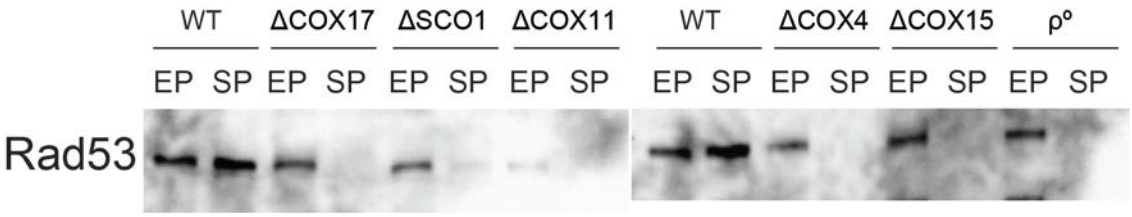

Figure 3.12 Abundance of Rad53 at different phases of growth (EP, Exponential phase; SP, stationary phase) was determined via Western blotting of whole cell lysates obtained from cultures grown in YPD and harvested at exponential and stationary phases. 55µg of protein were loaded in each lane.

3.8 Mitochondrial Defects Correlate with Increased Oxidative Stress

The mitochondrial electron transport chain is thought to be one of the main factors contributing to ROS generation within a cell. Accordingly, oxidative stress levels of cells carrying ETC-related defects are expected to be higher in comparison to respiratory competent cells. A specific role for COX in ROS production has not been identified yet, but COX deficiency has been associated with increased ROS levels in many instances. It has been hypothesized that in sequential systems, such as the electron transport chain, dysfunction of a single complex might influence ROS production at other ETC sites (Srinivasan & Avadhani, 2012).

In this study, several approaches were adopted to provide insights into a connection between the cell cycle defects described above and the physiological status of stationary phase cells. This was done by studying markers associated with oxidative stress levels in wild-type and respiratory deficient cells. ROS negatively impact a variety of cellular components and functions. For this reason, cells are equipped to counteract oxidative damage and defense mechanisms against ROS involve enzymes such as catalases, peroxidases and superoxide dismutase (Fridovich, 1999).

The enzyme superoxide dismutase converts superoxide (O_2^-), a known reactive oxygen species to hydrogen peroxide. Superoxide dismutase 1 (Sod1) localizes to both cytosol and the intermembrane space of mitochondria (Sturtz et al., 2001) and it is known to play a crucial role in the survival of cells at stationary phase (Longo et al., 1996).

The abundance of Sod1 in whole cell lysates from wild-type and mitochondrial mutant cells at late exponential and stationary phases was assayed. Cells were grown for 24 and 192 hours,

respectively, and processed to generate whole cell lysates that were used to detect the presence of the Sod1 protein via Western blotting and to determine its enzymatic activity.

As shown in Figure 3.13-A, a slight increase in the abundance of Sod1 from exponential to stationary phase was observed in whole cell lysates in wild-type cells. Sod1 steady-state protein levels in all the respiratory deficient strains, however, were lower than that of the wild-type at 24 hours, but increased strikingly at stationary phase, surpassing levels seen in the respiratory competent cells. The abundance of actin, Act1, showed no change between different phases of growth in any strain, demonstrating that differences in the levels of the protein detected were not due to erroneous loading onto the gel. From these results, it would be tempting to speculate that increased Sod1 steady-state levels at stationary phase might be related to increased levels of oxidative stress. An in-gel activity assay was performed to compare Sod1 enzymatic activity with its protein abundance. Unexpectedly, activity decreased in wild-type cells from exponential to stationary phase, despite the fact that protein levels showed a mild increase. Mitochondrial mutants, on the other hand, did not display significant variation in Sod1 activity levels between the different phases of growth, with the exception of *cox11* mutant cells, which displayed an increased enzymatic activity at stationary phase. Overall, it appears that Sod1 abundance in mitochondrial mutants is higher than in a wild-type strain at stationary phase, while the enzymatic activity does not seem to change from exponential to stationary phase but it remains higher in comparison to that of wild-type cells. The finding that only a small portion (approximately 2 %) of Sod1 is necessary to scavenge oxygen superoxide might be the reason for the disconnect between steady-state protein and activity levels we found (Reddi & Culotta, 2013).

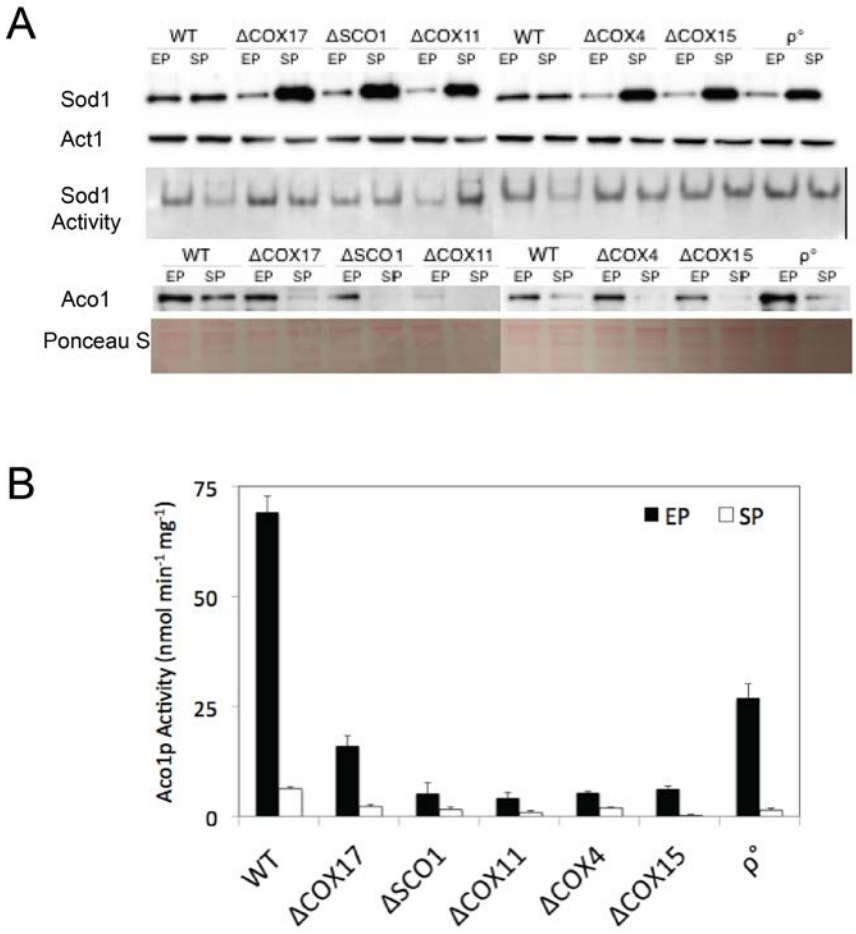

Figure 3.13 Oxidative stress analysis in wild-type (WT) and mitochondrial mutant cells. (A) Sod1 steady-state levels and enzymatic activity were measured. The respiratory competent, wild-type strain and the respiration-deficient strains were grown as previously described and whole cell lysates generated. 20 µg of protein were immunoblotted to assess the steady-state levels of Sod1 at exponential (EP) and stationary (SP) phases. Act1, which served as a loading control, was visualized on the same blot. Sod1 activity was measured in whole cell lysates (18 µg) using an in-gel assay originally developed by Beauchamp & Fridovich, (1971). Immunoblotting of mitochondria (10 µg) was carried out to detect the abundance of Aco1 at both exponential (EP) and stationary (SP) phases. Because we found that the abundance of Por1, which is used as a marker for mitochondrial proteins, decreased in our respiration deficient mutant strains, we have included the Ponceau S general protein stain to show that equal amounts of mitochondrial protein have been loaded into each well of the gel. (B) Aco1 activity was assayed in mitochondria isolated from the wild-type and the respiration deficient mutant strains at both the exponential and stationary phases. The spectrophotometric assay used citrate as the substrate and measured the production of NADPH at 340 nm. Activities (measured in duplicate) represent the average of 4 separate assays; error bars represent the standard error of the mean. These experiments were carried out by Alicia Dubinski and Seville Scarcello.

Investigating the abundance and activity levels of aconitase, Aco1, was another approach to assess oxidative stress. Aco1 localizes to both the cytoplasm and the mitochondrial matrix, where it carries out functions in citric acid cycle and mtDNA maintenance (Chen et al., 2005). This protein is easily inactivated by oxidative damage (Murakami & Yoshino, 1997) and for this reason provides a reliable marker for oxidative stress. Mitochondrial samples were isolated from exponential and stationary phase cultures of each strain and tested for aconitase activity. As shown in Figure 3.13-A, the transition from exponential to stationary phase of growth correlated with a marked decline in Aco1 steady-state protein levels. Despite the general trend being similar for all strains tested, Aco1 abundance seemed to vary based on the strain. A *cox11* mutant, for example, revealed lower steady state protein levels than any other strain at exponential phase while protein levels were below detection limit at stationary phase. Cells lacking mtDNA and all other COX assembly mutants were characterized by aconitase steady-state protein levels similar to wild-type at 24 hours, while the protein was barely detectable or below detection limit after 192 hours. Likewise, Aco1 steady-state protein levels decreased in wild-type cells at stationary phase, although the abundance of this protein was significantly higher when compared to mutant strains.

A dramatic difference between aconitase activity of wild-type and respiratory deficient cells at different growth stages was revealed by an indirect enzymatic activity assay. At 24 hours, Aco1 activity of the mutants varied between 7 and 30 % of that of wild-type strains. Among these strains, rho^0 cells and a *cox17* mutant showed activity levels that were two to five times higher than that measured in *cox4*, *cox11* and *cox15* mutants, despite the fact that steady-state protein levels did not show such diversity. At the stationary phase of growth, Aco1 activity decreased significantly in all of the strains tested, indicating increased oxidative stress in comparison to exponentially growing cultures. Aconitase activity, however, was preserved to a small extent in stationary phase wild-type cells while it was barely detectable in mutant samples.

Overall, these results are consistent with the hypothesis that oxidative stress is increased in cells bearing mitochondrial defects. It also seems that the effects of mitochondrial aberrations are more pronounced once cultures reach stationary phase.

3.9 Sensitivity to Hydroxyurea-Induced Oxidative Stress Is Increased in COX Assembly Mutants

Studies performed in the recent past have shed light on phenotypes caused by treatment of yeast cells with hydroxyurea (HU). While the effects of HU as a ribonucleotide reductase inhibitor, and the consequent depletion of the dNTPs pool are well known (Herman, 2002), induction of oxidative stress in eukaryotic cells is not. A study by Singh and Xu, 2017, demonstrated that a *Schizosaccharomyces pombe* heme-deficient strain was hypersensitive to HU treatment. In an effort to elucidate the mechanisms behind this phenotype, the authors hypothesized that ROS production was induced in HU-treated cells to levels that a heme-deficient strain, unlike wild-type, was unable to counteract (Singh & Xu, 2017).

This discovery prompted us to investigate whether HU exposure could produce a similar effect in *S. cerevisiae* cells lacking COX assembly factors. Among the proteins that are the subject of this study are Cox17, Cox11 and Sco1, which are known to bind copper ions, and the heme A synthase Cox15. Lack of these proteins might have yet unexplored implications in redox metabolism that could potentially correlate with the observed cell cycle defects.

As mentioned above, it could be that yeast cells lacking the cuproproteins Cox17, Cox11 and Sco1 reach an oxidative stress threshold earlier than other mitochondrial mutants due to higher ROS production rates. Oxidative damage above cellular scavenging capabilities would induce a bi-phasic cell cycle defect characterized by delayed S phase and subsequent G2/M arrest, similar to the results we found for cell cycle progression in synchronized cells, DNA content in non-synchronized cultures and budding index.

A standard spot assay was performed to assess the sensitivity of yeast cells to hydroxyurea. Wild-type and mitochondrial mutant cells were grown overnight in YPD media and normalized to OD_{600} = 1 the following day. Serial dilutions were then plated onto YPD (untreated control) and YPD containing 240 mM HU. Plates were incubated at 30 °C for six days and growth was then scored. All of the strains tested were characterized by lower growth when exposed to HU in comparison to untreated cells. However, as shown in Figure 3.14, sensitivity to HU varied among the strains tested. In the presence of HU, wild-type and rho^0 cells displayed the most abundant growth. Among the other strains, a *cox11* mutant displayed the highest sensitivity to HU, followed by strains defective for the other two cuproproteins

Sco1 and Cox17. Cells lacking Cox4 were characterized by sensitivity to HU similar to a *cox17* mutant strain. Intriguingly, a *cox15* null mutant, incapable of synthesizing the heme A synthase, was characterized by growth similar to wild-type even in the presence of HU. These results support the idea that mutants lacking cuproproteins might have higher endogenous ROS productions rates, and when treated with HU, these cells are not capable of counteracting the increased levels of ROS.

Strikingly, the cytotoxic effect of hydroxyurea among the mitochondrial mutants seemed to follow a pattern similar to that observed with cell cycle defects. A *cox15* mutant, for example, showed cell cycle progression very similar to wild-type. Similarly, this strain displayed a more robust growth in YPD+HU than the other mutants. In contrast, a *cox11* mutant, the strain most sensitive to HU, showed a cell cycle defect that manifested as a delayed S phase. Exceptions to this trend seem to be cells deprived of mtDNA, which did not show the hypersensitivity to HU that characterized other mitochondrial mutants. However, these cells are also characterized by cell cycle arrest at G1 (Crider et al., 2012). Moreover, as shown previously, rho^0 cells also differed from the other mitochondrial mutants by displaying a significantly lower budding index at stationary phase, which corresponds to a high proportion of cells at G1 phase.

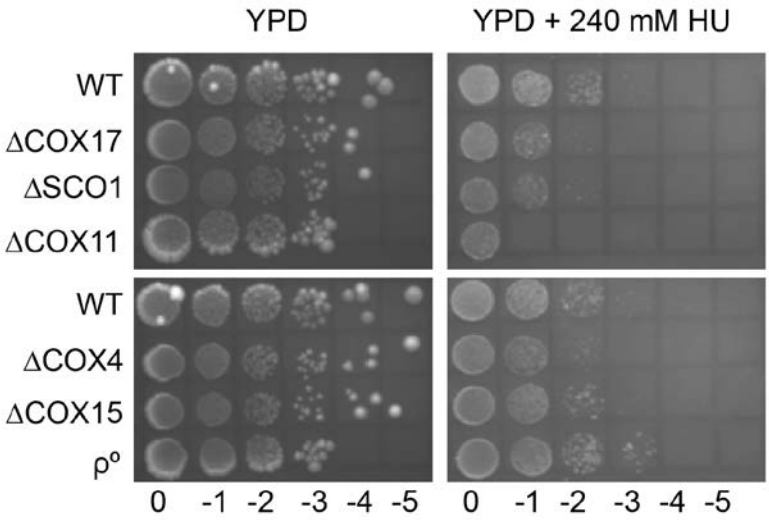

Figure 3.14 Spot assay of yeast cells treated with hydroxyurea. Cells were grown overnight at 30 °C in liquid YPD media and then normalized to OD_{600}=1. 5 µL of 10-fold serial dilutions of each strain were then plated onto YPD and YPD containing 240 mM HU agar plates. Cells were incubated for six days at 30 °C before growth was scored. HU, hydroxyurea.

3.10 Induced Oxidative Stress Correlates with Higher Death Rate in Certain COX Assembly Mutants at Stationary Phase

As mentioned previously, loss of COX assembly factors was found to have a deleterious impact on yeast growth and viability at stationary phase. While a respiratory competent strain had approximately $2.4*10^7$ viable cells/mL in stationary phase cultures, a rho^0 strain, the most viable mitochondrial mutant, only had approximately $1*10^7$ viable cells/mL. The media used contained glucose, which is rapidly exhausted by cells during fermentative metabolism. Once the diauxic shift is reached and glucose is no longer available, a switch from fermentative to respiratory metabolism is necessitated to utilize non-fermentable carbon sources. However, COX-deficient cells are unable to utilize non-fermentable carbon sources and this might be one of the causes of the low viability of mitochondrial mutants at stationary phase. Despite the fact that all of the mutants tested in this study were characterized by COX deficiency, it seemed clear that certain mutations had a more dramatic impact on survival at stationary phase.

Such variability among mutant phenotypes caused by mitochondrial defects led us to investigate what pathways might be involved. A common feature among the mitochondrial mutants is an increased oxidative stress due to COX deficiency. While cells are capable of counteracting ROS, in some cases programmed cell death pathways are activated to prevent necrotic death that could damage surrounding cells (Carmona-Gutierrez et al., 2010).

The involvement of apoptosis and necrosis in the low survival rate of respiratory deficient cells was investigated by using a flow cytometry-based approach.

Cells harvested from cultures at 24 and 192 hours, were normalized to OD_{600} = 1.0 and treated with hydrogen peroxide at concentrations that should induce cell death. It is known that treating cells with low peroxide concentrations will induce apoptosis, while high concentrations of peroxide will induce necrosis. Cells at late exponential phase of growth were therefore treated with 0 mM, 3 mM and 90 mM hydrogen peroxide concentrations respectively. As cells in stationary phase cultures tend to be more resistant to oxidative stress, 90 mM hydrogen peroxide was used to induce apoptosis while 180 mM hydrogen peroxide was used to trigger necrosis. Cultures were exposed to varying hydrogen peroxide concentrations for 3 hours at 30 ºC and then harvested and cell walls removed through Zymolyase 20T treatment. Exposure of phosphatidylserine on the outer leaflet of the plasma membrane, which is a hallmark of early apoptosis, was assayed by using Annexin V conjugated to the fluorophore FITC, while PI was used as counterstain to identify cell death via necrosis. Flow cytometry was performed to measure fluorescence signals from 30,000 cells and data acquired with this approach were plotted as shown in Figure 3.15. At exponential phase, a wild-type strain showed approximately a 20 % increase in the number of cells that stained positive for the cell death marker following treatment with 3 mM hydrogen peroxide, indicating a clear cellular response to the treatment. Among the mitochondrial mutants, a *sco*1 null mutant and the rho^0 were the only strains that showed a cell death induction similar to that of the wild-type upon peroxide treatment. Interestingly, the other strains, namely *cox15*, *cox17*, *cox4* and *cox11* null mutants, displayed activation of cell death pathways to a lower extent, even when compared to respiratory competent cells. Among these strains, a *cox17* mutant distinguished itself by displaying a mere 5 % increase in the number of Annexin V-FITC positive cells after treatment with peroxide.

At stationary phase, cells tend to be more resistant to peroxide treatment as shown by wild-type cells, which displayed a lower cell death induction after treatment in comparison to the same cells at exponential phase.

In contrast, all of the COX assembly mutants displayed cell death induction upon incubation with 90 mM hydrogen peroxide. Among these strains, *cox15* and *sco1* mutants showed the most dramatic effect of oxidative stress on cell death induction, with a 40-50 % increase in the number of cells that stained positively for the death marker. Cells defective for Cox17 or Cox4 displayed a milder response to hydrogen peroxide with a 25-30 % increase in cell death. Somewhat surprisingly, mtDNA-less cells were not affected by oxidative stress like the other mitochondrial mutants and were characterized by a number of cells positive for death markers before and after 90 mM very similar to what was observed in respiratory competent cells.

Taken together, these results suggest that while certain mitochondrial mutants revealed a correlation between oxidative stress and cell death, particularly at stationary phase, others seemed to be affected to a lesser extent. More specifically, *cox11*, *sco1* and *cox15* mutants displayed strong cell death induction after peroxide treatment at stationary phase while *cox4* and *Cox17* mutants had less robust induction levels. Overall it is also evident how cell death induction seems to be growth phase dependent in the mutants, with little to no induction in exponentially growing cultures and moderate to strong induction at stationary phase.

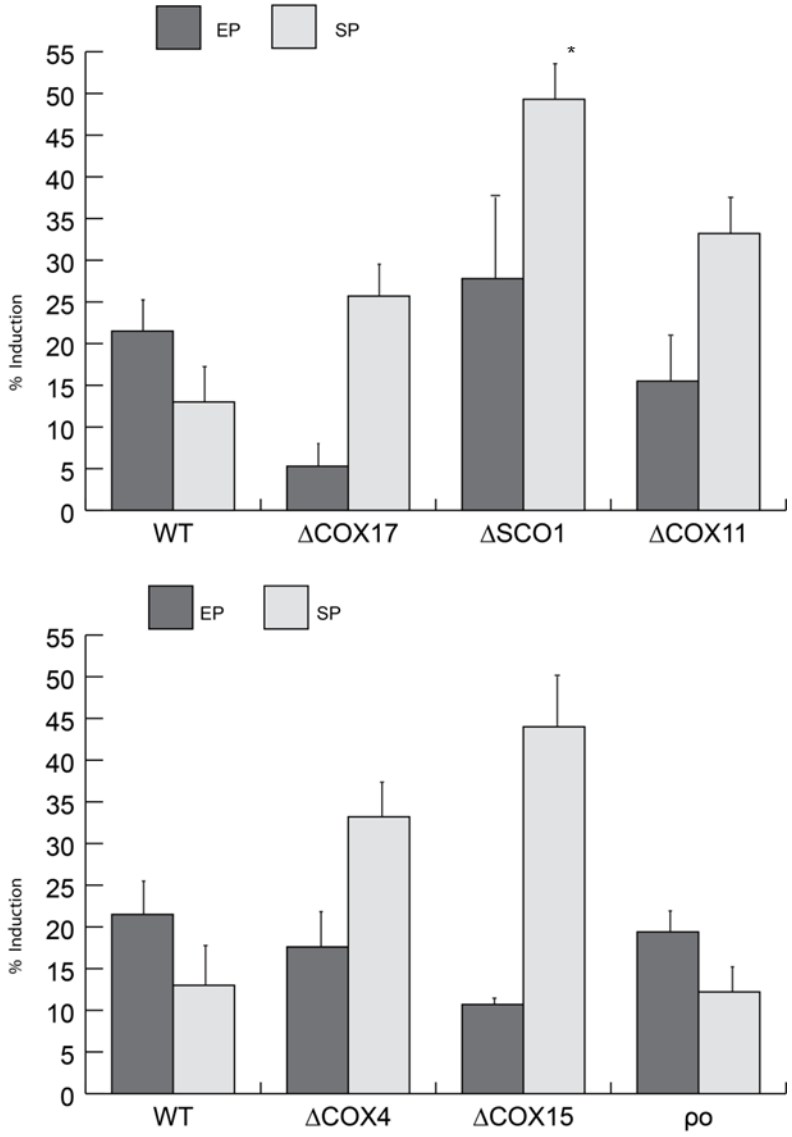

Figure 3.15 Cell death induction of yeast strains treated with hydrogen peroxide. Cells were grown and harvested at 24 and 192 hours (exponential and stationary phases), normalized to OD_{600} = 1 and incubated with different hydrogen peroxide concentrations. Exponential phase (EP) cells were incubated with 3 mM hydrogen peroxide while 90 mM peroxide was used for stationary phase cultures (SP), as these are more resistant to oxidative stress. As strain-dependent internal controls, 0 mM, 90 mM (induction of necrosis at exponential phase) and 180 mM (induction of necrosis at stationary phase) peroxide-treated cells were also analyzed. Each column represents the subtraction between the percentages of cells emitting fluorescence in the FITC and PI channels alone and in the double-stained channel after and before peroxide treatment. Asterisk denotes a statistically significant difference ($p < 0.05$: ΔSCO1 SP, 3.6E-02) between the induction levels of a wild type and mitochondrial mutant strains at a given time point. Statistical significance was determined by performing a one-way ANOVA followed by Games-Howell post hoc test (see Supplementary Table 6).

3.11 Summary

Taken together, the results of this study support the idea that functionally divergent COX assembly mutants are also phenotypically diverse, contrary to the belief that loss of COX assembly results in an identical phenotype characterized by loss of COX function. Yeast strains bearing selected COX assembly factor mutations were used to investigate the impact of COX deficiencies on a variety of cellular functions, with variability thought to be related to potential secondary functions of these COX assembly factors. Monitoring of cell cycle progression led to the novel finding that strains defective for proteins involved in COX copper metalation, such as Cox17, Cox11 and Sco1, are characterized by a cell cycle progression defect. The metal binding capability of these ancillary factors suggests that oxidative stress arising from an altered copper metabolism could be responsible for the cell cycle aberrations, with analysis of oxidative stress markers such as aconitase confirming that mitochondrial mutants are subject to higher oxidative stress levels than the respiratory competent strain. Together with a greater sensitivity to HU, which is a known oxidative stress agent in yeast, we propose that the cuproprotein mutants are characterized by higher levels of oxidative stress than mutants with defects in non-copper related pathways and that potential unbalances in cellular copper metabolism might be responsible for the cell cycle defect observed.

Chapter 4
Discussion

4.1. COX Assembly Mutants and the Yeast Stationary Phase

The identification of alternate functions for any given protein has become increasingly common, particularly in the era of large-scale proteomics screens.

Amongst the set of COX assembly factors, Sco1 and Cox11 have been proposed to have roles in redox metabolism. Strains defective for these cuproproteins bear a COX deficiency caused by the disruption of the COX copper metalation pathway. Sco1 was first associated with a role in redox metabolism given the similarities between the structure of this cuproprotein and the structures of peroxiredoxins and thioredoxins (Williams et al., 2005). Other studies have linked both Sco1 and another COX ancillary factor, Cox11, to secondary functions based on the hypersensitivity of the null mutant strains to hydrogen peroxide concentrations in the millimolar range (Banting & Glerum, 2006; Veniamin et al., 2011). These results suggested the possible involvement of these two COX assembly factors in redox metabolism, as peroxidases or, alternatively, as peroxide sensors.

In the course of experiments designed to determine whether peroxide sensing elements are present in the promoters of the *COX11* and *SCO1* genes, we found that the promoter for *COX17* drove increasing levels of expression with increased time in culture, raising the possibility that Cox17 expression levels might vary based on the phase of growth. The strains were selected to allow a comparison of the phenotypes caused by functionally diverse mutations. Cells incapable of synthesizing the cuproproteins Cox17, Sco1 and Cox11 cannot provide COX with copper.

A strain incapable of synthesizing heme A synthase, (ΔCox15), was included to study COX deficiency due to heme A assembly failure. A mutant strain defective for structural subunit Cox4 was also studied, as it differs from the mutants described above in that Cox4 is not involved in redox reactions. A rho^0 strain was also studied here, as loss of mtDNA makes rho^0 cells incapable of synthesizing the COX core subunits (Cox1, Cox2 and Cox3), as well as subunits for Complex III and Complex V. Since rho^0 strains carry defects that are not limited

to COX but rather affect the electron transport chain at multiple levels, they are employed extensively in mitochondria-related research, as a respiration-deficient reference strain.

A yeast culture is thought to reach full saturation after approximately one week (Herman, 2002) and so the time point chosen to represent the stationary phase in the present work was eight days. All the strains tested underwent an initial exponential phase of growth, as expected, and as reflected in the 24 h time point. At the diauxic shift (48 h time point), wild-type, respiratory competent cells kept growing and then reached a plateau, indicating stationary phase (144 and192 h). The respiratory deficient mutant strains cannot utilize non-fermentable carbon sources and their growth was characterized by lower OD_{600} than wild-type throughout the incubation period (Figure 3.2).

Even though all of the mutants share the common defect of a lack of COX activity, their growths were affected differently. The *cox11* mutant strain was the only strain showing a net OD_{600} decrease between exponential and stationary phase, which might be a consequence of a higher cell death rate.

Interestingly, cells lacking Cox17 grew to a higher optical density than cells lacking either Sco1 or Cox11, even though all three of these cuproproteins are involved in the COX copper metalation pathway. These data, while still preliminary, may mean that failure in the assembly of the Cu_B redox center has a stronger negative impact on cellular homeostasis.

Viabilities of wild-type and mutant strains were determined at late exponential and stationary phases and yielded results that correlated well with the growth curves. After 24 hours of incubation, mutant cells were approximately 20 % less viable than wild-type cells; at 192 hours, mitochondrial mutant strains had less than half the number of viable cells of a wild-type strain. *cox11* mutant cells were characterized by the lowest viability at stationary phase (Figure 3.3) while the rho^0 strain showed the biggest drop in viability. Despite their inability to synthesize COX core subunits, the viability of rho^0 cells at exponential phase was slightly higher than that of wild-type, as has also been observed by others (Stuart et al., 2006) while at stationary phase the viability decreased to levels that are similar to those of the other mutants. The residual viability of respiratory-deficient strains at stationary phase may be surprising due to the lack of fermentable carbon sources. However, it is possible that a portion of the yeast population is capable of surviving by utilizing nutrients released by apoptotic cells.

Taken together, these analyses show that COX assembly aberrations can result in phenotypes that differ to a greater extent than previously thought. In particular, a defect in copper delivery to redox center Cu_B seems to affect yeast growth and viability to a greater extent than other mutations. According to the accepted model for COX copper metalation, Cox17 delivers copper ions to Cox11 and Sco1 during COX assembly. Thus, it is somewhat surprising that a *cox17* mutant showed a more robust growth than strains lacking the other two cuproproteins. Direct interaction between Cox19, a protein capable of binding metals, and Cox11 was recently demonstrated and is required for Cox11 activity (Bode et al., 2015). In this study a *cox19* mutant was not tested, but based on our results it seems plausible that Cox19 and Cox17 might have some overlap in function so that loss of Cox17 does not have as dramatic an impact on cellular homeostasis as the loss of Cox11.

As originally suggested by our promoter studies, we found that steady-state levels of Cox17 increased from exponential to stationary phase in wild-type cells; Sod1 protein levels were also assayed and displayed an even stronger increase at stationary phase. Superoxide dismutase has long been known known for its critical role in cell survival in stationary phase yeast cultures (Longo et al., 1996). It should be noted that variation in the increase of Sod1 abundance at stationary phase likely depended on the method used to generate the whole cell lysate (Figures 3.4-3.13).

Higher Cox17 steady-state protein levels at stationary phase also led us to investigate the partitioning of this cuproprotein between cytosol and mitochondria at stationary phase. We found that, while the abundance of Cox17 decreased in mitochondria at stationary phase, it slightly increased in the post mitochondrial supernatant fraction (Figure 3.5-A). Under reducing environmental conditions, Cox17 and other intermembrane space proteins have been shown to retro-translocate to the cytosol (Bragoszewski et al., 2015), suggesting that the change in partitioning we observed in our mitochondrial preparations might be the result of a retro-translocation event that followed reduction of Cox17 disulfide bonds. A secondary function of Cox17 within the mitochondria has also been described (Chojnacka et al., 2015); although the increased abundance of Cox17 in its cytosolic pool at stationary phase combined with the redox-potential of the protein suggest that this protein might exert yet another function. Western blotting of mitochondrial preparations also revealed decreased steady-state levels of a number of mitochondrial proteins (Cox11, Sco1, Cox4 and Por1) between the

exponential and stationary phases in the *cox17* null mutant strain (Figure 3.5-B). Interestingly, no changes in the abundance of these proteins were observed in the wild-type. Ponceau S staining was regularly performed during Western Blotting to ensure equal loading of 10 μg of mitochondrial protein on the polyacrylamide gel. Lower abundance of mitochondrial proteins at stationary phase in the respiratory deficient strain could be due to increased mitophagy, which is known to be induced in stationary phase cultures (Kanki et al., 2015). Another hypothesis that could explain a decrease in Cox11 and Sco1 protein levels at stationary phase in a *cox17* mutant strain is that the absence of Cox17 might be responsible for a decrease in the abundance of the other two cuproproteins in a feedback-loop system.

4.2. COX Defects Adversely Impact the Cell Cycle

Visual inspection of yeast cells during growth curve experiments led to the initial observation that a *cox17* mutant strain seemed to have a higher proportion of budded cells when compared to wild-type cells at stationary phase. Budding indices of wild-type and mitochondrial mutant cells were determined to verify this initial observation and to explore whether this phenotype might be common to other respiratory deficient mutants. This approach revealed an unexpected scenario where mitochondrial mutants not only behaved differently from one another but also from the wild-type strain.

The budding index of respiratory competent cells was approximately 60 % at exponential phase, which decreased to 35 % at stationary phase. A lower budding index at stationary phase is expected as cells stop growing and should remain in a non-budded state (G_0 phase). In contrast, cells depleted of mtDNA were characterized by budding indices lower than any other strain at both phases of growth. As reported by Crider et al., (2012), yeast rho^0 cells manifest a defect while transitioning from G1 to S phase during the cell cycle, which might explain the lower budding index of a rho^0 strain when compared to respiratory competent cells. Furthermore, the increase in cellular volume associated with G1 arrest (Bryan et al., 2010) might be responsible for altering light absorption, ultimately leading to rho^0 cells displaying a faster growth rate than other mitochondrial mutants at exponential phase (Figure 3.2).

Budding index analyses of the other mitochondrial mutants provided further proof of diversity between COX deficiencies caused by different defects. At the exponential phase of growth, the COX assembly factors mutant strains had budding indices similar to that of the wild-type, with

differences emerging at the stationary phase. Confirming initial observations, the budding index of a *cox17* mutant was about 15 % higher than that of the wild-type after 192 hours. *cox4* and *cox15* mutants also displayed budding indices slightly higher than that of wild-type. On the other hand, strains defective for Cox11 and Sco1 revealed proportions of budded cells at 192 hours that were lower than the other COX assembly mutants but not lower than wild-type (Figure 3.6). This approach thus served to distinguish defects caused by the loss of mtDNA from those with a loss of assembled COX. The anomalous budding indices of the COX assembly mutants suggested the presence of possible cell cycle-related defects distinct from that of the rho^0 strain.

In an effort to explore the connection between mitochondrial defects and the cell cycle, flow cytometry-based approaches were adopted to assess the DNA content of cells from both synchronous and non-synchronous cultures. Flow cytometry of non-synchronous cultures at different growth phases revealed a general trend among all strains, defined by an increased G1/G2 ratio in moving from exponential to stationary phase. This was not surprising since synchronization in an non-budded state is a known hallmark of quiescent cells in stationary phase cultures (Gray et al., 2004). The increased G1/G2 ratios after eight days of incubation also provided further evidence that cultures had indeed reached stationary phase.

The highest G1/G2 ratios at both exponential and stationary phases were found in the rho^0 strain. Evidence that the majority of mtDNA-less cells had 1-N DNA content also matched the low budding indices determined for this strain, suggesting that this phenotype is likely linked to the known cell cycle defect of mtDNA-less cells.

DNA content analysis of COX assembly mutants provided a clear contrast with rho^0 cells, providing an indication of different cell cycle anomalies affecting these strains. At stationary phase, *cox17*, *cox4* and *cox15* null mutant strains were characterized by G1/G2 ratios that were half of that of wild-type, indicating a greater number of cells at G2/M, which was in keeping with the high budding indices found in these strains at stationary phase.

The G1/G2 ratios of *sco1* and *cox11* mutants were also lower than that of the wild-type at stationary phase. Interestingly, the budding indices for these two strains at stationary phase did not show differences from wild-type, unlike the other assembly mutants.

Overall, these results provided evidence that higher percentages of budded cells in certain mitochondrial mutants at stationary phase correlated with higher proportions of cells at

G2/M. This pattern was not observed in exponentially growing cultures, where G1/G2 ratios of COX assembly mutants were approximately half of that of the wild-type after 24 hours, but with no differences in budding indices. A rho^0 strain, on the other hand, showed the highest G1/G2 ratios, in keeping with low budding indices at both growth phases. Because this strain is characterized by a known cell cycle defect, it served as internal control for a comparison with the COX assembly mutants.

Techniques typically used to monitor cell cycle progression in *S. cerevisiae* involve flow cytometry and visual analysis. In the work presented here, visual analysis was employed to determine the budding index of each strain. Generally, morphological changes in cells are associated with cell cycle transitions. A limitation of visual analysis, however, is that it requires a correlation between cytoskeletal events and DNA replication (Calvert et al., 2008). Uncoupling between bud emergence and DNA replication has been reported in specific mutant strains and under specific growth conditions, such as nitrogen starvation (Piatti et al., 1995; Rivin & Fangman, 1980; Schwob & Nasmyth, 1993), and may underlie the discrepancies between DNA content analysis and budding indices we found in our mutants. The effects of COX assembly aberrations on the cell cycle were further investigated by analyzing cell cycle progression of cultures synchronized at G1.

These experiments led to a further diversification of phenotypes caused by mutations of different COX assembly factors. It was found that *cox15* and *cox4* null mutants were characterized by a cell cycle progression very similar to that of respiratory competent, wild-type cells. Interestingly, *cox4* and *cox15* mutants, together with cells defective for Cox17 were the strains that presented with the highest percentages of budded cells at stationary phase. However, progression between cell cycle phases seemed slightly delayed in a *cox17* mutant strain (Figure 3.9). A delayed progression through cell cycle phases was even more evident in cells lacking the other two cuproproteins, Sco1 and Cox11, respectively. In contrast to the DNA content analysis of non-synchronous cultures, which showed higher numbers of cells at G2/M in COX assembly mutants, the analysis of DNA content post-synchronization allowed us to identify a cell cycle defect that appears limited to the cuproproteins mutants, at least in cells grown for less than 24 h. Indeed, FACS analyses of synchronized cultures revealed that strains lacking cuproproteins showed a delayed cell cycle progression that appeared similar to the delayed G1-S transition observed in a rho^0 strain (Crider et al., 2012). However, the defect

shared among cuproprotein mutants seemed to differ from that of a rho^0 strain. The latter, in fact, showed a delay in progression through cell cycle phases as well as a high proportion of cells that arrest at G1, whereas the cuproprotein mutants displayed higher proportions of cells that arrest at G2 at both phases of growth in non-synchronous cultures. In addition, the cell cycle progression of cuproprotein mutants was not characterized by the post-release predominant G1 peak shown by cells that lack mtDNA, which arrested at G1. To our knowledge, this is the first report of cell cycle defects associated with COX assembly mutants. In summary, while minimal or no apparent difference from respiratory competent cells was found for the *cox15* and *cox4* mutants, strains defective for the cuproproteins were characterized by a slower cell cycle progression, displaying 2-N DNA content at a later time point after release.

The strategies applied to investigate the cell cycle in wild-type and respiratory deficient cells generated results that led to seemingly contradictory conclusions. While initial experiments revealed impaired growth and lower viability of cells that are unable to respire, analysis of budding indices identified COX assembly mutants with increased proportions of budded cells at stationary phase. Because the anomalous budding indices observed in *cox17*, *cox4* and *cox15* mutants could have been related to their replicative capability, the replicative lifespan (RLS) of each strain was determined. RLS is defined as the number of times a virgin cell divides before becoming senescent (Mortimer & Johnston, 1959). This technique is currently a common tool in aging studies. RLS analyses of the mutants used in this study did not reveal significant differences between lifespans of the wild-type and those of the mitochondrial mutants ($p > 0.01$), thereby ruling out the possibility that these mitochondrial mutants could be more prolific than the respiratory competent cells. However, while our strains did not show differences in RLS, results reported in the literature are contradictory. It appears that yeast lifespan may vary depending on genetic background and on growth conditions (Longo et al., 2012). Indeed, the RLS of certain rho^0 strains was found to be higher than that of the wild-type, although this phenotype was not observed in rho^0 strains with different genetic backgrounds (Kirchman et al., 1999).

The rho^0 strain used in this study was in the W303 genetic background and its replicative lifespan was not different from that of the parent, respiratory competent strain, as described by others (Kirchman et al., 1999). A *cox4* null mutant has been studied in the YPK9-background

and its lifespan was found to be mildly higher than that of the wild-type, although it should be noted that the "corresponding rho^0 strain was characterized by a strong RLS increase.

A discrepancy between our results and data from the literature is the overall lower RLS that characterized our strains. Pioneering RLS experiments estimated a yeast lifespan ranging between 20-25 divisions (Mortimer & Johnston, 1959), while recent studies have estimated that yeast RLS varies between 20 and 30 divisions (Steffen et al., 2009). Cells with the W303 background, like the ones used in the work presented here, fall in the category of "short-lived" strains and their RLS was reported to be approximately 20 to 23 divisions (Kaeberlein et al., 1999). In contrast with what was reported in the literature, our strains were characterized by shorter lifespans, with mean RLS ranging from 12 to 15.

The reason(s) for this discrepancy are not clear as a nearly identical methodology was used. One possibility is that long-term storage of our strains may have played a role in the shorter lifespans. Given the lack of an observable defect in replicative lifespan, experiments were undertaken to further explore the possibility that COX assembly mutants might still be proliferating at stationary phase, as suggested by the anomalous budding indices.

Western blotting for Mcm2, a component of the Mcm2-7 hexameric helicase complex, showed high levels of this protein in proliferating cells, as expected (Young & Tye, 1997). Immunoblotting of whole cell lysates revealed that Mcm2 steady-state protein levels in all of the mitochondrial mutants were below detection limits, after 192 hours in culture. This contrasted with Mcm2 steady-state levels in the wild-type strain, which did not appear to change based on the growth phase. This was somewhat surprising, as little to no cell replication would be expected to happen in stationary phase cultures.

In summary, these results suggest that the anomalous budding indices of certain COX assembly mutants are not connected to the replicative lifespan of the strains investigated.

4.3. Role of Oxidative Stress in Cell Cycle Defects

On the basis of the cell cycle progression analyses, mutants that could not express the COX assembly cuproproteins, together with a rho^0 strain, were characterized by delays in cell cycle progression. However, based on subtle differences, we hypothesized that lack of mtDNA and the lack of cuproproteins interfered with the cell cycle in different ways. This hypothesis was based on evidence that, after 192 hours of incubation, rho^0 cells displayed the lowest

budding indices and the highest proportion of cells at G1, reflecting G1 arrest. In comparison, the G1/G2 ratios of cuproprotein mutants indicated a much higher abundance of cells at G2/M at both exponential and stationary phases, suggesting they may be undergoing a G2/M arrest. Steady-state levels of Rad53, one of the key players in G2/M arrest in *S. cerevisiae*, were below detection limits in all of the mitochondrial mutants at stationary phase. In contrast, Rad53 steady-state levels did not appear to change from exponential to stationary phases in wild-type cells, possibly representing the need for this protein in response to DNA damage due to increased oxidative stress levels (Schroeder & Shadel, 2014). Why Rad53 was not detected in whole cell lysates from mitochondrial mutant cultures at stationary phase remains unclear, although it is possible that the cell cycle defects in COX assembly mutants affect mechanisms that act upstream of Rad53.

In the absence of obvious replicative defects among our strains, we considered another potential source of cell cycle defects, namely oxidative stress. Reactive oxygen species are involved in a myriad of cellular pathways and in most cases have a negative impact on cellular homeostasis. Because mitochondria are thought to be one of the main sources of cellular ROS, the idea that oxidative stress could be linked to the phenotypes observed in our mutants seem plausible, given that induced oxidative stress has been reported to cause a bi-phasic cell cycle arrest in yeast, with S phase arrest followed by G2/M arrest at a later point in time (Shapira et al., 2004). The behaviours of our COX assembly mutants fit with the model of a bi-phasic cell cycle arrest, as high budding indices and low G1/G2 ratios of COX assembly mutants could be indicative of G2/M phase arrest. *cox17*, *sco1* and *cox11* mutants displayed a delayed cell cycle progression, leading to the possibility that strains lacking proteins involved in COX copper metalation might have higher endogenous ROS production rates. *cox4* and *cox15* mutants, on the other hand, displayed cell cycle progression similar to that of the wild-type, but the high budding indices and low G1/G2 ratios of these strains at stationary phase suggest that these cells might reach deleterious ROS intracellular levels at a later point. In fact, a culturing period of 192 hours implies a prolonged exposure of cells to oxidative stress, ultimately inducing the cell cycle defect observed in the cuproprotein mutants at an earlier time point, in late exponential phase (Figure 4.1).

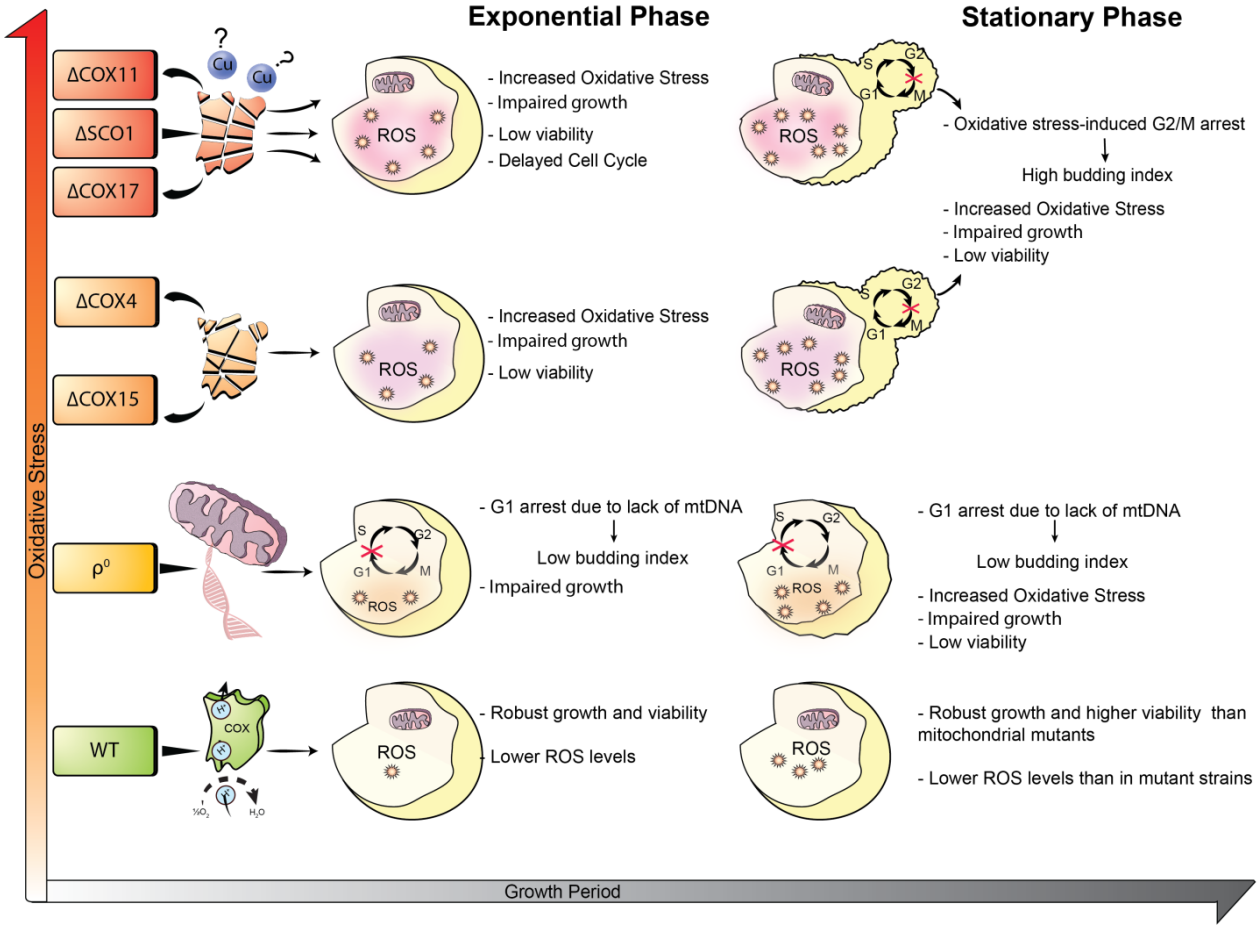

Figure 4.1 Differential impact of mitochondrial defects on cellular homeostasis. Oxidative stress levels, which increase in all strains from exponential to stationary phase, vary depending on the nature of COX deficiency. A wild-type strain is characterized by higher growth, higher viability and lower oxidative stress than mutant strains. Depletion of mtDNA in rho^0 cells causes G1 arrest, impaired growth and low budding indices. COX assembly mutants are characterized by higher ROS generation rates that associate with bi-phasic cell cycle arrest, impaired growth and low viability, especially at stationary phase. These effects are especially pronounced in cuproprotein mutant strains *cox17*, *sco1* and *cox11*, which also displayed higher sensitivity to hydroxyurea treatment. WT, wild-type; ROS, reactive oxygen species; COX, Cytochrome *c* Oxidase

Mitochondria are a known source of ROS through different intra-organellar sites such as the external mitochondrial NADH dehydrogenase (Davidson & Schiestl, 2001), coenzyme Q (Guo & Lemire, 2003) and succinate dehydrogenase (Outten & Culotta, 2003).

Aconitase is used as a sensitive detector of oxidative stress and we found decreased steady-state levels of Aco1 at stationary phase in both the wild-type and mutant strains, with the mutants having no or barely detectable Aco1 levels. Enzymatic activity of this protein was also marked by a significant decrease at stationary phase (Figure 3.13), suggesting that an intact electron transport chain is necessary for cells to be able to counteract oxidative damage. Alternatively, defects of individual complexes could lead to increased ROS production through electron slippage.

Likewise, increased steady-state levels of Sod1were found at stationary phase in mutant strains, although superoxide dismutase activity levels did not increase accordingly, possibly due to the fact that only a rather small portion of Sod1 is required to scavenge cellular oxygen superoxide (Reddi & Culotta, 2013) Further experiments will be required to determine whether mutant strains have higher rates of Sod1 protein turnover.

The discrepancy between Sod1 activity and steady-state protein levels has also been described in a *cmc1* null mutant in which mitochondrial Sod1 activity increased, while steady-state protein levels did not; the same study reported no differences in Sod1 activity in whole cell lysates (Horn et al., 2008). The inability to grow on non-fermentable carbon sources of another Cmc1 mutant was rescued with the addition of the anti-oxidant dithiothreitol (DTT), without notable increase in either Sod1 activity or steady-state levels (Bode et al., 2013). It should be noted that these studies examined mitochondria isolated from cells harvested at exponential phase/early diauxic shift, conditions that are different from those described here. A more recent investigation of Sod1 at stationary phase has found increased amounts of the Sod1 protein in soluble aggregates (Martins & English, 2014). Neither this possibility nor the involvement of Sod2, the mitochondrial matrix Mn-superoxide dismutase, was assessed during this work. Taken together, analyses of oxidative stress markers such as aconitase and superoxide dismutase protein levels and enzymatic activities suggest that mitochondrial mutants are subject to higher oxidative stress levels than the wild-type strain, especially at stationary phase.

The approaches discussed above analyzed endogenous oxidative stress levels in stationary phase culture, and we wondered how our mitochondrial mutants would respond to an exogenously-induced oxidative offense.

It has very recently been reported that a *S. pombe* heme-deficient strain is hypersensitive to treatment with hydroxyurea, with the cytotoxic effect of hydroxyurea due to induction of ROS levels beyond the capacity of cellular scavenging mechanisms (Singh & Xu, 2017). The strains studied in the work presented here responded differently, based on the nature of the COX defect, when exposed to hydroxyurea. Interestingly, as reported in Figure 3.14, a *cox15* null mutant, which is defective for the heme A synthase, was the least affected by HU treatment among the assembly mutants. On the other hand, the cuproprotein mutants showed the strongest sensitivity to HU, supporting the hypothesis that COX assembly mutants lacking one of the cuproproteins might be subject to higher endogenous ROS production rates.

Similarly to what was shown in heme deficient *S. pombe* cells (Singh & Xu, 2017), HU treatment might induce oxidative damage to levels that the cuproprotein mutants cannot manage. Experiments aimed at confirming that the reduced growth of the cuproprotein mutants in the presence of HU is due to increased ROS levels and not to the depletion of the dNTP pool are currently ongoing. Interestingly, the *cox11* and *sco1* mutants are known to be hypersensitive to hydrogen peroxide, while the *cox17* and *cox4* null mutants are not characterized by sensitivity to peroxide (Banting & Glerum, 2006). An investigation of the promoter regions of the genes encoding Cox17, Cox11 and Sco1 failed to find any evidence of peroxide-responsive elements (Figure 3.1). While potential roles for Cox11 and Sco1 in redox metabolism cannot be excluded, it is possible that the peroxide sensitivity of the null mutants is a consequence of the same mechanism that results in the sensitivity of these strains to hydroxyurea. It should be noted that while a *cox17* mutant did not show hypersensitivity to induced oxidative stress as reported previously (Banting & Glerum, 2006), it could be that 6 mM hydrogen peroxide was too low a concentration to affect this mutant. Our FACS analysis of cell death markers in cells treated with hydrogen peroxide showed that *cox17* mutant cells hardly responded to treatment with 3 mM hydrogen peroxide. On the other hand, when the same cells were treated with 90 mM hydrogen peroxide after 192 hours in culture, induction of cell death pathways was significant (Figure 3.15).

Mutation of any of the COX assembly factors described in the present work results in COX assembly failure and the subsequent loss of activity. Still, cuproproteins mutants were found to be more sensitive to an oxidative offense than the other mutants and the underlying mechanisms are not clear and require further investigation. The presence of copper ions within the cell needs to be tightly regulated as these ions can otherwise contribute to formation of dangerous hydroxyl radicals through Fenton reactions in the presence of hydrogen peroxide (Halliwell & Gutteridge, 1990). Because Cox17, Cox11 and Sco1 are all proteins capable of binding copper ions, it is possible that their loss could interfere with mitochondrial copper metabolism, leading to increased ROS production rates. Mitochondrial copper regulation is still poorly understood and a matter of debate, especially with regard to how copper reaches the IMS and the mitochondrial copper pool in the matrix. A study performed in human cells showed that a COX17 deficiency was associated with increased mitochondrial copper concentration, suggesting that COX17 could play a role in copper efflux from mitochondria (Wang et al., 2013). Another protein thought to be playing a role in copper efflux is SCO1, as cells with mutated *SCO1* have a mitochondrial copper deficiency, although similar effects were found in *sco2* and *cox15* backgrounds (Leary et al., 2007). Another more recent study contributed to the development of a model that involves SCO1, SCO2, COX19 and ATP7A in coordinating copper efflux from the cell. Briefly, according to this model, mutant SCO1 is characterized by an altered status of its redox-active cysteines, which simulates a status of "copper overload" and triggers release of COX19 from the IMS. COX19 release ultimately leads to cellular copper efflux mediated by the Golgi-localized, ATP7A copper-transporting ATPase (Leary et al., 2013). In this regard, it would be interesting to study Cox19, Cmc1, Sco2 and Cox23, which are all localized to mitochondria and have metal-binding functions. Among these proteins, Cox23 is thought to have a role in copper homeostasis and to act in a common pathway upstream of Cox17 (Barros et al., 2004). It would be interesting to investigate the phenotypes of mutants for the proteins with regards to cell cycle and sensitivity to oxidative stress, especially when considering the recent discovery of a direct interaction between Cox19 and Cox11 prior to copper delivery to Cox1 (Bode et al., 2015).

The requirement of copper in mitochondria is not limited to the electron transport chain, but extends to other enzymes such as the superoxide dismutase Sod1. Thus, unbalances in copper homeostasis might have repercussions on the functions of this protein as well. Interestingly, it

was previously reported that the lack of Sod1 interferes with the regulation of copper genes in response to DNA damaging agents such as methyl methanesulfonate, suggesting a direct role for this protein in a pathway that connects copper metabolism with cellular antioxidant defense mechanisms (Dong et al., 2013).

The mitochondrial mutants studied in this work showed differences in viability, as discussed earlier, suggesting the possibility of diversified activation of cell death pathways. Moreover, respiratory deficient strains revealed increased oxidative stress, which is known to trigger the apoptotic pathway.

Cell death in the wild-type and COX deficient strains at different phases of growth was therefore investigated by testing for the externalization of phosphatidylserine to the outer leaflet of the plasma membrane. However, these data should be considered preliminary, as it is recommended that more than one approach should be used when investigating apoptosis (Carmona-Gutierrez et al., 2010), especially considering the challenges of the strong autofluorescence, especially in a wild-type strain. Despite adopting gating strategies specific for individual strains and using unstained cells as "negative control", a clear distinction between early apoptotic cells (single stained, FITC positive cells) and late apoptotic/necrotic cells (double stained, FITC+PI) was not achievable. For this reason, "cell death induction" was determined as the difference between numbers of single and double stained events after and before incubation with peroxide.

Interestingly, exposure of exponentially growing cells to 3 mM hydrogen peroxide did not appear to trigger cell death in mutant cells to a greater extent than in wild-type cells, with the exception of the *sco1* mutant strain. On the other hand, *cox17*, *cox4* and *cox15* mutant strains displayed lower cell death induction rates in comparison to the wild-type. In particular, the *cox17* mutant showed a mere 5 % increase in the number of cells undergoing cell death upon treatment with peroxide, while the induction rate in wild-type cells at exponential phase was about 20 %.

In contrast, at the stationary phase of growth, all of the COX assembly mutants displayed higher levels of cell death upon incubation with 90 mM hydrogen peroxide. Among these strains, *sco1*, *cox15 cox11* and *cox4* mutants were found to be particularly sensitive to peroxide treatment and were characterized by an increase in the numbers of events positive for cell death markers of between 30 and 50 % (Figure 3.15). Rho^0 cells did not appear more

sensitive to peroxide-induced cell death than the wild-type strain at stationary phase, as has been reported by others (Büttner et al., 2007), and both strains displayed lower cell death levels at stationary phase as compared to exponential phase.

Taken together, our analysis of cell death in wild-type and mitochondrial mutants revealed that stationary phase COX assembly mutant cells were more sensitive to oxidative damage than wild-type or rho^0 cells. Moreover, among the COX assembly mutants, cells defective for Cox17 appeared less sensitive to peroxide, potentially unveiling a role for this protein in cell death pathways.

In summary, results of this study revealed divergent phenotypes of yeast strains that were characterized by failure in COX assembly and the subsequent loss of COX function. Analysis of the phenotypic variability among these mitochondrial mutants led us to uncover a cell cycle defect associated with the loss of COX assembly factors that is likely due to higher oxidative stress levels that were observed in respiratory deficient strains. To our knowledge, this is the first report of a cell cycle aberration caused by COX assembly factors mutations.

Chapter 5
Conclusions and Future Directions

5.1. COX Assembly Factors Defects Lead to Diverse Phenotypes

In the recent past, the common belief that all COX assembly mutants present a virtually identical phenotype has been challenged by studies that have unveiled novel, secondary functions for some of these proteins. The experiments described here revealed a phenotypic diversity caused by mutations in different ancillary factors. Analyses of growth curves and cellular viabilities at different phases of growth uncovered divergent phenotypes among the strains studied, with *cox11* exhibiting the lowest growth and viability, while a *cox17* mutant was found to grow to higher density levels than any of the other COX mutants, both during the exponential and stationary phases.

Phenotypic differences among the COX assembly mutants extended to cell cycle progression, with strains defective for proteins involved in COX copper metalation displaying a defect that was not observed in other COX assembly mutants such as *cox15* and *cox4*.

The COX assembly mutant strains selected for this work included cells defective for proteins involved in the assembly of the COX complex at different levels. However, scientific research makes COX assembly factors a group of proteins that is still growing in number and that includes functions that have not been considered in this study. Cox17, Cox11 and Sco1 are not the only copper-binding COX assembly factors; Cox23, Cmc1 and Cox19 are also capable of binding copper and localize to the IMS. It would be interesting to see whether strains defective for these proteins show a cell cycle defect similar to that of the *cox17*, *sco1* and *cox11* mutants. Another protein that was not investigated in this study, but that falls within the category of proteins involved in COX assembly, is Sco2. The function of Sco2 is believed to be partially redundant with that of Sco1 (Lode et al., 2000), although overexpression of this protein cannot rescue the loss of Sco1 (Glerum et al., 1996b). The approaches used in the present work could be applied to study a *sco2* null mutant, possibly leading to an improved understanding of the functional relationship between Sco1 and Sco2 as homologous COX assembly factors.

5.2. Novel Functions of COX Assembly Factors

Since the hypothesis for secondary roles of Cox11 and Sco1 was initially formulated (Banting & Glerum, 2006), definitive evidence of their specific roles in redox metabolism has not been attained. Some of the functions proposed for these cuproproteins included roles as peroxidases or, alternatively, as peroxide sensors in the IMS. Other studies have linked human SCO1 with a pathway that regulates copper efflux from the mitochondria (Leary et al., 2013). In the work described here, no peroxide-responsive elements in the *SCO1* and *COX11* promoter regions were identified, ruling out roles for these two cuproproteins in peroxide sensing. An alternate function in redox metabolism, however, cannot be excluded. Experiments aimed at finding whether Cox11 and Sco1 can function as peroxidases would be another step towards exploring the roles of these proteins in peroxide metabolism. To this aim, His-tag versions of Sco1 and Cox11 could be purified via affinity chromatography and tested for peroxidase activity using an Amplex Red assay. Alternatively, these cuproproteins could be acting by regulating the activity of other peroxidases. In this case, co-immunoprecipitation experiments might reveal new interactions between Sco1 and Cox11 and proteins involved in peroxide metabolism, such as the mitochondrial peroxiredoxin Prx1, and Ccp1, a cytochrome *c* peroxidase localized to the IMS.

Cox17, the cuproprotein functioning upstream of Cox11 and Sco1, has also been associated with functions not directly related to COX assembly. The interaction between Cox17 and a core component of the MICOS complex, Mic60, indicates the involvement of Cox17 in a pathway required for the maintenance of the IMM integrity (Chojnacka et al., 2015). Another study linked this small cuproprotein to a role in copper efflux from human mitochondria (Wang et al., 2013). Experiments described here, which were aimed at characterizing broader phenotypes of the COX assembly mutants, showed that the growth of cells defective for Cox17 is not affected as much as observed in other strains, such as a *cox15* mutant. The cell cycle defect that was observed in a *cox17* mutant, as well as in cells defective for Sco1 and Cox11, might be related to the metal-binding ability of these proteins rather than being specific to the function of a single protein. However, the exact cause of the cell cycle delay that was found in the cuproproteins mutants requires further investigation. To further confirm the role of oxidative stress as the cause of the cell cycle defect we observed,

experiments will be aimed at demonstrating that under certain growth conditions such as the absence of oxygen and/or the presence of N-acetylcysteine, a strong anti-oxidant, the sensitivity of the cuproprotein mutants to HU can be reversed.

Flow cytometric analysis of cell death markers has shown that treating cells with hydrogen peroxide induces cell death to a lesser extent in a *cox17* mutant than in the other strains tested at late exponential phase. While these results are preliminary, they suggest the potential involvement of Cox17 in cell death pathways. As mentioned previously, multiple approaches should be adopted when investigating apoptosis (Carmona-Gutierrez et al., 2010) and other methods that could be used to confirm these preliminary data include terminal deoxynucleotidyl transferase dUTP nick end labeling (TUNEL), a technique that is commonly used to detect apoptosis in its late stages and DAPI staining to observe the status of chromatin.

The retro-translocation of Cox17 from the IMS to the cytosol we observed in our mitochondrial preparations had been previously reported already and demonstrated to be linked to the reduction of Cox17 disulfide bonds (Bragoszewski et al., 2015). However, we also found that Cox17 steady-state protein levels increased in whole cell lysates between exponential to stationary phases. Thus, it is possible that the increased abundance and retro-translocation of Cox17 associate with yet another function of the protein in the cytosol.

5.3. Correlation between COX Deficiency and Cell Cycle Defects

The initial observation that some COX assembly mutants had more cells with buds than the wild-type strain at stationary phase prompted us to explore a possible association between COX defects and the cell cycle. Visual analysis, followed by determination of budding indices, confirmed that *cox17, cox4* and *cox15* mutants had a higher abundance of budding cells in comparison to the wild-type. Flow cytometric data supported the budding indices, revealing that *cox4*, *cox15* and *cox17* mutants have a high proportion of cells at G2/M in the stationary phase. Monitoring of cell cycle progression allowed us to discriminate between two different cell cycle defects: a G1-S transition defect that had previously been described in a rho^0 strain (Crider et al., 2012), and a second anomaly consisting of a delayed cycle progression, as seen in the cuproprotein mutants. Treating cells with a known ROS, such as hydrogen peroxide, induces a bi-phasic cell cycle arrest, first at G1-S phase and later at G2/M, leading us to hypothesize that cuproprotein mutants could be under increased oxidative stress. Indeed,

analysis of oxidative stress revealed that the mitochondrial mutants displayed increased oxidative damage, as shown by the reduced aconitase activity. Furthermore, the cuproproteins mutants displayed hypersensitivity to hydroxyurea, which is known to increase cellular oxidative stress levels (Singh & Xu, 2017). The mechanisms that underlie the oxidative stress-dependent cell cycle defect are not yet clear and require further investigation. Proteins such as the transducer, Mec1, and the downstream effector proteins Rad53 and Rad9, which are known to function in a checkpoint in response to DNA damage, represent a starting point for future experiments aimed at elucidating the mechanisms underlying the cell cycle defect described here. Studying the phosphorylation of Pif1, a downstream player in the Rad53-induced response to DNA damage (Makovets & Blackburn, 2009) could give a first indication of the involvement of Rad53 in the cell cycle defect observed in a subset of our mutants.

While human disease associated with COX deficiency has not been the focus of this work, the results described in this study shed light on the phenotypic variability caused by COX deficiencies in yeast cells and uncovered a potential link between the loss of certain COX assembly factors and cell cycle defects. These findings are therefore relevant to the phenotypic impact of COX deficiencies associated with human disease, particularly in terminally differentiated cells, such as neurons.

Mitochondrial disease is commonly defined as defects of the respiratory chain, and despite the efforts of scientific research, no cures currently exist. Therapeutic approaches to treat mitochondrial disorders are mainly limited to pharmacological and surgical treatment. A common approach in treating mitochondrial disease consists of enhancing the respiratory chain function to attenuate the energy deficiency and to prevent ROS accumulation and the subsequent oxidative stress. A compound frequently used to treat respiratory deficiencies is coenzyme Q_{10}, thanks to its antioxidant properties and the important role that it plays in the electron transport (Dimauro et al., 2012). This pharmacological strategy, however, lead to modest and often subjective results (Glover et al., 2010). The experiments performed in the work presented here unveiled a connection between the loss of COX assembly factors and cell cycle defects. This connection bears the potential of becoming a starting point for future research aimed at exploring new therapeutic approaches that are not solely focused on the energy-related aspect of mitochondrial disorders.

References

Abajian, C., Yatsunyk, L. A., Ramirez, B. E., & Rosenzweig, A. C. (2004). Yeast Cox17 solution structure and copper(I) binding. *Journal of Biological Chemistry*, *279*(51), 53584–53592. https://doi.org/10.1074/jbc.M408099200

Ahmed, S., Thomas, G., Ghoussaini, M., Healey, C. S., Humphreys, M. K., Platte, R., Morrison, J., Maranian, M., Pooley, K. A., … Easton, D. F. (2009). Newly discovered breast cancer susceptibility loci on 3p24 and 17q23.2. *Nature Genetics*, *41*(5), 585–90. https://doi.org/10.1038/ng.354

Allen, C., Büttner, S., Aragon, A. D., Thomas, J. A., Jaetao, J. E., Benn, D., Ruby, S. W., Veenhuis, M., Madeo, F., Werner-washburne, M., Buttner, S., & Meirelles, O. (2012). of from yeast cells quiescent and nonquiescent cultures stationary-phase. *Cell*, *174*(1), 89–100. https://doi.org/10.1083/jcb.200604072

Anderson, S., Bankier, A. T., Barrell, B. G., de Bruijn, M. H., Coulson, A. R., Drouin, J., Eperon, I. C., Nierlich, D. P., Roe, B. A., Sanger, F., Schreier, P. H., Smith, A. J., Staden, R., & Young, I. G. (1981). Sequence and organization of the human mitochondrial genome. *Nature*, *290*(5806), 457–465. https://doi.org/10.1038/290457a0

Aragon, A. D., Rodriguez, A. L., Meirelles, O., Roy, S., Davidson, G. S., Tapia, P. H., Allen, C., Joe, R., Benn, D., & Werner-Washburne, M. (2007). Characterization of Differentiated Quiescent and Nonquiescent Cells in Yeast Stationary-Phase Cultures. *Molecular Biology of the Cell*, *19*(3), 1271–1280. https://doi.org/10.1091/mbc.E07-07-0666

Banci, L., & Bertini, I. (2013). Metallomics and the cell: some definitions and general comments. *Metal Ions in Life Sciences*, *12*, 1–13. https://doi.org/10.1007/978-94-007-5561-1_1

Banci, L., Bertini, I., Cefaro, C., Ciofi-Baffoni, S., Gallo, A., Martinelli, M., Sideris, D. P., Katrakili, N., & Tokatlidis, K. (2009). MIA40 is an oxidoreductase that catalyzes oxidative protein folding in mitochondria. *Nature Structural & Molecular Biology*, *16*(2), 198–206. https://doi.org/10.1038/nsmb.1553; 10.1038/nsmb.1553

Banting, G. S., & Glerum, D. M. (2006). Mutational analysis of the Saccharomyces cerevisiae cytochrome c oxidase assembly protein Cox11p. *Eukaryotic Cell*, *5*(3), 568–578. https://doi.org/10.1128/EC.5.3.568-578.2006

Bareth, B., Dennerlein, S., Mick, D. U., Nikolov, M., Urlaub, H., & Rehling, P. (2013). The heme a synthase Cox15 associates with cytochrome c oxidase assembly intermediates during Cox1 maturation. *Molecular and Cellular Biology*, *33*(20), 4128–4137. https://doi.org/10.1128/MCB.00747-13

Barnum, K. J., & O'Connell, M. J. (2014). Cell cycle regulation by checkpoints. *Methods in Molecular Biology*, *1170*, 29–40. https://doi.org/10.1007/978-1-4939-0888-2_2

Barrientos, A., Zambrano, A., & Tzagoloff, A. (2004). Mss51p and Cox14p jointly regulate mitochondrial Cox1p expression in Saccharomyces cerevisiae. *The EMBO Journal*, *23*(17), 3472–3482. https://doi.org/10.1038/sj.emboj.7600358

Barros, M. H., Carlson, C. G., Glerum, D. M., & Tzagoloff, A. (2001). Involvement of mitochondrial ferredoxin and Cox15p in hydroxylation of heme O. *FEBS Letters*, *492*(1–2), 133–138. https://doi.org/10.1016/S0014-5793(01)02249-9

Barros, M. H., Johnson, A., & Tzagoloff, A. (2004). COX23, a homologue of COX17, is required for cytochrome oxidase assembly. *Journal of Biological Chemistry*, *279*(30), 31943–31947. https://doi.org/10.1074/jbc.M405014200

Beauchamp, C., & Fridovich, I. (1971). Superoxide dismutase: Improved assays and an assay applicable to acrylamide gels. *Analytical Biochemistry*, *44*(1), 276–287. https://doi.org/10.1016/0003-2697(71)90370-8

Beers, J., Glerum, D. M., & Tzagoloff, A. (1997). Purification, characterization, and localization of yeast Cox17p, a mitochondrial copper shuttle. *Journal of Biological Chemistry*, *272*(52), 33191–33196. https://doi.org/10.1074/jbc.272.52.33191

Bender, C. E., Fitzgerald, P., Tait, S. W. G., Llambi, F., McStay, G. P., Tupper, D. O., Pellettieri, J., Sánchez Alvarado, A., Salvesen, G. S., & Green, D. R. (2012). Mitochondrial pathway of apoptosis is ancestral in metazoans. *Proc. Natl. Acad. Sci. USA*, *109*(13), 4904–9. https://doi.org/10.1073/pnas.1120680109

Bénit, P., Slama, A., Cartault, F., Giurgea, I., Chretien, D., Lebon, S., Marsac, C., Munnich, A., Rötig, A., & Rustin, P. (2004). Mutant NDUFS3 subunit of mitochondrial complex I causes Leigh syndrome. *Journal of Medical Genetics*, *41*(1), 14–7. https://doi.org/10.1136/JMG.2003.014316

Bertoli, C., Skotheim, J. M., & de Bruin, R. A. M. (2013). Control of cell cycle transcription during G1 and S phases. *Nature Reviews. Molecular Cell Biology*, *14*(8), 518–28. https://doi.org/10.1038/nrm3629

Bode, M., Longen, S., Morgan, B., Peleh, V., Dick, T. P., Bihlmaier, K., & Herrmann, J. M. (2013). Inaccurately Assembled Cytochrome *c* Oxidase Can Lead to Oxidative Stress-Induced Growth Arrest. *Antioxidants & Redox Signaling*, *18*(13), 1597–1612. https://doi.org/10.1089/ars.2012.4685

Bode, M., Woellhaf, M. W., Bohnert, M., Laan, M. V. D., Sommer, F., Jung, M., Zimmermann, R., Schroda, M., & Herrmann, J. M. (2015). Redox-regulated dynamic interplay between Cox19 and the copper-binding protein Cox11 in the intermembrane space of mitochondria facilitates biogenesis of cytochrome c oxidase. *Molecular Biology of the Cell*, *26*(13), 2385–2401. https://doi.org/10.1091/mbc.E14-11-1526

Bragoszewski, P., Wasilewski, M., Sakowska, P., Gornicka, A., Böttinger, L., Qiu, J., Wiedemann, N., & Chacinska, A. (2015). Retro-translocation of mitochondrial intermembrane space proteins. *Proceedings of the National Academy of Sciences of the United States of America*, *112*(25), 7713–8. https://doi.org/10.1073/pnas.1504615112

Brown, N. G., Costanzo, M. C., & Fox, T. D. (1994). *Interactions among three proteins that specifically activate translation of the mitochondrial COX3 mRNA in Saccharomyces cerevisiae*. *Molecular and cellular biology* (Vol. 14). Section of Genetics and Development, Cornell University, Ithaca, New York 14853-2703.

Brown, R. M., & Brown, G. K. (1996). Complementation analysis of systemic cytochrome oxidase deficiency presenting as Leigh syndrome. *Journal of Inherited Metabolic Disease*, *19*(6), 752–60. https://doi.org/10.1007/BF01799168

Bryan, A. K., Goranov, A., Amon, A., & Manalis, S. R. (2010). Measurement of mass, density, and volume during the cell cycle of yeast. *Proceedings of the National Academy of Sciences*, *107*(3), 999–1004. https://doi.org/10.1073/pnas.0901851107

Büttner, S., Eisenberg, T., Carmona-Gutierrez, D., Ruli, D., Knauer, H., Ruckenstuhl, C., Sigrist, C., Wissing, S., Kollroser, M., Fröhlich, K. U., Sigrist, S., & Madeo, F. (2007). Endonuclease G Regulates Budding Yeast Life and Death. *Molecular Cell*, *25*(2), 233–246. https://doi.org/10.1016/j.molcel.2006.12.021

Büttner, S., Ruli, D., Vögtle, F.-N., Galluzzi, L., Moitzi, B., Eisenberg, T., Kepp, O., Habernig, L., Carmona-Gutierrez, D., Rockenfeller, P., Laun, P., Breitenbach, M., Khoury, C., Fröhlich, K.-U., Rechberger, G., Meisinger, C., Kroemer, G., & Madeo, F. (2011). A yeast BH3-only protein mediates the mitochondrial pathway of apoptosis. *The EMBO Journal*, *30*(14), 2779–2792. https://doi.org/10.1038/emboj.2011.197

Calvert, M. E. K., Lannigan, J. A., & Pemberton, L. F. (2008). Optimization of yeast cell cycle analysis and morphological characterization by multispectral imaging flow cytometry. *Cytometry. Part A : The Journal of the International Society for Analytical Cytology*, *73*(9), 825–833. https://doi.org/10.1002/cyto.a.20609

Carlson, C. G., Barrientos, A., Tzagoloff, A., & Glerum, D. M. (2003). COX16 encodes a novel protein required for the assembly of cytochrome oxidase in Saccharomyces cerevisiae. *The Journal of Biological Chemistry*, *278*(6), 3770–5. https://doi.org/10.1074/jbc.M209893200

Carmona-Gutierrez, D., Eisenberg, T., Büttner, S., Meisinger, C., Kroemer, G., & Madeo, F. (2010). Apoptosis in yeast: triggers, pathways, subroutines. *Cell Death & Differentiation*, *17*(5), 763–773. https://doi.org/10.1038/cdd.2009.219

Carr, H. S., Maxfield, A. B., Horng, Y. C., & Winge, D. R. (2005). Functional analysis of the domains in Cox11. *Journal of Biological Chemistry*, *280*(24), 22664–22669. https://doi.org/10.1074/jbc.M414077200

Chen, X. J., Wang, X., Kaufman, B. A., & Butow, R. A. (2005). Aconitase Couples Metabolic Regulation to Mitochondrial DNA Maintenance. *Science*, *307*(5710), 714–717. https://doi.org/10.1126/science.1106391

Chojnacka, M., Gornicka, A., Oeljeklaus, S., Warscheid, B., & Chacinska, A. (2015). Cox17 Protein Is an Auxiliary Factor Involved in the Control of the Mitochondrial Contact Site and Cristae Organizing System. *The Journal of Biological Chemistry*, *290*(24), 15304–12. https://doi.org/10.1074/jbc.M115.645069

Church, C., Goehring, B., Forsha, D., Wazny, P., & Poyton, R. O. (2005). A role for Pet100p in the assembly of yeast cytochrome c oxidase: Interaction with a subassembly that accumulates in a pet100 mutant. *Journal of Biological Chemistry*, *280*(3), 1854–1863. https://doi.org/10.1074/jbc.M410726200

Clark-Walker, G. D., & Linnane, A. W. (1966). In Vivo Differentiation of Yeast Cytoplasmic and Mitochondrial Protein Synthesis with Antibiotics. *Biochemical and Biophysical Research Communications*, *25*(1), 8–13. https://doi.org/10.1016/0006-291X(66)90631-0

Cobine, P. A., Ojeda, L. D., Rigby, K. M., & Winge, D. R. (2004). Yeast Contain A Non-proteinaceous Pool of Copper in the Mitochondrial Matrix. *Journal of Biological Chemistry*, *279*(14), 14447–14455. https://doi.org/10.1074/jbc.M312693200

Coenen, M. J. H., van den Heuvel, L. P., Nijtmans, L. G. J., Morava, E., Marquardt, I., Girschick, H. J., Trijbels, F. J. M., Grivell, L. A., & Smeitink, J. A. M. (1999). SURFEIT-1 Gene Analysis and Two-Dimensional Blue Native Gel Electrophoresis in Cytochrome c Oxidase Deficiency. *Biochemical and Biophysical Research Communications*, *265*(2), 339–344. https://doi.org/10.1006/bbrc.1999.1662

Cooper, M. P., Qu, L., Rohas, L. M., Lin, J., Yang, W., Erdjument-Bromage, H., Tempst, P., & Spiegelman, B. M. (2006). Defects in energy homeostasis in Leigh syndrome French Canadian variant through PGC-1α/LRP130 complex. *Genes and Development*, *20*(21), 2996–3009. https://doi.org/10.1101/gad.1483906

Crider, D. G., García-Rodríguez, L. J., Srivastava, P., Peraza-Reyes, L., Upadhyaya, K., Boldogh, I. R., & Pon, L. A. (2012). Rad53 is essential for a mitochondrial DNA inheritance checkpoint regulating G1 to S progression. *The Journal of Cell Biology*, *198*(5), 793–798. Retrieved from http://jcb.rupress.org/content/198/5/793

Danial, N. N., Korsmeyer, S. J., Acehan, D., Jiang, X., Morgan, D. G., Heuser, J. E., Wang, X., Akey, C. W., Alimonti, J. B., … Wang, X. (2004). Cell death: critical control points. *Cell*, *116*(2), 205–19. https://doi.org/10.1016/S0092-8674(04)00046-7

Davidson, G. S., Joe, R. M., Roy, S., Meirelles, O., Allen, C. P., Wilson, M. R., Tapia, P. H., Manzanilla, E. E., Dodson, A. E., Chakraborty, S., Carter, M., Young, S., Edwards, B., Sklar, L., & Werner-Washburne, M. (2011). The proteomics of quiescent and nonquiescent cell differentiation in yeast stationary-phase cultures. *Molecular Biology of the Cell*, *22*(7), 988–998. https://doi.org/10.1091/mbc.E10-06-0499

Davidson, J. F., & Schiestl, R. H. (2001). Mitochondrial Respiratory Electron Carriers Are Involved in Oxidative Stress during Heat Stress inSaccharomyces cerevisiae Mitochondrial Respiratory Electron Carriers Are Involved in Oxidative Stress during Heat Stress in Saccharomyces cerevisiae. *Molecular and Cellular Biology*, *21*(24), 8483–8489. https://doi.org/10.1128/MCB.21.24.8483

Debray, F. G., Lambert, M., Lortie, A., Vanasse, M., & Mitchell, G. A. (2007). Long-term outcome of leigh syndrome caused by the NARP-T8993C mtDNA mutation. *American Journal of Medical Genetics, Part A*, *143*(17), 2046–2051. https://doi.org/10.1002/ajmg.a.31880

Delobel, P., & Tesnière, C. (2014). A Simple FCM Method to Avoid Misinterpretation in Saccharomyces cerevisiae Cell Cycle Assessment between G0 and Sub-G1. *PLoS ONE*, *9*(1), e84645. https://doi.org/10.1371/journal.pone.0084645

Dickinson, E. K., Adams, D. L., Schon, E. A., & Glerum, D. M. (2000). A human SCO2 mutation helps define the role of scolp in the cytochrome oxidase assembly pathway. *Journal of Biological Chemistry*, *275*(35), 26780–26785. https://doi.org/10.1074/jbc.M004032200

DiMauro, S., Schon, E. A., Carelli, V., & Hirano, M. (2013). The clinical maze of mitochondrial neurology. *Nature Reviews Neurology*, *9*(8), 429–444.

Dimauro, S., Tanji, K., & Schon, E. A. (2012). The many clinical faces of cytochrome c oxidase deficiency. *Advances in Experimental Medicine and Biology*, *748*, 341–357. https://doi.org/10.1007/978-1-4614-3573-0_14

Dong, K., Addinall, S. G., Lydall, D., & Rutherford, J. C. (2013). The yeast copper response is regulated by DNA damage. *Molecular and Cellular Biology*, *33*(20), 4041–50. https://doi.org/10.1128/MCB.00116-13

Drummond-Barbosa, D. (2008). Stem cells, their niches and the systemic environment: An aging network. *Genetics*. https://doi.org/10.1534/genetics.108.098244

Eser, U., Falleur-Fettig, M., Johnson, A., & Skotheim, J. M. (2011). Commitment to a cellular transition precedes genome-wide transcriptional change. *Molecular Cell*, *43*(4), 515–27. https://doi.org/10.1016/j.molcel.2011.06.024

Fasching, P. A., Pharoah, P. D. P., Cox, A., Nevanlinna, H., Bojesen, S. E., Karn, T., Broeks, A., Van Leeuwen, F. E., Van't Veer, L. J., … Schmidt, M. K. (2012). The role of genetic breast cancer susceptibility variants as prognostic factors. *Human Molecular Genetics*, *21*(17), 3926–3939. https://doi.org/10.1093/hmg/dds159

Finsterer, J., Leigh, D., Pronicki, M., Matyja, E., Piekutowska-Abramczuk, D., Al., E., Debray, F. G., Lambert, M., Lortie, A., … Al., E. (2008). Leigh and Leigh-like syndrome in children and adults. *Pediatric Neurology*, *39*(4), 223–35. https://doi.org/10.1016/j.pediatrneurol.2008.07.013

Fontanesi, F., Jin, C., Tzagoloff, A., & Barrientos, A. (2008). Transcriptional activators HAP/NF-Y rescue a cytochrome c oxidase defect in yeast and human cells. *Human Molecular Genetics*, *17*(6), 775–788. https://doi.org/10.1093/hmg/ddm349

Fontanesi, F., Soto, I. C., & Barrientos, A. (2008, September). Cytochrome c oxidase biogenesis: New levels of regulation. *IUBMB Life*. NIH Public Access. https://doi.org/10.1002/iub.86

Forsburg, S. L., & Nurse, P. (1991). Cell Cycle Regulation in the Yeasts Saccharomyces cerevisiae and Schizosaccharomyces pombe. *Annual Review of Cell Biology*, *7*(1), 227–256. https://doi.org/10.1146/annurev.cb.07.110191.001303

Fowler, L. R., Richardson, S. H., & Hatefi, Y. (1962). *A rapid method for the preparation of highly purified cytochrome oxidase*. *Biochimica et biophysica acta* (Vol. 64). Elsevier.

Fridovich, I. (1999). Fundamental aspects of reactive oxygen species, or what's the matter with oxygen? *Annals of the New York Academy of Sciences*, *893*, 13–8. https://doi.org/10.1111/j.1749-6632.1999.tb07814.x

Giannattasio, S., Atlante, A., Antonacci, L., Guaragnella, N., Lattanzio, P., Passarella, S., & Marra, E. (2008). Cytochrome c is released from coupled mitochondria of yeast en route to acetic acid-induced programmed cell death and can work as an electron donor and a ROS scavenger. *FEBS Letters*, *582*(10), 1519–1525. https://doi.org/10.1016/j.febslet.2008.03.048

Giannattasio, S., Guaragnella, N., Corte-Real, M., Passarella, S., & Marra, E. (2005). Acid stress adaptation protects Saccharomyces cerevisiae from acetic acid-induced programmed cell death. In *Gene* (Vol. 354, pp. 93–98). https://doi.org/10.1016/j.gene.2005.03.030

Glerum, D. M., Shtanko, A., & Tzagoloff, A. (1996a). Characterization of COX17, a yeast gene involved in copper metabolism and assembly of cytochrome oxidase. *Journal of Biological Chemistry*, *271*(24), 14504–14509. https://doi.org/10.1074/jbc.271.24.14504

Glerum, D. M., Shtanko, A., & Tzagoloff, A. (1996b). SCO1 and SCO2 act as high copy suppressors of a mitochondrial copper recruitment defect in Saccharomyces cerevisiae. *Journal of Biological Chemistry*, *271*(34), 20531–20535. https://doi.org/10.1074/jbc.271.34.20531

Glover, E. I., Martin, J., Maher, A., Thornhill, R. E., Moran, G. R., & Tarnopolsky, M. A. (2010). A randomized trial of coenzyme Q10 in mitochondrial disorders. *Muscle & Nerve*, *42*(5), 739–748. https://doi.org/10.1002/mus.21758

Gonzalez, C., Hadany, L., Ponder, R. G., Price, M., Hastings, P. J., & Rosenberg, S. M. (2008). Mutability and importance of a hypermutable cell subpopulation that produces stress-induced mutants in Escherichia coli. *PLoS Genetics*, *4*(10), e1000208. https://doi.org/10.1371/journal.pgen.1000208

Gray, J. V, Petsko, G. A., Johnston, G. C., Ringe, D., Singer, R. A., & Werner-Washburne, M. (2004). "Sleeping beauty": quiescence in Saccharomyces cerevisiae. *Microbiology and Molecular Biology Reviews : MMBR*, *68*(2), 187–206. https://doi.org/10.1128/MMBR.68.2.187-206.2004

Guaragnella, N., Antonacci, L., Giannattasio, S., Marra, E., & Passarella, S. (2008). Catalase T and Cu, Zn-superoxide dismutase in the acetic acid-induced programmed cell death in Saccharomyces cerevisiae. *FEBS Letters*, *582*(2), 210–214. https://doi.org/10.1016/j.febslet.2007.12.007

Guaragnella, N., Bobba, A., Passarella, S., Marra, E., & Giannattasio, S. (2010). Yeast acetic acid-induced programmed cell death can occur without cytochrome c release which requires metacaspase YCA1. *FEBS Letters*, *584*(1), 224–228. https://doi.org/10.1016/j.febslet.2009.11.072

Guaragnella, N., Passarella, S., Marra, E., & Giannattasio, S. (2010). Knock-out of metacaspase and/or cytochrome c results in the activation of a ROS-independent acetic acid-induced programmed cell death pathway in yeast. *FEBS Letters*, *584*(16), 3655–3660. https://doi.org/10.1016/j.febslet.2010.07.044

Guaragnella, N., Passarella, S., Marra, E., & Giannattasio, S. (2011). Cytochrome c Trp65Ser substitution results in inhibition of acetic acid-induced programmed cell death in Saccharomyces cerevisiae. *Mitochondrion*, *11*(6), 987–991. https://doi.org/10.1016/j.mito.2011.08.007

Guaragnella, N., Pereira, C., Sousa, M. J., Antonacci, L., Passarella, S., Côrte-Real, M., Marra, E., & Giannattasio, S. (2006). YCA1 participates in the acetic acid induced yeast programmed cell death also in a manner unrelated to its caspase-like activity. *FEBS Letters*, *580*(30), 6880–6884. https://doi.org/10.1016/j.febslet.2006.11.050

Guaragnella, N., Zdralević, M., Antonacci, L., Passarella, S., Marra, E., & Giannattasio, S. (2012). The role of mitochondria in yeast programmed cell death. *Frontiers in Oncology*, *2*(July), 70. https://doi.org/10.3389/fonc.2012.00070

Guaragnella et al. (2007). Hydrogen Peroxide and Superoxide Anion production during acetic-acid-induced yeast programmed cell death. *Folia Microbiol*, *52*(3), 237–240. https://doi.org/10.1007/BF02931304

Guo, J., & Lemire, B. D. (2003). The Ubiquinone-binding Site of the Saccharomyces cerevisiae Succinate-Ubiquinone Oxidoreductase Is a Source of Superoxide. *Journal of Biological Chemistry*, *278*(48), 47629–47635. https://doi.org/10.1074/jbc.M306312200

Halliwell, B., & Gutteridge, J. M. C. (1990). Role of free radicals and catalytic metal ions in human disease: An overview. *Methods in Enzymology*, *186*(C), 1–85. https://doi.org/10.1016/0076-6879(90)86093-B

Hangen, E., Blomgren, K., Bénit, P., Kroemer, G., & Modjtahedi, N. (2010). Life with or without AIF. *Trends in Biochemical Sciences*. https://doi.org/10.1016/j.tibs.2009.12.008

Harner, M. E., Unger, A. K., Izawa, T., Walther, D. M., Özbalci, C., Geimer, S., Reggiori, F., Brügger, B., Mann, M., Westermann, B., & Neupert, W. (2014). Aim24 and MICOS modulate respiratory function, tafazzin-related cardiolipin modification and mitochondrial architecture. *eLife*, *2014*(3), e01684. https://doi.org/10.7554/eLife.01684

Hartwell, L. H.; Mortimer, R. K. ; Culotti, J.; and Culotti, M. (1973). Genetic control of the cell division cycle in yeast: V. genetic analyis of cdc mutants. *Genetics*, *74*(2), 74: 267-268. https://doi.org/74(2): 267–286.

Hartwell, L. H. (1974). Saccharomyces cerevisiae cell cycle. *Bacteriological Reviews*, *38*(2), 164–198. https://doi.org/38(2): 164–198.

Heaton, D. N., George, G. N., Garrison, G., & Winge, D. R. (2001). The mitochondrial copper metallochaperone Cox17 exists as an oligomeric, polycopper complex. *Biochemistry*, *40*(3), 743–751.

Hederstedt, L. (2012). Heme A biosynthesis. *BBA-Bioenergetics*, *1817*(6), 920–927. https://doi.org/10.1016/j.bbabio.2012.03.025

Hell, K., Herrmann, J. M., Pratje, E., Neupert, W., & Stuart, R. A. (1998). Oxa1p, an essential component of the N-tail protein export machinery in mitochondria. *Proceedings of the National Academy of Sciences*, *95*(5), 2250–2255. https://doi.org/10.1073/pnas.95.5.2250

Hell, K., Tzagoloff, A., Neupert, W., & Stuart, R. A. (2000). Identification of Cox20p, a novel protein involved in the maturation and assembly of cytochrome oxidase subunit 2. *Journal of Biological Chemistry*, *275*(7), 4571–4578. https://doi.org/10.1074/jbc.275.7.4571

Herker, E., Jungwirth, H., Lehmann, K. A., Maldener, C., Fröhlich, K. U., Wissing, S., Büttner, S., Fehr, M., Sigrist, S., & Madeo, F. (2004). Chronological aging leads to apoptosis in yeast. *Journal of Cell Biology*, *164*(4), 501–507. https://doi.org/10.1083/jcb.200310014

Herman, P. K. (2002, December). Stationary phase in yeast. *Current Opinion in Microbiology*. https://doi.org/10.1016/S1369-5274(02)00377-6

Herrero, E., Ros, J., Bellí, G., & Cabiscol, E. (2008). Redox control and oxidative stress in yeast cells. *Biochimica et Biophysica Acta (BBA) - General Subjects*, *1780*(11), 1217–1235. https://doi.org/10.1016/j.bbagen.2007.12.004

Holley, R. W., & Kiernan, J. A. (1974). Control of the initiation of DNA synthesis in 3T3 cells: low-molecular weight nutrients. *Proceedings of the National Academy of Sciences*, *71*(8), 2942–5.

Holt, I. J., Harding, A. E., Cooper, J. M., Schapira, A. H. V., Toscano, A., Clark, J. B., & Morgan-Hughes, J. A. (1989). Mitochondrial myopathies: Clinical and biochemical features of 30 patients with major deletions of muscle mitochondrial DNA. *Annals of Neurology*, *26*(6), 699–708. https://doi.org/10.1002/ana.410260603

Horan, S., Bourges, I., Taanman, J.-W., & Meunier, B. (2005). Analysis of COX2 mutants reveals cytochrome oxidase subassemblies in yeast. *The Biochemical Journal*, *390*(Pt 3), 703–8. https://doi.org/10.1042/BJ20050598

Horn, D., Al-Ali, H., & Barrientos, A. (2008). Cmc1p is a conserved mitochondrial twin CX9C protein involved in cytochrome c oxidase biogenesis. *Molecular and Cellular Biology*, *28*(13), 4354–4364. https://doi.org/10.1128/MCB.01920-07

Horng, Y. C., Cobine, P. A., Maxfield, A. B., Carr, H. S., & Winge, D. R. (2004). Specific copper transfer from the Cox17 metallochaperone to both Sco1 and Cox11 in the assembly of yeast cytochrome c oxidase. *Journal of Biological Chemistry*, *279*(34), 35334–35340. https://doi.org/10.1074/jbc.M404747200

Horváth, R., Abicht, A., Holinski-Feder, E., Laner, A., Gempel, K., Prokisch, H., Lochmüller, H., Klopstock, T., & Jaksch, M. (2006). Leigh syndrome caused by mutations in the flavoprotein (Fp) subunit of succinate dehydrogenase (SDHA). *Journal of Neurology, Neurosurgery, and Psychiatry*, *77*(1), 74–6. https://doi.org/10.1136/jnnp.2005.067041

Hüttemann, M., Pecina, P., Rainbolt, M., Sanderson, T. H., Kagan, V. E., Samavati, L., Doan, J. W., & Lee, I. (2011). The multiple functions of cytochrome c and their regulation in life and death decisions of the mammalian cell: From respiration to apoptosis. *Mitochondrion*, *11*(3), 369–381. https://doi.org/10.1016/j.mito.2011.01.010

John, G. B., Shang, Y., Li, L., Renken, C., Mannella, C. A., Selker, J. M. L., Rangell, L., Bennett, M. J., & Zha, J. (2005). The mitochondrial inner membrane protein mitofilin controls cristae morphology. *Molecular Biology of the Cell*, *16*(3), 1543–54. https://doi.org/10.1091/mbc.E04-08-0697

Joseph-Horne, T., Hollomon, D. W., & Wood, P. M. (2001). Fungal respiration: A fusion of standard and alternative components. *Biochimica et Biophysica Acta - Bioenergetics*. https://doi.org/10.1016/S0005-2728(00)00251-6

Kaeberlein, M., McVey, M., & Guarente, L. (1999). The SIR2/3/4 complex and SIR2 alone promote longevity in Saccharomyces cerevisiae by two different mechanisms. *Genes and Development*, *13*(19), 2570–2580. https://doi.org/10.1101/gad.13.19.2570

Kanki, T., Furukawa, K., & Yamashita, S. I. (2015). Mitophagy in yeast: Molecular mechanisms and physiological role. *Biochimica et Biophysica Acta - Molecular Cell Research*. https://doi.org/10.1016/j.bbamcr.2015.01.005

Kannan, F., Jain, G. A., Meyer, B. I., Roth, K. A., Gruss, P., Karasuyama, H., Su, M. S., Rakic, P., Flavell, R. A., Khoo, W., Potter, J., Yoshida, R., Kaufman, S. A., Lowe, S. W., Penninger, J. M., & Mak, T. W. (2000). Oxidative stress and apoptosis. *Pathophysiology : The Official Journal of the International Society for Pathophysiology*, *7*(3), 153–163. https://doi.org/10.1016/S0928-4680(00)00053-5

Khalimonchuk, O., Rigby, K., Bestwick, M., Pierrel, F., Cobine, P. A., & Winge, D. R. (2008). Pet191 is a cytochrome c oxidase assembly factor in Saccharomyces cerevisiae. *Eukaryotic Cell*, *7*(8), 1427–1431. https://doi.org/10.1128/EC.00132-08

Kirchman, P. A., Kim, S., Lai, C. Y., & Michal Jazwinski, S. (1999). Interorganelle signaling is a determinant of longevity in Saccharomyces cerevisiae. *Genetics*, *152*(1), 179–190. https://doi.org/10.1023/a:1006847319162

Kluck, R. M., Ellerby, L. M., Ellerby, H. M., Naiem, S., Yaffe, M. P., Margoliash, E., Bredesen, D., Mauk, A. G., Sherman, F., & Newmeyer, D. D. (2000). Determinants of cytochrome c pro-apoptotic activity. The role of lysine 72 trimethylation. *The Journal of Biological Chemistry*, *275*(21), 16127–33. https://doi.org/10.1074/JBC.275.21.16127

Koenig, M. K. (2008). Presentation and Diagnosis of Mitochondrial Disorders in Children. *Pediatric Neurology*. https://doi.org/10.1016/j.pediatrneurol.2007.12.001

Labib, K. (2010). How do Cdc7 and cyclin-dependent kinases trigger the initiation of chromosome replication in eukaryotic cells? *Genes & Development*, *24*(12), 1208–1219. https://doi.org/10.1101/gad.1933010

Lasserre, J. P., Dautant, A., Aiyar, R. S., Kucharczyk, R., Glatigny, A., Tribouillard-Tanvier, D., Rytka, J., Blondel, M., Skoczen, N., Reynier, P., Pitayu, L., Rotig, A., Delahodde, A., Steinmetz, L. M., Dujardin, G., Procaccio, V., & di Rago, J. P. (2015). Yeast as a system for modeling mitochondrial disease mechanisms and discovering therapies. *Disease Models & Mechanisms*, *8*(6), 509–526. https://doi.org/10.1242/dmm.020438 [doi]

Laun, P., Rinnerthaler, M., Bogengruber, E., Heeren, G., & Breitenbach, M. (2006). Yeast as a model for chronological and reproductive aging - A comparison. *Experimental Gerontology*. https://doi.org/10.1016/j.exger.2006.11.001

Leary, S. C., Cobine, P. A., Kaufman, B. A., Guercin, G.-H., Mattman, A., Palaty, J., Lockitch, G., Winge, D. R., Rustin, P., Horvath, R., & Shoubridge, E. A. (2007). The Human Cytochrome c Oxidase Assembly Factors SCO1 and SCO2 Have Regulatory Roles in the Maintenance of Cellular Copper Homeostasis. *Cell Metabolism*, *5*(1), 9–20. https://doi.org/10.1016/j.cmet.2006.12.001

Leary, S. C., Cobine, P. A., Nishimura, T., Verdijk, R. M., de Krijger, R., de Coo, R., Tarnopolsky, M. A., Winge, D. R., & Shoubridge, E. A. (2013). COX19 mediates the transduction of a mitochondrial redox signal from SCO1 that regulates ATP7A-mediated cellular copper efflux. *Molecular Biology of the Cell*, *24*(6), 683–91. https://doi.org/10.1091/mbc.E12-09-0705

Leary, S. C., Winge, D. R., & Cobine, P. A. (2009). "Pulling the plug" on cellular copper: The role of mitochondria in copper export. *Biochimica et Biophysica Acta - Molecular Cell Research*. https://doi.org/10.1016/j.bbamcr.2008.05.002

Lee, I. H., & Finkel, T. (2013). Metabolic regulation of the cell cycle. *Current Opinion in Cell Biology*. https://doi.org/10.1016/j.ceb.2013.07.002

Leigh, D. (1951). *Subacute necrotizing encephalomyelopathy in an infant*. *Journal of neurology, neurosurgery, and psychiatry* (Vol. 14). Not Available.

Li, L. Y., Luo, X., & Wang, X. (2001). Endonuclease G is an apoptotic DNase when released from mitochondria. *Nature*, *412*(6842), 95–99. https://doi.org/10.1038/35083620

Li, W., Sun, L., Liang, Q., Wang, J., Mo, W., & Zhou, B. (2006). Yeast AMID homologue Ndi1p displays respiration-restricted apoptotic activity and is involved in chronological aging. *Molecular Biology of the Cell*, *17*(4), 1802–11. https://doi.org/10.1091/mbc.E05-04-0333

Lode, A., Kuschel, M., Paret, C., & Rödel, G. (2000). Mitochondrial copper metabolism in yeast: Interaction between Sco1p and Cox2p. *FEBS Letters*, *485*(1), 19–24. https://doi.org/10.1016/S0014-5793(00)02176-1

Longo, V. D., Gralla, E. B., & Valentine, J. S. (1996). Superoxide Dismutase Activity Is Essential for Stationary Phase Survival in Saccharomyces cerevisiae. *Biochemistry*, *271*(21), 12275–12280.

Longo, V. D., Shadel, G. S., Kaeberlein, M., & Kennedy, B. (2012). Replicative and chronological aging in saccharomyces cerevisiae. *Cell Metabolism*, *16*(1), 18–31. https://doi.org/10.1016/j.cmet.2012.06.002

Lowry, O. H., Roserbrough, N. J., Farr, A. L., & Randall, R. J. (1951). Protein measurement with the Folin phenol reagent. *The Journal of Biological Chemistry*, *193*(1), 265–75.

Ludovico, P., Rodrigues, F., Almeida, A., Silva, M. T., Barrientos, A., & Côrte-Real, M. (2002). Cytochrome c Release and Mitochondria Involvement in Programmed Cell Death Induced by Acetic Acid in Saccharomyces cerevisiae. *Molecular Biology of the Cell*, *13*(8), 2598–2606. https://doi.org/10.1091/mbc.E01-12-0161

Luft, R. (1995). The development of mitochondrial medicine. *BBA - Molecular Basis of Disease*, *1271*(1), 1–6. https://doi.org/10.1016/0925-4439(95)00002-L

Luft, R., Ikkos, D., Palmieri, G., Ernster, L., & Afzelius, B. (1962). A case of severe hypermetabolism of nonthyroid origin with a defect in the maintenance of mitochondrial respiratory control: a correlated clinical, biochemical, and morphological study. *The Journal of Clinical Investigation*, *41*, 1776–1804. https://doi.org/10.1172/JCI104637

Madeo, F., Carmona-Gutierrez, D., Ring, J., Büttner, S., Eisenberg, T., & Kroemer, G. (2009). Caspase-dependent and caspase-independent cell death pathways in yeast. *Biochemical and Biophysical Research Communications*. https://doi.org/10.1016/j.bbrc.2009.02.117

Madeo, F., Fröhlich, E., & Fröhlich, K. U. (1997). A yeast mutant showing diagnostic markers of early and late apoptosis. *Journal of Cell Biology*, *139*(3), 729–734. https://doi.org/10.1083/jcb.139.3.729

Madeo, F., Herker, E., Maldener, C., Wissing, S., Lächelt, S., Herlan, M., Fehr, M., Lauber, K., Sigrist, S. J., Wesselborg, S., & Fröhlich, K. U. (2002). A caspase-related protease regulates apoptosis in yeast. *Molecular Cell*, *9*(4), 911–917. https://doi.org/10.1016/S1097-2765(02)00501-4

Makovets, S., & Blackburn, E. H. (2009). DNA damage signalling prevents deleterious telomere addition at DNA breaks. *Nature Cell Biology*, *11*(11), 1383–1386. https://doi.org/10.1038/ncb1985

Mandal, S., Freije, W. A., Guptan, P., & Banerjee, U. (2010). Metabolic control of G1-S transition: Cyclin E degradation by p53-induced activation of the ubiquitin-proteasome system. *Journal of Cell Biology*, *188*(4), 473–479. https://doi.org/10.1083/jcb.200912024

Mandal, S., Guptan, P., Owusu-Ansah, E., & Banerjee, U. (2005). Mitochondrial regulation of cell cycle progression during development as revealed by the tenured mutation in Drosophila. *Developmental Cell*, *9*(6), 843–854. https://doi.org/10.1016/j.devcel.2005.11.006

Mannella, C. A. (2006). *Structure and dynamics of the mitochondrial inner membrane cristae*. *Biochimica et Biophysica Acta (BBA)-Molecular Cell Research* (Vol. 1763). Elsevier.

Manon, S., Chaudhuri, B., & Guérin, M. (1997). Release of cytochrome c and decrease of cytochrome c oxidase in Bax-expressing yeast cells, and prevention of these effects by coexpression of Bcl-x L. *FEBS Letters*, *415*(1), 29–32. https://doi.org/10.1016/S0014-5793(97)01087-9

Manthey, G. M., & McEwen, J. E. (1995). The product of the nuclear gene PET309 is required for translation of mature mRNA and stability or production of intron-containing RNAs derived from the mitochondrial COX1 locus of Saccharomyces cerevisiae. *The EMBO Journal*, *14*(16), 4031–4043.

Martínez-Morentin, L., Martínez, L., Piloto, S., Yang, H., Schon, E. A., Garesse, R., Bodmer, R., Ocorr, K., Cervera, M., & Arredondo, J. J. (2015). Cardiac deficiency of single cytochrome oxidase assembly factor scox induces p53-dependent apoptosis in a Drosophila cardiomyopathy model. *Human Molecular Genetics*, *24*(13), 3608–3622. https://doi.org/10.1093/hmg/ddv106

Martins, D., & English, A. M. (2014). SOD1 oxidation and formation of soluble aggregates in yeast: Relevance to sporadic ALS development. *Redox Biology*, *2*(1), 632–639. https://doi.org/10.1016/j.redox.2014.03.005

Mashkevich, G., Repetto, B., Glerum, D. M., Jin, C., & Tzagoloff, A. (1997). SHY1, the Yeast Homolog of the MammalianSURF-1 Gene, Encodes a Mitochondrial Protein Required for Respiration. *Journal of Biological Chemistry*, *272*(22), 14356–14364. https://doi.org/10.1074/jbc.272.22.14356

Maxfield, A. B., Heaton, D. N., & Winge, D. R. (2004). Cox17 Is Functional When Tethered to the Mitochondrial Inner Membrane. *Journal of Biological Chemistry*, *279*(7), 5072–5080. https://doi.org/10.1074/jbc.M311772200

McEwan, A. G., Lewin, A., Davy, S. L., Boetzel, R., Leech, A., Walker, D., Wood, T., & Moore, G. R. (2002). PrrC from Rhodobacter sphaeroides, a homologue of eukaryotic Sco proteins, is a copper-binding protein and may have a thiol-disulfide oxidoreductase activity. *FEBS Letters*, *518*(1), 10–16. https://doi.org/10.1016/S0014-5793(02)02532-2

McFarland, R., Taylor, R. W., & Turnbull, D. M. (2002). The neurology of mitochondrial DNA disease. *Lancet Neurology*. https://doi.org/10.1016/S1474-4422(02)00159-X

McFarland, R., Taylor, R. W., & Turnbull, D. M. (2010). A neurological perspective on mitochondrial disease. *The Lancet Neurology*. https://doi.org/10.1016/S1474-4422(10)70116-2

McStay, G. P., Su, C. H., & Tzagoloff, A. (2013). Modular assembly of yeast cytochrome oxidase. *Molecular Biology of the Cell*, *24*(4), 440–52. https://doi.org/10.1091/mbc.E12-10-0749

Mick, D. U., Vukotic, M., Piechura, H., Meyer, H. E., Warscheid, B., Deckers, M., & Rehling, P. (2010). Coa3 and Cox14 are essential for negative feedback regulation of COX1 translation in mitochondria. *Journal of Cell Biology*, *191*(1), 141–154. https://doi.org/10.1083/jcb.201007026

Moore, J. K., & Miller, R. K. (2007). The cyclin-dependent kinase Cdc28p regulates multiple aspects of Kar9p function in yeast. *Mol Biol Cell*, *18*(4), 1187–1202. https://doi.org/10.1091/mbc.E06-04-0360

Moraes, C. T., Diaz, F., & Barrientos, A. (2004). Defects in the biosynthesis of mitochondrial heme c and heme a in yeast and mammals. In *Biochimica et Biophysica Acta - Bioenergetics* (Vol. 1659, pp. 153–159). https://doi.org/10.1016/j.bbabio.2004.09.002

Morgan, D. O. (1995, March 9). Principles of CDK regulation. *Nature*. https://doi.org/10.1038/374131a0

Mortimer, R. K., & Johnston, J. R. (1959). Life Span of Individual Yeast Cells. *Nature*, *183*(4677), 1751–1752. https://doi.org/10.1038/1831751a0

Mulero, J. J., & Fox, T. D. (1993). PET111 acts in the 5'-leader of the Saccharomyces cerevisiae mitochondrial COX2 mRNA to promote its translation. *Genetics*, *133*(3), 509–516.

Munaro, M., Tiranti, V., Sandonà, D., Lamantea, E., Uziel, G., Bisson, R., & Zeviani, M. (1997). A single cell complementation class is common to several cases of cytochrome c oxidase-defective Leigh's syndrome. *Human Molecular Genetics*, *6*(2), 221–228. https://doi.org/10.1093/hmg/6.2.221

Murakami, K., & Yoshino, M. (1997). Inactivation of aconitase in yeast exposed to oxidative stress. *IUBMB Life*, *41*(3), 481–486. https://doi.org/10.1080/15216549700201501

Murray, A. W. (2004). Recycling the Cell Cycle: Cyclins Revisited. *Cell*. https://doi.org/10.1016/S0092-8674(03)01080-8

Nasmyth, K. (1996). At the heart of the budding yeast cell cycle. *Trends in Genetics*, *12*(10), 405–412. https://doi.org/10.1016/0168-9525(96)10041-X

Nijtmans, L. G. J., Taanman, J., Muijsers, A. O., Speijer, D., & Van den Bogert, C. (1998). *Assembly of cytochrome-c oxidase in cultured human cells*. *European Journal of Biochemistry* (Vol. 254). Wiley Online Library.

Ott, M., Prestele, M., Bauerschmitt, H., Funes, S., Bonnefoy, N., & Herrmann, J. M. (2006). Mba1, a membrane-associated ribosome receptor in mitochondria. *{EMBO} J.*, *25*(8), 1603–1610. https://doi.org/10.1038/sj.emboj.7601070

Outten, C. E., & Culotta, V. C. (2003). A novel NADH kinase is the mitochondrial source of NADPH in Saccharomyces cerevisiae. *The EMBO Journal*, *22*(9), 2015–24. https://doi.org/10.1093/emboj/cdg211

Owusu-Ansah, E., Yavari, A., Mandal, S., & Banerjee, U. (2008). Distinct mitochondrial retrograde signals control the G1-S cell cycle checkpoint. *Nature Genetics*, *40*(3), 356–61. https://doi.org/10.1038/ng.2007.50

Papadopoulou, L. C., Sue, C. M., Davidson, M. M., Tanji, K., Nishino, I., Sadlock, J. E., Krishna, S., Walker, W., Selby, J., Glerum, D. M., Coster, R. Van, Lyon, G., Scalais, E., Lebel, R., Kaplan, P., Shanske, S., De Vivo, D. C., Bonilla, E., Hirano, M., DiMauro, S., & Schon, E. A. (1999). Fatal infantile cardioencephalomyopathy with COX deficiency and mutations in SCO2, a COX assembly gene. *Nature Genetics*, *23*(3), 333–7. https://doi.org/10.1038/15513

Paupe, V., Prudent, J., Dassa, E. P., Rendon, O. Z., & Shoubridge, E. A. (2015). *CCDC90A (MCUR1) Is a Cytochrome c Oxidase Assembly Factor and Not a Regulator of the Mitochondrial Calcium Uniporter*. *Cell Metabolism* (Vol. 21). https://doi.org/10.1016/j.cmet.2014.12.004

Pereira, C., Camougrand, N., Manon, S., Sousa, M. J., & Côrte-Real, M. (2007). ADP/ATP carrier is required for mitochondrial outer membrane permeabilization and cytochrome c release in yeast apoptosis. *Molecular Microbiology*, *66*(3), 571–582. https://doi.org/10.1111/j.1365-2958.2007.05926.x

Piao, Y.-S., Tang, G.-C., Yang, H., & Lu, D.-H. (2006). Clinico-neuropathological study of a Chinese case of familial adult Leigh syndrome. *Neuropathology*, *26*(3), 218–221. https://doi.org/10.1111/j.1440-1789.2006.00686.x

Piatti, S., Lengauer, C., & Nasmyth, K. (1995). Cdc6 is an unstable protein whose de novo synthesis in G1 is important for the onset of S phase and for preventing a “reductional” anaphase in the budding yeast Saccharomyces cerevisiae. *The EMBO Journal*, *14*(15), 3788–3799. Retrieved from http://www.ncbi.nlm.nih.gov/pubmed/7641697

Pierrel, F., Bestwick, M. L., Cobine, P. A., Khalimonchuk, O., Cricco, J. A., & Winge, D. R. (2007). Coa1 links the Mss51 post-translational function to Cox1 cofactor insertion in cytochrome c oxidase assembly. *The EMBO Journal*, *26*, 4335–4346. https://doi.org/10.1038/

Porcelli, D., Oliva, M., Duchi, S., Latorre, D., Cavaliere, V., Barsanti, P., Villani, G., Gargiulo, G., & Caggese, C. (2010). Genetic, functional and evolutionary characterization of scox, the Drosophila melanogaster ortholog of the human SCO1 gene. *Mitochondrion*, *10*(5), 433–448. https://doi.org/10.1016/j.mito.2010.04.002

Poyton, R. O., & Schatz, G. (1975). Cytochrome c oxidase from bakers' yeast. III. Physical characterization of isolated subunits and chemical evidence for two different classes of polypeptides. *The Journal of Biological Chemistry*, *250*(2), 752–761.

Punter, F. A., & Glerum, D. M. (2003). Mutagenesis reveals a specific role for Cox17p in copper transport to cytochrome oxidase. *Journal of Biological Chemistry*, *278*(33), 30875–30880. https://doi.org/10.1074/jbc.M302358200

Rabl, R., Soubannier, V., Scholz, R., Vogel, F., Mendl, N., Vasiljev-Neumeyer, A., Körner, C., Jagasia, R., Keil, T., Baumeister, W., Cyrklaff, M., Neupert, W., & Reichert, A. S. (2009). Formation of cristae and crista junctions in mitochondria depends on antagonism between Fcj1 and Su e/g. *The Journal of Cell Biology*, *185*(6), 1047–63. https://doi.org/10.1083/jcb.200811099

Rahman, S., Blok, R. B., Dahl, H.-H. H. M., Danks, D. M., Kirby, D. M., Chow, C. W., Christodoulou, J., & Thorburn, D. R. (1996). Leigh syndrome: Clinical features and biochemical and DNA abnormalities. *Annals of Neurology*, *39*(3), 343–351. https://doi.org/10.1002/ana.410390311

Reddi, A. R., & Culotta, V. C. (2013). SOD1 integrates signals from oxygen and glucose to repress respiration. *Cell*, *152*(1–2), 224–235. https://doi.org/10.1016/j.cell.2012.11.046

Ribeiro, G. F., Côrte-Real, M., & Johansson, B. (2006). Characterization of DNA damage in yeast apoptosis induced by hydrogen peroxide, acetic acid, and hyperosmotic shock. *Molecular Biology of the Cell*, *17*(10), 4584–91. https://doi.org/10.1091/mbc.E06-05-0475

Rich, P. R., & Marechal, A. (2010). The mitochondrial respiratory chain. *Essays in Biochemistry*, *47*, 1–23. https://doi.org/10.1042/bse0470001; 10.1042/bse0470001

Rivin, C. J., & Fangman, W. L. (1980). Cell cycle phase expansion in nitrogen-limited cultures of Saccharomyces Cerevisiae. *Journal of Cell Biology*, *85*(1), 96–107. https://doi.org/10.1083/jcb.85.1.96

Rossi, D. J., Jamieson, C. H. M., & Weissman, I. L. (2008). Stems Cells and the Pathways to Aging and Cancer. *Cell*. https://doi.org/10.1016/j.cell.2008.01.036

Rubin, M. S., & Tzagoloff, A. (1973a). Assembly of the mitochondrial membrane system. IX. Purification, characterization, and subunit structure of yeast and beef cytochrome oxidase. *The Journal of Biological Chemistry*, *248*(12), 4269–4274.

Rubin, M. S., & Tzagoloff, A. (1973b). Assembly of the mitochondrial membrane system. X. Mitochondrial synthesis of three of the subunit proteins of yeast cytochrome oxidase. *The Journal of Biological Chemistry*, *248*(12), 4275–4279.

Saracco, S. A., & Fox, T. D. (2002). Cox18p Is Required for Export of the Mitochondrially Encoded Saccharomyces cerevisiae Cox2p C-Tail and Interacts with Pnt1p and Mss2p in the Inner Membrane. *Molecular Biology of the Cell*, *13*(6), 1122–1131. https://doi.org/10.1091/mbc.01

Saraste, M. (1999). Oxidative phosphorylation at the fin de siecle. *Science (New York, N.Y.)*, *283*(5407), 1488–1493.

Scheffler, I. E. (1999). *Mitochondria* (1st ed.). New York: Wiley-Liss.

Scheffler, I. E. (2007). *Mitochondria* (2nd ed.). Hoboken, New Jersey: Wiley-Liss.

Schroeder, E. A., & Shadel, G. S. (2014). Crosstalk between mitochondrial stress signals regulates yeast chronological lifespan. *Mechanisms of Ageing and Development*, *135*(1), 41–49. https://doi.org/10.1016/j.mad.2013.12.002

Schwob, E., & Nasmyth, K. (1993). CLB5 and CLB6, a new pair of B cyclins involved in DNA replication in Saccharomyces cerevisiae. *Genes and Development*, *7*(7 A), 1160–1175. https://doi.org/10.1101/gad.7.7a.1160

Seib, K. L., Jennings, M. P., & McEwan, A. G. (2003). A Sco homologue plays a role in defence against oxidative stress in pathogenic Neisseria. *FEBS Letters*, *546*(2–3), 411–415. https://doi.org/10.1016/S0014-5793(03)00632-X

Shapira, M., Segal, E., & Botstein, D. (2004). Disruption of yeast forkhead-associated cell cycle transcription by oxidative stress. *Mol Biol Cell*, *15*(12), 5659–5669. https://doi.org/10.1091/mbc.E04-04-0340

Sherer, T. B., Betarbet, R., Testa, C. M., Seo, B. B., Richardson, J. R., Kim, J. H., Miller, G. W., Yagi, T., Matsuno-Yagi, A., & Greenamyre, J. T. (2003). Mechanism of toxicity in rotenone models of Parkinson's disease. *The Journal of Neuroscience : The Official Journal of the Society for Neuroscience*, *23*(34), 10756–10764. https://doi.org/23/34/10756 [pii]

Singh, A., & Xu, Y. J. (2017). Heme deficiency sensitizes yeast cells to oxidative stress induced by hydroxyurea. *Journal of Biological Chemistry*, *292*(22), 9088–9103. https://doi.org/10.1074/jbc.M117.781211

Smith, D., Gray, J., Mitchell, L., Antholine, W. E., & Hosler, J. P. (2005). Assembly of cytochrome-c oxidase in the absence of assembly protein Surf1p leads to loss of the active site heme. *Journal of Biological Chemistry*, *280*(18), 17652–17656. https://doi.org/10.1074/jbc.C500061200

Smits, P. H. M., de Haan, M., Maat, C., & Grivell, L. A. (1994). II. Yeast sequencing reports. The complete sequence of a 33 kb fragment on the right arm of chromosome II from Saccharomyces cerevisiae reveals 16 open reading frames, including ten new open reading frames, five previously identified genes and a homologue. *Yeast*, *10*(S1994A), S75–S80. https://doi.org/10.1002/yea.320100010

Sniegowski, P. D. (1995). The origin of adaptive mutants: Random or nonrandom? *Journal of Molecular Evolution*, *40*(1), 94–101. https://doi.org/10.1007/BF00166600

Soto, I. C., Fontanesi, F., Liu, J., & Barrientos, A. (2012). Biogenesis and assembly of eukaryotic cytochrome c oxidase catalytic core. *Biochimica et Biophysica Acta - Bioenergetics*. https://doi.org/10.1016/j.bbabio.2011.09.005

Srikumar, T., Lewicki, M. C., Costanzo, M., Tkach, J. M., van Bakel, H., Tsui, K., Johnson, E. S., Brown, G. W., Andrews, B. J., Boone, C., Giaever, G., Nislow, C., & Raught, B. (2013). Global analysis of SUMO chain function reveals multiple roles in chromatin regulation. *Journal of Cell Biology*, *201*(1), 145–163. https://doi.org/10.1083/jcb.201210019

Srinivasan, S., & Avadhani, N. G. (2012). Cytochrome c oxidase dysfunction in oxidative stress. *Free Radical Biology & Medicine*, *53*(6), 1252–63. https://doi.org/10.1016/j.freeradbiomed.2012.07.021

Steffen, K. K., Kennedy, B. K., & Kaeberlein, M. (2009). Measuring replicative life span in the budding yeast. *Journal of Visualized Experiments : JoVE*, (28), 1–5. https://doi.org/10.3791/1209

Steller, H. (1995). Mechanisms and genes of cellular suicide. *Science (New York, N.Y.)*, *267*(5203), 1445–1449. https://doi.org/10.1126/science.7878463

Stuart, G. R., Santos, J. H., Strand, M. K., Van Houten, B., & Copeland, W. C. (2006). Mitochondrial and nuclear DNA defects in Saccharomyces cerevisiae with mutations in DNA polymerase {gamma} associated with progressive external ophthalmoplegia. *Hum. Mol. Genet.*, *15*(2), 363–374. https://doi.org/10.1093/hmg/ddi454

Stuart, R. A. (2008). *Supercomplex organization of the oxidative phosphorylation enzymes in yeast mitochondria*. *Journal of Bioenergetics and Biomembranes* (Vol. 40). Springer. https://doi.org/10.1007/s10863-008-9168-4

Sturtz, L. A., Diekert, K., Jensen, L. T., Lill, R., & Culotta, V. C. (2001). A fraction of yeast Cu,Zn-superoxide dismutase and its metallochaperone, CCS, localize to the intermembrane space of mitochondria. A physiological role for SOD1 in guarding against mitochondrial oxidative damage. *Journal of Biological Chemistry*, *276*(41), 38084–38089. https://doi.org/10.1074/jbc.M105296200

Sundin, G. W., & Weigand, M. R. (2007, December). The microbiology of mutability. *FEMS Microbiology Letters*. Oxford University Press. https://doi.org/10.1111/j.1574-6968.2007.00901.x

Taylor, N. G., Swenson, S., Harris, N. J., Germany, E. M., Fox, J. L., & Khalimonchuk, O. (2017). The assembly factor Pet117 couples heme a synthase activity to cytochrome oxidase assembly. *Journal of Biological Chemistry*, *292*(5), 1815–1825. https://doi.org/10.1074/jbc.M116.766980

Tiranti, V., Hoertnagel, K., Carrozzo, R., Galimberti, C., Munaro, M., Granatiero, M., Zelante, L., Gasparini, P., Marzella, R., Rocchi, M., Bayona-Bafaluy, M. P., Enriquez, J. A., Uziel, G., Bertini, E., Dionisi-Vici, C., Franco, B., Meitinger, T., & Zeviani, M. (1998). Mutations of SURF-1 in Leigh disease associated with cytochrome c oxidase deficiency. *American Journal of Human Genetics*, *63*(6), 1609–21. https://doi.org/10.1086/302150

Tsukihara, T., Aoyama, H., Yamashita, E., Tomizaki, T., Yamaguchi, H., Shinzawa-Itoh, K., Nakashima, R., Yaono, R., & Yoshikawa, S. (1995). Structures of metal sites of oxidized bovine heart cytochrome c oxidase at 2.8 A. *Science*, *269*(5227), 1069–1074. https://doi.org/10.1126/science.7652554

Tsukihara, T., Aoyama, H., Yamashita, E., Tomizaki, T., Yamaguchi, H., Shinzawa-Itoh, K., Nakashima, R., Yaono, R., & Yoshikawa, S. (1996). The whole structure of the 13-subunit oxidized cytochrome c oxidase at 2.8 A. *Science (New York, N.Y.)*, *272*(5265), 1136–1144. https://doi.org/10.1126/science.272.5265.1136

Turner, J. J., Ewald, J. C., & Skotheim, J. M. (2012). Cell size control in yeast. *Current Biology : CB*, *22*(9), R350-9. https://doi.org/10.1016/j.cub.2012.02.041

Tzagoloff, A., Nobrega, M., Gorman, N., & Sinclair, P. (1993). On the functions of the yeast COX10 and COX11 gene products. *Biochemistry and Molecular Biology International*, *31*(3), 593–598.

Vander Heiden, M. G., Chandel, N. S., Li, X. X., Schumacker, P. T., Colombini, M., & Thompson, C. B. (2000). Outer mitochondrial membrane permeability can regulate coupled respiration and cell survival. *Proceedings of the National Academy of Sciences of the United States of America*, *97*, 4666–4671. https://doi.org/10.1073/pnas.090082297

Veniamin, S., Sawatzky, L. G., Banting, G. S., & Glerum, D. M. (2011). Characterization of the peroxide sensitivity of COX-deficient yeast strains reveals unexpected relationships between COX assembly proteins. *Free Radical Biology and Medicine*, *51*(8), 1589–1600. https://doi.org/10.1016/j.freeradbiomed.2011.06.024

Vest, K. E., Leary, S. C., Winge, D. R., & Cobine, P. A. (2013). Copper import into the mitochondrial matrix in Saccharomyces cerevisiae is mediated by Pic2, a mitochondrial carrier family protein. *Journal of Biological Chemistry*, *288*(33), 23884–23892. https://doi.org/10.1074/jbc.M113.470674

Wallenfang, M. R. (2007). Aging within the Stem Cell Niche. *Developmental Cell*, *13*(5), 603–604. https://doi.org/10.1016/j.devcel.2007.10.011

Wang, B., Dong, D., & Kang, Y. J. (2013). Copper chaperone for superoxide dismutase-1 transfers copper to mitochondria but does not affect cytochrome c oxidase activity. *Experimental Biology and Medicine (Maywood, N.J.)*, *238*(9), 1017–23. https://doi.org/10.1177/1535370213497327

Werner-Washburne, M., Braun, E., Johnston, G. C., & Singer, R. A. (1993). Stationary phase in the yeast Saccharomyces cerevisiae. *Microbiological Reviews*, *57*(2), 383–401. Retrieved from http://www.ncbi.nlm.nih.gov/pubmed/8393130

Werner-Washburne, M., Roy, S., & Davidson, G. S. (2015). Aging and the survival of quiescent and non-quiescent cells in yeast stationary-phase cultures. *Sub-Cellular Biochemistry*. https://doi.org/10.1007/978-94-007-2561-4_6

Wielburski, A., & Nelson, B. D. (1983). Evidence for the sequential assembly of cytochrome oxidase subunits in rat liver mitochondria. *Biochem. J*, *212*, 829–834.

Wilkinson, D., & Ramsdale, M. (2011). Proteases and caspase-like activity in the yeast Saccharomyces cerevisiae. *Biochemical Society Transactions*, *39*(5), 1502–8. https://doi.org/10.1042/BST0391502

Williams, J. C., Sue, C., Banting, G. S., Yang, H., Glerum, D. M., Hendrickson, W. A., & Schon, E. A. (2005). Crystal structure of human SCO1: Implications for redox signaling by a mitochondrial cytochrome c oxidaxse "assembly" protein. *Journal of Biological Chemistry*, *280*(15), 15202–15211. https://doi.org/10.1074/jbc.M410705200

Williams, S. L., Valnot, I., Rustin, P., & Taanman, J. W. (2004). Cytochrome c Oxidase Subassemblies in Fibroblast Cultures from Patients Carrying Mutations in COX10, SCO1, or SURF1. *Journal of Biological Chemistry*, *279*(9), 7462–7469. https://doi.org/10.1074/jbc.M309232200

Winey, M., & O'Toole, E. T. (2001). The spindle cycle in budding yeast. *Nature Cell Biology*, *3*(1), E23–E27. https://doi.org/10.1038/35050663

Wissing, S., Ludovico, P., Herker, E., Büttner, S., Engelhardt, S. M., Decker, T., Link, A., Proksch, A., Rodrigues, F., Corte-Real, M., Fröhlich, K.-U., Manns, J., Candé, C., Sigrist, S. J., Kroemer, G., & Madeo, F. (2004). An AIF orthologue regulates apoptosis in yeast. *The Journal of Cell Biology*, *166*(7), 969–74. https://doi.org/10.1083/jcb.200404138

Xu, C., Wang, J., Gao, Y., Lin, H., Du, L., Yang, S., Long, S., She, Z., Cai, X., Zhou, S., & Lu, Y. (2010). The anthracenedione compound bostrycin induces mitochondria-mediated apoptosis in the yeast Saccharomyces cerevisiae. *FEMS Yeast Research*, *10*(3), 297–308. https://doi.org/10.1111/j.1567-1364.2010.00615.x

Ye, Q., Imriskova-Sosova, I., Hill, B. C., & Jia, Z. (2005). Identification of a disulfide switch in BsSco, a member of the Sco family of cytochrome c oxidase assembly proteins. *Biochemistry*, *44*(8), 2934–2942. https://doi.org/10.1021/bi0480537

Yoshikawa, S., Shinzawa-Itoh, K., Nakashima, R., Yaono, R., Yamashita, E., Inoue, N., Yao, M., Fei, M. J., Libeu, C. P., Mizushima, T., Yamaguchi, H., Tomizaki, T., & Tsukihara, T. (1998). Redox-Coupled Crystal Structural Changes in Bovine Heart Cytochrome c Oxidase. *Science*, *280*(5370), 1723–1729. https://doi.org/10.1126/science.280.5370.1723

Young, M. R., & Tye, B. K. (1997). Mcm2 and Mcm3 are constitutive nuclear proteins that exhibit distinct isoforms and bind chromatin during specific cell cycle stages of Saccharomyces cerevisiae. *Molecular Biology of the Cell*, *8*(8), 1587–601. https://doi.org/10.1091/mbc.8.8.1587

Ždralević, M., Guaragnella, N., Antonacci, L., Marra, E., & Giannattasio, S. (2012). Yeast as a Tool to Study Signaling Pathways in Mitochondrial Stress Response and Cytoprotection. *The Scientific World Journal*, *2012*, 1–10. https://doi.org/10.1100/2012/912147

Zee, J. M., & Glerum, D. M. (2006). Defects in cytochrome oxidase assembly in humans: lessons from yeast. *Biochemistry and Cell Biology = Biochimie et Biologie Cellulaire*, *84*(6), 859–869. https://doi.org/10.1139/O06-201

Zhang, H., & Siede, W. (2004). Analysis of the budding yeast Saccharomyces cerevisiae cell cycle by morphological criteria and flow cytometry. *Methods in Molecular Biology (Clifton, N.J.)*, *241*(2), 77–91.

Zhu, Z., Yao, J., Johns, T., Fu, K., De Bie, I., Macmillan, C., Cuthbert, A. P., Newbold, R. F., Wang, J., Chevrette, M., Brown, G. K., Brown, R. M., & Shoubridge, E. A. (1998). SURF1, encoding a factor involved in the biogenesis of cytochrome c oxidase, is mutated in Leigh syndrome. *Nature Genetics*, *20*(4), 337–343. https://doi.org/10.1038/3804

Appendix

Supplementary Table 1 Statistical analysis of the LacZ assay reported in Figure 3.1. A one way ANOVA test was performed to determine the significance ($p < 0.05$) of the differences among the data groups. A post-hoc Games-Howell test was performed to determine the significance of the differences between the means of anyone data group. Games-Howell test accounts for unequal sample sizes. df, degrees of freedom; A_{420}, absorbance at 420 nm.

ANOVA

A_{420}	Sum of Squares	df	Mean Square	F	p
Between Groups	2.441	11	0.222	2.871	0.008
Within Groups	2.783	36	0.077		
Total	5.225	47			

Games-Howell Post Hoc Test

Sample for multiple comparison	Compared to	p	Sample for multiple comparison	Compared to	p
plCOX17 0 mM H_2O_2	plCOX17 0.02 mM H_2O_2	1.000	plSCO1 0.2 mM H_2O_2	plCOX17 0 mM H_2O_2	0.158
	plCOX17 0.2 mM H_2O_2	1.000		plCOX17 0.02 mM H_2O_2	0.235
	plCOX17 0.5 mM H_2O_2	1.000		plCOX17 0.2 mM H_2O_2	0.525
	plSCO1 0 mM H_2O_2	0.136		plCOX17 0.5 mM H_2O_2	0.482
	plSCO1 0.02 mM H_2O_2	0.258		plSCO1 0 mM H_2O_2	1.000
	plSCO1 0.2 mM H_2O_2	0.158		plSCO1 0.02 mM H_2O_2	0.990
	plSCO1 0.5 mM H_2O_2	0.105		plSCO1 0.5 mM H_2O_2	1.000
	plCOX11 0 mM H_2O_2	0.911		plCOX11 0 mM H_2O_2	0.674
	plCOX11 0.02 mM H_2O_2	0.309		plCOX11 0.02 mM H_2O_2	0.562
	plCOX11 0.2 mM H_2O_2	0.264		plCOX11 0.2 mM H_2O_2	0.813
	plCOX11 0.5 H_2O_2	0.136		plCOX11 0.5 mM H_2O_2	0.806
plCOX17 0.02 mM H_2O_2	plCOX17 0 mM H_2O_2	1.000	plSCO1 0.5 mM H_2O_2	plCOX17 0 mM H_2O_2	0.105
	plCOX17 0.2 mM H_2O_2	1.000		plCOX17 0.02 mM H_2O_2	0.202
	plCOX17 0.5 mM H_2O_2	1.000		plCOX17 0.2 mM H_2O_2	0.494
	plSCO1 0 mM H_2O_2	0.326		plCOX17 0.5 mM H_2O_2	0.432
	plSCO1 0.02 mM H_2O_2	0.449		plSCO1 0 mM H_2O_2	0.999
	plSCO1 0.2 mM H_2O_2	0.235		plSCO1 0.02 mM H_2O_2	0.982
	plSCO1 0.5 mM H_2O_2	0.202		plSCO1 0.2 mM H_2O_2	1.000
	plCOX11 0 mM H_2O_2	0.914		plCOX11 0 mM H_2O_2	0.617
	plCOX11 0.02 mM H_2O_2	0.646		plCOX11 0.02 mM H_2O	0.452
	plCOX11 0.2 mM H_2O_2	0.527		plCOX11 0.2 mM H_2O_2	0.731
	plCOX11 0.5 mM H_2O_2	0.484		plCOX11 0.5 mM H_2O_2	0.715

	plCOX17 0 mM H_2O_2	1.000		plCOX17 0 mM H_2O_2	0.911
	plCOX17 0.02 mM H_2O_2	1.000		plCOX17 0.02 mM H_2O_2	0.914
	plCOX17 0.5 mM H_2O_2	1.000		plCOX17 0.2 mM H_2O_2	0.994
	plSCO1 0 mM H_2O_2	0.672		plCOX17 0.5 mM H_2O_2	0.999
	plSCO1 0.02 mM H_2O_2	0.787		plSCO1 0 mM H_2O_2	0.836
plCOX17 0.2 mM H_2O_2	plSCO1 0.2 mM H_2O_2	0.525	plCOX11 0 mM H_2O_2	plSCO1 0.02 mM H_2O_2	0.950
	plSCO1 0.5 mM H_2O_2	0.494		plSCO1 0.2 mM H_2O_2	0.674
	plCOX11 0 mM H_2O_2	0.994		plSCO1 0.5 mM H_2O_2	0.617
	plCOX11 0.02 mM H_2O_2	0.933		plCOX11 0.02 mM H_2O_2	1.000
	plCOX11 0.2 mM H_2O_2	0.854		plCOX11 0.2 mM H_2O_2	0.982
	plCOX11 0.5 mM H_2O_2	0.819		plCOX11 0.5 mM H_2O_2	0.955
	plCOX17 0 mM H_2O_2	1.000		plCOX17 0 mM H_2O_2	0.309
	plCOX17 0.02 mM H_2O_2	1.000		plCOX17 0.02 mM H_2O_2	0.646
	plCOX17 0.2 mM H_2O_2	1.000		plCOX17 0.2 mM H_2O_2	0.933
	plSCO1 0 mM H_2O_2	0.644		plCOX17 0.5 mM H_2O_2	0.954
	plSCO1 0.02 mM H_2O_2	0.797		plSCO1 0 mM H_2O_2	0.712
plCOX17 0.5 mM H_2O_2	plSCO1 0.2 mM H_2O_2	0.482	plCOX11 0.02 mM H_2O_2	plSCO1 0.02 mM H_2O_2	0.939
	plSCO1 0.5 mM H_2O_2	0.432		plSCO1 0.2 mM H_2O_2	0.562
	plCOX11 0 mM H_2O_2	0.999		plSCO1 0.5 mM H_2O_2	0.452
	plCOX11 0.02 mM H_2O_2	0.954		plCOX11 0 mM H_2O_2	1.000
	plCOX11 0.2 mM H_2O_2	0.863		plCOX11 0.2 mM H_2O_2	0.930
	plCOX11 0.5 mM H_2O_2	0.809		plCOX11 0.5 mM H_2O_2	0.594
	plCOX17 0 mM H_2O_2	0.136		plCOX17 0 mM H_2O_2	0.264
	plCOX17 0.02 mM H_2O_2	0.326		plCOX17 0.02 mM H_2O_2	0.527
	plCOX17 0.2 mM H_2O_2	0.672		plCOX17 0.2 mM H_2O_2	0.854
	plCOX17 0.5 mM H_2O_2	0.644		plCOX17 0.5 mM H_2O_2	0.863
	plSCO1 0.02 mM H_2O_2	1.000		plSCO1 0 mM H_2O_2	0.972
plSCO1 0 mM H_2O_2	plSCO1 0.2 mM H_2O_2	1.000	plCOX11 0.2 mM H_2O_2	plSCO1 0.02 mM H_2O_2	1.000
	plSCO1 0.5 mM H_2O_2	0.999		plSCO1 0.2 mM H_2O_2	0.813
	plCOX11 0 mM H_2O_2	0.836		plSCO1 0.5 mM H_2O_2	0.731
	plCOX11 0.02 mM H_2O_2	0.712		plCOX11 0 mM H_2O_2	0.982
	plCOX11 0.2 mM H_2O_2	0.972		plCOX11 0.02 mM H_2O_2	0.930
	plCOX11 0.5 mM H_2O_2	0.971		plCOX11 0.5 mM H_2O_2	1.000
	plCOX17 0 mM H_2O_2	0.258		plCOX17 0 mM H_2O_2	0.136
	plCOX17 0.02 mM H_2O_2	0.449		plCOX17 0.02 mM H_2O_2	0.484
	plCOX17 0.2 mM H_2O_2	0.787		plCOX17 0.2 mM H_2O_2	0.819
	plCOX17 0.5 mM H_2O_2	0.797		plCOX17 0.5 mM H_2O_2	0.809
	plSCO1 0 mM H_2O_2	1.000		plSCO1 0 mM H_2O_2	0.971
plSCO1 0.02 mM H_2O_2	plSCO1 0.2 mM H_2O_2	0.990	plCOX11 0.5 mM H_2O_2	plSCO1 0.02 mM H_2O_2	1.000
	plSCO1 0.5 mM H_2O_2	0.982		plSCO1 0.2 mM H_2O_2	0.806
	plCOX11 0 mM H_2O_2	0.950		plSCO1 0.5 mM H_2O_2	0.715
	plCOX11 0.02 mM H_2O_2	0.939		plCOX11 0 mM H_2O_2	0.955
	plCOX11 0.2 mM H_2O_2	1.000		plCOX11 0.02 mM H_2O_2	0.594
	plCOX11 0.5 mM H_2O_2	1.000		plCOX11 0.2 mM H_2O_2	1.000

Supplementary Table 2 Statistical analysis of growth curves data depicted in Figure 3.2. A one way ANOVA test was performed to determine the significance ($p < 0.05$) of the differences among the data groups. A post-hoc Games-Howell test was performed to determine the significance of the differences between the means of anyone data group. Games-Howell test accounts for unequal sample sizes. df, degrees of freedom; OD_{600}, absorbance at 600 nm.

ANOVA

OD_{600}	Sum of Squares	df	Mean Square	F	p
Between Groups	131.101	13	10.085	15.807	3.0E-21
Within Groups	85.491	134	0.638		
Total	216.592	147			

Games-Howell Post Hoc Test

Sample for multiple comparison	Compared to	p	Sample for multiple comparison	Compared to	p
WT EP	WT SP	0.015	WT SP	WT EP	1.5E-02
	ΔCOX17 EP	0.992		ΔCOX17 EP	2.6E-03
	ΔCOX17 SP	1.000		ΔCOX17 SP	0.135
	ΔSCO1 EP	0.277		ΔSCO1 EP	2.1E-04
	ΔSCO1 SP	0.276		ΔSCO1 SP	1.2E-03
	ΔCOX11 EP	1.0E-03		ΔCOX11 EP	5.5E-07
	ΔCOX11 SP	1.5E-12		ΔCOX11 SP	2.0E-11
	ΔCOX4 EP	0.262		ΔCOX4 EP	1.6E-04
	ΔCOX4 SP	1.000		ΔCOX4 SP	0.425
	ΔCOX15 EP	1.4E-07		ΔCOX15 EP	4.6E-08
	ΔCOX15 SP	4.5E-08		ΔCOX15 SP	3.2E-08
	Rho0 EP	5.5E-06		Rho0 EP	3.2E-07
	Rho0 SP	2.9E-03		Rho0 SP	3.6E-06
ΔCOX17 EP	WT EP	0.992	ΔCOX17 SP	WT EP	1.000
	WT SP	2.6E-03		WT SP	0.135
	ΔCOX17 SP	0.987		ΔCOX17 EP	0.987
	ΔSCO1 EP	0.932		ΔSCO1 EP	0.387
	ΔSCO1 SP	0.783		ΔSCO1 SP	0.307
	ΔCOX11 EP	4.8E-02		ΔCOX11 EP	1.0E-02
	ΔCOX11 SP	1.2E-07		ΔCOX11 SP	3.8E-06
	ΔCOX4 EP	0.956		ΔCOX4 EP	0.409
	ΔCOX4 SP	1.000		ΔCOX4 SP	1.000
	ΔCOX15 EP	2.1E-03		ΔCOX15 EP	2.1E-03
	ΔCOX15 SP	1.1E-03		ΔCOX15 SP	1.4E-03
	Rho0 EP	2.3E-02		Rho0 EP	1.0E-02
	Rho0 SP	0.326		Rho0 SP	7.0E-02

ΔSCO1 EP	WT EP	0.277	ΔSCO1 SP	WT EP	0.276
	WT SP	2.1E-04		WT SP	1.2E-03
	ΔCOX17 EP	0.932		ΔCOX17 EP	0.783
	ΔCOX17 SP	0.387		ΔCOX17 SP	0.307
	ΔSCO1 SP	1.000		ΔSCO1 EP	1.000
	ΔCOX11 EP	0.790		ΔCOX11 EP	1.000
	ΔCOX11 SP	0.000		ΔCOX11 SP	1.6E-02
	ΔCOX4 EP	1.000		ΔCOX4 EP	0.999
	ΔCOX4 SP	0.998		ΔCOX4 SP	0.978
	ΔCOX15 EP	0.287		ΔCOX15 EP	0.959
	ΔCOX15 SP	0.194		ΔCOX15 SP	0.901
	Rho0 EP	0.803		Rho0 EP	1.000
	Rho0 SP	1.000		Rho0 SP	1.000
ΔCOX11 EP	WT EP	1.0E-03	ΔCOX11 SP	WT EP	1.5E-12
	WT SP	5.5E-07		WT SP	2.0E-11
	ΔCOX17 EP	4.8E-02		ΔCOX17 EP	1.2E-07
	ΔCOX17 SP	1.0E-02		ΔCOX17 SP	3.8E-06
	ΔSCO1 EP	0.790		ΔSCO1 EP	3.6E-04
	ΔSCO1 SP	1.000		ΔSCO1 SP	1.6E-02
	ΔCOX11 SP	8.8E-04		ΔCOX11 EP	0.001
	ΔCOX4 EP	0.542		ΔCOX4 EP	0.000
	ΔCOX4 SP	0.747		ΔCOX4 SP	7.3E-02
	ΔCOX15 EP	1.000		ΔCOX15 EP	2.0E-05
	ΔCOX15 SP	0.997		ΔCOX15 SP	4.7E-05
	Rho0 EP	1.000		Rho0 EP	2.9E-06
	Rho0 SP	0.807		Rho0 SP	9.2E-06
ΔCOX4 EP	WT EP	0.262	ΔCOX4 SP	WT EP	1.000
	WT SP	1.6E-04		WT SP	0.425
	ΔCOX17 EP	0.956		ΔCOX17 EP	1.000
	ΔCOX17 SP	0.409		ΔCOX17 SP	1.000
	ΔSCO1 EP	1.000		ΔSCO1 EP	0.998
	ΔSCO1 SP	0.999		ΔSCO1 SP	0.978
	ΔCOX11 EP	0.542		ΔCOX11 EP	0.747
	ΔCOX11 SP	2.6E-04		ΔCOX11 SP	7.3E-02
	ΔCOX4 SP	0.999		ΔCOX4 EP	0.999
	ΔCOX15 EP	0.121		ΔCOX15 EP	0.580
	ΔCOX15 SP	0.080		ΔCOX15 SP	0.523
	Rho0 EP	0.488		Rho0 EP	0.797
	Rho0 SP	0.997		Rho0 SP	0.968

ΔCOX15 EP	WT EP	1.4E-07	ΔCOX15 SP	WT EP	4.5E-08
	WT SP	4.6E-08		WT SP	3.2E-08
	ΔCOX17 EP	2.1E-03		ΔCOX17 EP	1.1E-03
	ΔCOX17 SP	2.1E-03		ΔCOX17 SP	1.4E-03
	ΔSCO1 EP	0.287		ΔSCO1 EP	0.194
	ΔSCO1 SP	0.959		ΔSCO1 SP	0.901
	ΔCOX11 EP	1.000		ΔCOX11 EP	0.997
	ΔCOX11 SP	2.0E-05		ΔCOX11 SP	4.7E-05
	ΔCOX4 EP	0.121		ΔCOX4 EP	8.0E-02
	ΔCOX4 SP	0.580		ΔCOX4 SP	0.523
	ΔCOX15 SP	1.000		ΔCOX15 EP	1.000
	Rho0 EP	0.537		Rho0 EP	0.210
	Rho0 SP	6.8E-02		Rho0 SP	3.3E-02
Rho0 EP	WT EP	5.5E-06	Rho0 SP	WT EP	2.9E-03
	WT SP	3.2E-07		WT SP	3.6E-06
	ΔCOX17 EP	2.3E-02		ΔCOX17 EP	0.326
	ΔCOX17 SP	1.0E-02		ΔCOX17 SP	7.0E-02
	ΔSCO1 EP	0.803		ΔSCO1 EP	1.000
	ΔSCO1 SP	1.000		ΔSCO1 SP	1.000
	ΔCOX11 EP	1.000		ΔCOX11 EP	0.807
	ΔCOX11 SP	0.000		ΔCOX11 SP	9.2E-06
	ΔCOX4 EP	0.488		ΔCOX4 EP	0.997
	ΔCOX4 SP	0.797		ΔCOX4 SP	0.968
	ΔCOX15 EP	0.537		ΔCOX15 EP	6.8E-02
	ΔCOX15 SP	0.210		ΔCOX15 SP	3.3E-02
	Rho0 SP	0.641		Rho0 EP	0.641

Supplementary Table 3 Statistical analysis of cell viability data depicted in Figure 3.3. A one way ANOVA test was performed to determine the significance ($p < 0.05$) of the differences among the data groups. A post-hoc Games-Howell test was performed to determine the significance of the differences between the means of anyone data group. Games-Howell test accounts for unequal sample sizes. df, degrees of freedom.

ANOVA

Viability	Sum of Squares	df	Mean Square	F	p
Between Groups	6387.531	13	491.349	21.255	4.6E-18
Within Groups	1433.226	62	23.117		
Total	7820.758	75			

Games-Howell Post Hoc Test

Sample for multiple comparison	Compared to	p	Sample for multiple comparison	Compared to	p
WT EP	WT SP	0.329	WT SP	WT EP	0.329
	ΔCOX17 EP	0.068		ΔCOX17 EP	1.000
	ΔCOX17 SP	1.7E-12		ΔCOX17 SP	2.3E-07
	ΔSCO1 EP	0.997		ΔSCO1 EP	1.000
	ΔSCO1 SP	3.0E-05		ΔSCO1 SP	3.0E-04
	ΔCOX11 EP	0.098		ΔCOX11 EP	0.595
	ΔCOX11 SP	1.8E-12		ΔCOX11 SP	5.0E-09
	ΔCOX4 EP	0.857		ΔCOX4 EP	1.000
	ΔCOX4 SP	0.066		ΔCOX4 SP	0.120
	ΔCOX15 EP	0.318		ΔCOX15 EP	0.999
	ΔCOX15 SP	2.1E-11		ΔCOX15 SP	1.3E-06
	Rho0 EP	0.705		Rho0 EP	0.062
	Rho0 SP	9.8E-03		Rho0 SP	5.0E-02
ΔCOX17 EP	WT EP	0.068	ΔCOX17 SP	WT EP	1.7E-12
	WT SP	1.000		WT SP	2.3E-07
	ΔCOX17 SP	0.000		ΔCOX17 EP	4.1E-05
	ΔSCO1 EP	0.999		ΔSCO1 EP	0.089
	ΔSCO1 SP	2.0E-03		ΔSCO1 SP	0.903
	ΔCOX11 EP	0.812		ΔCOX11 EP	0.318
	ΔCOX11 SP	5.3E-06		ΔCOX11 SP	1.5E-03
	ΔCOX4 EP	1.000		ΔCOX4 EP	0.228
	ΔCOX4 SP	0.173		ΔCOX4 SP	0.993
	ΔCOX15 EP	1.000		ΔCOX15 EP	0.041
	ΔCOX15 SP	1.3E-04		ΔCOX15 SP	0.968
	Rho0 EP	2.6E-02		Rho0 EP	6.0E-04
	Rho0 SP	0.101		Rho0 SP	0.821

	WT EP	0.997		WT EP	3.0E-05
	WT SP	1.000		WT SP	3.0E-04
	ΔCOX17 EP	0.999		ΔCOX17 EP	2.0E-03
	ΔCOX17 SP	0.089		ΔCOX17 SP	0.903
	ΔSCO1 SP	0.136		ΔSCO1 EP	0.136
	ΔCOX11 EP	0.744		ΔCOX11 EP	0.693
ΔSCO1 EP	ΔCOX11 SP	3.8E-02	ΔSCO1 SP	ΔCOX11 SP	0.054
	ΔCOX4 EP	1.000		ΔCOX4 EP	0.291
	ΔCOX4 SP	0.190		ΔCOX4 SP	1.000
	ΔCOX15 EP	0.996		ΔCOX15 EP	0.080
	ΔCOX15 SP	0.112		ΔCOX15 SP	0.999
	Rho0 EP	0.770		Rho0 EP	2.7E-04
	Rho0 SP	0.238		Rho0 SP	1.000
	WT EP	0.098		WT EP	1.8E-12
	WT SP	0.595		WT SP	5.0E-09
	ΔCOX17 EP	0.812		ΔCOX17 EP	5.3E-06
	ΔCOX17 SP	0.318		ΔCOX17 SP	1.5E-03
	ΔSCO1 EP	0.744		ΔSCO1 EP	3.8E-02
	ΔSCO1 SP	0.693		ΔSCO1 SP	0.054
ΔCOX11 EP	ΔCOX11 SP	0.065	ΔCOX11 SP	ΔCOX11 EP	0.065
	ΔCOX4 EP	0.899		ΔCOX4 EP	0.138
	ΔCOX4 SP	0.851		ΔCOX4 SP	0.469
	ΔCOX15 EP	0.965		ΔCOX15 EP	1.4E-02
	ΔCOX15 SP	0.455		ΔCOX15 SP	2.6E-03
	Rho0 EP	0.027		Rho0 EP	5.3E-04
	Rho0 SP	0.973		Rho0 SP	0.155
	WT EP	0.857		WT EP	0.066
	WT SP	1.000		WT SP	0.120
	ΔCOX17 EP	1.000		ΔCOX17 EP	0.173
	ΔCOX17 SP	0.228		ΔCOX17 SP	0.993
	ΔSCO1 EP	1.000		ΔSCO1 EP	0.190
	ΔSCO1 SP	0.291		ΔSCO1 SP	1.000
ΔCOX4 EP	ΔCOX11 EP	0.899	ΔCOX4 SP	ΔCOX11 EP	0.851
	ΔCOX11 SP	0.138		ΔCOX11 SP	0.469
	ΔCOX4 SP	0.335		ΔCOX4 EP	0.335
	ΔCOX15 EP	1.000		ΔCOX15 EP	0.252
	ΔCOX15 SP	0.263		ΔCOX15 SP	1.000
	Rho0 EP	0.512		Rho0 EP	2.3E-02
	Rho0 SP	0.415		Rho0 SP	1.000

ΔCOX15 EP	WT EP	0.318	ΔCOX15 SP	WT EP	2.1E-11
	WT SP	0.999		WT SP	1.3E-06
	ΔCOX17 EP	1.000		ΔCOX17 EP	1.3E-04
	ΔCOX17 SP	0.041		ΔCOX17 SP	0.968
	ΔSCO1 EP	0.996		ΔSCO1 EP	0.112
	ΔSCO1 SP	0.080		ΔSCO1 SP	0.999
	ΔCOX11 EP	0.965		ΔCOX11 EP	0.455
	ΔCOX11 SP	0.014		ΔCOX11 SP	2.6E-03
	ΔCOX4 EP	1.000		ΔCOX4 EP	0.263
	ΔCOX4 SP	0.252		ΔCOX4 SP	1.000
	ΔCOX15 SP	0.059		ΔCOX15 EP	0.059
	Rho0 EP	0.084		Rho0 EP	8.7E-04
	Rho0 SP	0.282		Rho0 SP	0.966
Rho0 EP	WT EP	0.705	Rho0 SP	WT EP	0.010
	WT SP	0.062		WT SP	0.050
	ΔCOX17 EP	2.6E-02		ΔCOX17 EP	0.101
	ΔCOX17 SP	6.0E-04		ΔCOX17 SP	0.821
	ΔSCO1 EP	0.770		ΔSCO1 EP	0.238
	ΔSCO1 SP	2.7E-04		ΔSCO1 SP	1.000
	ΔCOX11 EP	2.7E-02		ΔCOX11 EP	0.973
	ΔCOX11 SP	5.3E-04		ΔCOX11 SP	0.155
	ΔCOX4 EP	0.512		ΔCOX4 EP	0.415
	ΔCOX4 SP	2.3E-02		ΔCOX4 SP	1.000
	ΔCOX15 EP	0.084		ΔCOX15 EP	0.282
	ΔCOX15 SP	8.7E-04		ΔCOX15 SP	0.966
	Rho0 SP	2.6E-03		Rho0 EP	2.6E-03

Supplementary Table 4 Statistical analysis of budding indices data depicted in Figure 3.6. A one way ANOVA test was performed to determine the significance ($p < 0.05$) of the differences among the data groups. A post-hoc Games-Howell test was performed to determine the significance of the differences between the means of anyone data group. Games-Howell test accounts for unequal sample sizes. df, degrees of freedom.

ANOVA

Budding Index	Sum of Squares	df	Mean Square	F	p
Between Groups	7648.557	13	588.351	18.829	1.5E-14
Within Groups	1499.851	48	31.247		
Total	9148.407	61			

Games-Howell Post Hoc Test

Sample for multiple comparison	Compared to	p	Sample for multiple comparison	Compared to	p
WT EP	WT SP	1.3E-05	WT SP	WT EP	1.3E-05
	ΔCOX17 EP	0.921		ΔCOX17 EP	2.2E-02
	ΔCOX17 SP	0.559		ΔCOX17 SP	0.001
	ΔSCO1 EP	1.000		ΔSCO1 EP	8.5E-02
	ΔSCO1 SP	0.252		ΔSCO1 SP	1.000
	ΔCOX11 EP	0.997		ΔCOX11 EP	1.6E-03
	ΔCOX11 SP	0.166		ΔCOX11 SP	1.000
	ΔCOX4 EP	1.000		ΔCOX4 EP	1.3E-06
	ΔCOX4 SP	0.349		ΔCOX4 SP	0.558
	ΔCOX15 EP	0.996		ΔCOX15 EP	8.9E-03
	ΔCOX15 SP	0.423		ΔCOX15 SP	0.258
	Rho0 EP	4.0E-05		Rho0 EP	1.000
	Rho0 SP	2.1E-03		Rho0 SP	0.168
ΔCOX17 EP	WT EP	0.921	ΔCOX17 SP	WT EP	0.559
	WT SP	2.2E-02		WT SP	7.6E-04
	ΔCOX17 SP	0.334		ΔCOX17 EP	0.334
	ΔSCO1 EP	0.995		ΔSCO1 EP	0.746
	ΔSCO1 SP	0.135		ΔSCO1 SP	0.441
	ΔCOX11 EP	0.619		ΔCOX11 EP	0.892
	ΔCOX11 SP	0.081		ΔCOX11 SP	0.327
	ΔCOX4 EP	0.925		ΔCOX4 EP	0.113
	ΔCOX4 SP	0.170		ΔCOX4 SP	0.864
	ΔCOX15 EP	0.999		ΔCOX15 EP	0.308
	ΔCOX15 SP	0.221		ΔCOX15 SP	0.961
	Rho0 EP	3.6E-02		Rho0 EP	5.1E-03
	Rho0 SP	5.1E-03		Rho0 SP	1.9E-02

ΔSCO1 EP	WT EP	1.000	ΔSCO1 SP	WT EP	0.252
	WT SP	0.085		WT SP	1.000
	ΔCOX17 EP	0.995		ΔCOX17 EP	0.135
	ΔCOX17 SP	0.746		ΔCOX17 SP	0.441
	ΔSCO1 SP	0.233		ΔSCO1 EP	0.233
	ΔCOX11 EP	0.982		ΔCOX11 EP	0.328
	ΔCOX11 SP	0.158		ΔCOX11 SP	1.000
	ΔCOX4 EP	1.000		ΔCOX4 EP	0.249
	ΔCOX4 SP	0.432		ΔCOX4 SP	0.872
	ΔCOX15 EP	1.000		ΔCOX15 EP	0.194
	ΔCOX15 SP	0.535		ΔCOX15 SP	0.689
	Rho0 EP	0.115		Rho0 EP	1.000
	Rho0 SP	2.1E-02		Rho0 SP	0.721
ΔCOX11 EP	WT EP	0.997	ΔCOX11 SP	WT EP	0.166
	WT SP	1.6E-03		WT SP	1.000
	ΔCOX17 EP	0.619		ΔCOX17 EP	0.081
	ΔCOX17 SP	0.892		ΔCOX17 SP	0.327
	ΔSCO1 EP	0.982		ΔSCO1 EP	0.158
	ΔSCO1 SP	0.328		ΔSCO1 SP	1.000
	ΔCOX11 SP	0.234		ΔCOX11 EP	0.234
	ΔCOX4 EP	0.684		ΔCOX4 EP	0.181
	ΔCOX4 SP	0.543		ΔCOX4 SP	0.779
	ΔCOX15 EP	0.703		ΔCOX15 EP	0.126
	ΔCOX15 SP	0.647		ΔCOX15 SP	0.557
	Rho0 EP	1.5E-02		Rho0 EP	1.000
	Rho0 SP	1.3E-02		Rho0 SP	0.665
ΔCOX4 EP	WT EP	1.000	ΔCOX4 SP	WT EP	0.349
	WT SP	1.3E-06		WT SP	0.558
	ΔCOX17 EP	0.925		ΔCOX17 EP	0.170
	ΔCOX17 SP	0.113		ΔCOX17 SP	0.864
	ΔSCO1 EP	1.000		ΔSCO1 EP	0.432
	ΔSCO1 SP	0.249		ΔSCO1 SP	0.872
	ΔCOX11 EP	0.684		ΔCOX11 EP	0.543
	ΔCOX11 SP	0.181		ΔCOX11 SP	0.779
	ΔCOX4 SP	0.260		ΔCOX4 EP	0.260
	ΔCOX15 EP	0.996		ΔCOX15 EP	0.207
	ΔCOX15 SP	0.315		ΔCOX15 SP	1.000
	Rho0 EP	2.7E-04		Rho0 EP	0.519
	Rho0 SP	2.0E-02		Rho0 SP	0.064

ΔCOX15 EP	WT EP	0.996	ΔCOX15 SP	WT EP	0.423
	WT SP	8.9E-03		WT SP	0.258
	ΔCOX17 EP	0.999		ΔCOX17 EP	0.221
	ΔCOX17 SP	0.308		ΔCOX17 SP	0.961
	ΔSCO1 EP	1.000		ΔSCO1 EP	0.535
	ΔSCO1 SP	0.194		ΔSCO1 SP	0.689
	ΔCOX11 EP	0.703		ΔCOX11 EP	0.647
	ΔCOX11 SP	0.126		ΔCOX11 SP	0.557
	ΔCOX4 EP	0.996		ΔCOX4 EP	0.315
	ΔCOX4 SP	0.207		ΔCOX4 SP	1.000
	ΔCOX15 SP	0.255		ΔCOX15 EP	0.255
	Rho0 EP	3.2E-02		Rho0 EP	0.275
	Rho0 SP	6.0E-03		Rho0 SP	4.1E-02
Rho0 EP	WT EP	4.0E-05	Rho0 SP	WT EP	2.1E-03
	WT SP	1.000		WT SP	0.168
	ΔCOX17 EP	3.6E-02		ΔCOX17 EP	5.1E-03
	ΔCOX17 SP	5.1E-03		ΔCOX17 SP	0.019
	ΔSCO1 EP	0.115		ΔSCO1 EP	2.1E-02
	ΔSCO1 SP	1.000		ΔSCO1 SP	0.721
	ΔCOX11 EP	1.5E-02		ΔCOX11 EP	1.3E-02
	ΔCOX11 SP	1.000		ΔCOX11 SP	0.665
	ΔCOX4 EP	0.000		ΔCOX4 EP	2.0E-02
	ΔCOX4 SP	0.519		ΔCOX4 SP	0.064
	ΔCOX15 EP	3.2E-02		ΔCOX15 EP	6.0E-03
	ΔCOX15 SP	0.275		ΔCOX15 SP	4.1E-02
	Rho0 SP	0.194		Rho0 EP	0.194

Supplementary Table 5 Statistical analysis of G1/G2 ratios obtained by flow cytometry, depicted in Figure 3.8. A one way ANOVA test was performed to determine the significance ($p < 0.05$) of the differences among the data groups. A post-hoc Games-Howell test was performed to determine the significance of the differences between the means of anyone data group. Games-Howell tests accounts for unequal sample sizes. df, degrees of freedom.

ANOVA

G1/G2 Ratio	Sum of Squares	df	Mean Square	F	p
Between Groups	82.788	13	6.368	28.873	3.1E-16
Within Groups	8.823	40	0.221		
Total	91.611	53			

Games-Howell Post Hoc Test

Sample for multiple comparison	Compared to	p	Sample for multiple comparison	Compared to	p
WT EP	WT SP	0.186	WT SP	WT EP	0.186
	ΔCOX17 EP	3.2E-03		ΔCOX17 EP	3.7E-04
	ΔCOX17 SP	0.024		ΔCOX17 SP	1.1E-03
	ΔSCO1 EP	8.0E-03		ΔSCO1 EP	9.7E-04
	ΔSCO1 SP	0.573		ΔSCO1 SP	3.6E-02
	ΔCOX11 EP	1.0E-02		ΔCOX11 EP	4.6E-04
	ΔCOX11 SP	0.950		ΔCOX11 SP	4.6E-02
	ΔCOX4 EP	1.4E-02		ΔCOX4 EP	1.5E-03
	ΔCOX4 SP	0.056		ΔCOX4 SP	2.1E-03
	ΔCOX15 EP	1.4E-02		ΔCOX15 EP	1.1E-03
	ΔCOX15 SP	0.262		ΔCOX15 SP	7.7E-03
	Rho0 EP	0.244		Rho0 EP	0.962
	Rho0 SP	0.008		Rho0 SP	0.367
ΔCOX17 EP	WT EP	3.2E-03	ΔCOX17 SP	WT EP	2.4E-02
	WT SP	3.7E-04		WT SP	1.1E-03
	ΔCOX17 SP	0.718		ΔCOX17 EP	0.718
	ΔSCO1 EP	0.791		ΔSCO1 EP	0.986
	ΔSCO1 SP	0.309		ΔSCO1 SP	0.709
	ΔCOX11 EP	1.000		ΔCOX11 EP	0.988
	ΔCOX11 SP	0.100		ΔCOX11 SP	0.168
	ΔCOX4 EP	0.421		ΔCOX4 EP	1.000
	ΔCOX4 SP	0.522		ΔCOX4 SP	1.000
	ΔCOX15 EP	0.380		ΔCOX15 EP	1.000
	ΔCOX15 SP	2.2E-02		ΔCOX15 SP	0.244
	Rho0 EP	3.8E-02		Rho0 EP	4.7E-02
	Rho0 SP	2.0E-03		Rho0 SP	1.8E-03

	WT EP	0.008		WT EP	0.573
	WT SP	9.7E-04		WT SP	3.6E-02
	ΔCOX17 EP	0.791		ΔCOX17 EP	0.309
	ΔCOX17 SP	0.986		ΔCOX17 SP	0.709
	ΔSCO1 SP	0.461		ΔSCO1 EP	0.461
	ΔCOX11 EP	1.000		ΔCOX11 EP	0.442
ΔSCO1 EP	ΔCOX11 SP	0.196	ΔSCO1 SP	ΔCOX11 SP	0.915
	ΔCOX4 EP	0.736		ΔCOX4 EP	0.576
	ΔCOX4 SP	0.837		ΔCOX4 SP	0.895
	ΔCOX15 EP	0.811		ΔCOX15 EP	0.666
	ΔCOX15 SP	3.1E-03		ΔCOX15 SP	1.000
	Rho0 EP	5.0E-02		Rho0 EP	8.4E-02
	Rho0 SP	4.9E-03		Rho0 SP	9.2E-03
	WT EP	1.0E-02		WT EP	0.950
	WT SP	4.6E-04		WT SP	4.6E-02
	ΔCOX17 EP	1.000		ΔCOX17 EP	0.100
	ΔCOX17 SP	0.988		ΔCOX17 SP	0.168
	ΔSCO1 EP	1.000		ΔSCO1 EP	0.196
	ΔSCO1 SP	0.442		ΔSCO1 SP	0.915
ΔCOX11 EP	ΔCOX11 SP	0.085	ΔCOX11 SP	ΔCOX11 EP	0.085
	ΔCOX4 EP	0.970		ΔCOX4 EP	0.248
	ΔCOX4 SP	0.891		ΔCOX4 SP	0.248
	ΔCOX15 EP	0.942		ΔCOX15 EP	0.195
	ΔCOX15 SP	0.125		ΔCOX15 SP	0.687
	Rho0 EP	3.2E-02		Rho0 EP	0.151
	Rho0 SP	6.9E-04		Rho0 SP	1.4E-02
	WT EP	1.4E-02		WT EP	0.056
	WT SP	1.5E-03		WT SP	2.1E-03
	ΔCOX17 EP	0.421		ΔCOX17 EP	0.522
	ΔCOX17 SP	1.000		ΔCOX17 SP	1.000
	ΔSCO1 EP	0.736		ΔSCO1 EP	0.837
	ΔSCO1 SP	0.576		ΔSCO1 SP	0.895
ΔCOX4 EP	ΔCOX11 EP	0.970	ΔCOX4 SP	ΔCOX11 EP	0.891
	ΔCOX11 SP	0.248		ΔCOX11 SP	0.248
	ΔCOX4 SP	0.982		ΔCOX4 EP	0.982
	ΔCOX15 EP	1.000		ΔCOX15 EP	1.000
	ΔCOX15 SP	5.9E-03		ΔCOX15 SP	0.455
	Rho0 EP	5.6E-02		Rho0 EP	0.052
	Rho0 SP	6.5E-03		Rho0 SP	2.1E-03

ΔCOX15 EP	WT EP	1.4E-02	ΔCOX15 SP	WT EP	0.262
	WT SP	1.1E-03		WT SP	7.7E-03
	ΔCOX17 EP	0.380		ΔCOX17 EP	2.2E-02
	ΔCOX17 SP	1.000		ΔCOX17 SP	0.244
	ΔSCO1 EP	0.811		ΔSCO1 EP	3.1E-03
	ΔSCO1 SP	0.666		ΔSCO1 SP	1.000
	ΔCOX11 EP	0.942		ΔCOX11 EP	0.125
	ΔCOX11 SP	0.195		ΔCOX11 SP	0.687
	ΔCOX4 EP	1.000		ΔCOX4 EP	5.9E-03
	ΔCOX4 SP	1.000		ΔCOX4 SP	0.455
	ΔCOX15 SP	2.4E-02		ΔCOX15 EP	2.4E-02
	Rho0 EP	0.055		Rho0 EP	0.106
	Rho0 SP	3.7E-03		Rho0 SP	9.9E-03
Rho0 EP	WT EP	0.244	Rho0 SP	WT EP	8.3E-03
	WT SP	0.962		WT SP	0.367
	ΔCOX17 EP	3.8E-02		ΔCOX17 EP	2.0E-03
	ΔCOX17 SP	4.7E-02		ΔCOX17 SP	1.8E-03
	ΔSCO1 EP	5.0E-02		ΔSCO1 EP	0.005
	ΔSCO1 SP	0.084		ΔSCO1 SP	9.2E-03
	ΔCOX11 EP	3.2E-02		ΔCOX11 EP	6.9E-04
	ΔCOX11 SP	0.151		ΔCOX11 SP	1.4E-02
	ΔCOX4 EP	0.056		ΔCOX4 EP	6.5E-03
	ΔCOX4 SP	0.052		ΔCOX4 SP	2.1E-03
	ΔCOX15 EP	0.055		ΔCOX15 EP	3.7E-03
	ΔCOX15 SP	0.106		ΔCOX15 SP	9.9E-03
	Rho0 SP	1.000		Rho0 EP	1.000

Supplementary Table 6 Statistical evaluation of cell death marker analysis performed by flow cytometry depicted in Figure 3.15. A one way ANOVA test was performed to determine the significance ($p < 0.05$) of the differences among the data groups. A post-hoc Games-Howell test was performed to determine the significance of the differences between the means of anyone data group. Games-Howell test accounts for unequal sample sizes. df, degrees of freedom.

ANOVA

Induction	Sum of Squares	df	Mean Square	F	p
Between Groups	6693.094	13	514.853	6.551	3.6E-06
Within Groups	2829.287	36	78.591		
Total	9522.381	49			

Games-Howell Post Hoc Test

Sample for multiple comparison	Compared to	p	Sample for multiple comparison	Compared to	p
WT EP	WT SP	0.893	WT SP	WT EP	0.893
	ΔCOX17 EP	6.2E-02		ΔCOX17 EP	0.859
	ΔCOX17 SP	0.996		ΔCOX17 SP	0.512
	ΔSCO1 EP	0.999		ΔSCO1 EP	0.893
	ΔSCO1 SP	4.0E-02		ΔSCO1 SP	1.2E-02
	ΔCOX11 EP	0.992		ΔCOX11 EP	1.000
	ΔCOX11 SP	0.583		ΔCOX11 SP	0.157
	ΔCOX4 EP	0.999		ΔCOX4 EP	0.999
	ΔCOX4 SP	0.583		ΔCOX4 SP	0.157
	ΔCOX15 EP	0.205		ΔCOX15 EP	1.000
	ΔCOX15 SP	0.250		ΔCOX15 SP	0.099
	Rho0 EP	1.000		Rho0 EP	0.931
	Rho0 SP	0.586		Rho0 SP	1.000
ΔCOX17 EP	WT EP	6.2E-02	ΔCOX17 SP	WT EP	0.996
	WT SP	0.859		WT SP	0.512
	ΔCOX17 SP	0.195		ΔCOX17 EP	0.195
	ΔSCO1 EP	0.598		ΔSCO1 EP	1.000
	ΔSCO1 SP	1.8E-02		ΔSCO1 SP	0.158
	ΔCOX11 EP	0.777		ΔCOX11 EP	0.832
	ΔCOX11 SP	6.4E-02		ΔCOX11 SP	0.889
	ΔCOX4 EP	0.427		ΔCOX4 EP	0.850
	ΔCOX4 SP	6.4E-02		ΔCOX4 SP	0.889
	ΔCOX15 EP	0.611		ΔCOX15 EP	0.376
	ΔCOX15 SP	0.077		ΔCOX15 SP	0.421
	Rho0 EP	0.151		Rho0 EP	0.826
	Rho0 SP	0.656		Rho0 SP	0.383

ΔSCO1 EP	WT EP	0.999	ΔSCO1 SP	WT EP	0.040
	WT SP	0.893		WT SP	1.2E-02
	ΔCOX17 EP	0.598		ΔCOX17 EP	1.8E-02
	ΔCOX17 SP	1.000		ΔCOX17 SP	0.158
	ΔSCO1 SP	0.661		ΔSCO1 EP	0.661
	ΔCOX11 EP	0.968		ΔCOX11 EP	0.082
	ΔCOX11 SP	1.000		ΔCOX11 SP	0.385
	ΔCOX4 EP	0.983		ΔCOX4 EP	5.2E-02
	ΔCOX4 SP	1.000		ΔCOX4 SP	0.385
	ΔCOX15 EP	0.765		ΔCOX15 EP	5.5E-02
	ΔCOX15 SP	0.886		ΔCOX15 SP	0.998
	Rho0 EP	0.991		Rho0 EP	0.067
	Rho0 SP	0.838		Rho0 SP	2.9E-02
ΔCOX11 EP	WT EP	0.992	ΔCOX11 SP	WT EP	0.583
	WT SP	1.000		WT SP	0.157
	ΔCOX17 EP	0.777		ΔCOX17 EP	0.064
	ΔCOX17 SP	0.832		ΔCOX17 SP	0.889
	ΔSCO1 EP	0.968		ΔSCO1 EP	1.000
	ΔSCO1 SP	0.082		ΔSCO1 SP	0.385
	ΔCOX11 SP	0.433		ΔCOX11 EP	0.433
	ΔCOX4 EP	1.000		ΔCOX4 EP	0.385
	ΔCOX4 SP	0.433		ΔCOX4 SP	1.000
	ΔCOX15 EP	0.986		ΔCOX15 EP	0.150
	ΔCOX15 SP	0.193		ΔCOX15 SP	0.861
	Rho0 EP	0.999		Rho0 EP	0.365
	Rho0 SP	1.000		Rho0 SP	0.139
ΔCOX4 EP	WT EP	0.999	ΔCOX4 SP	WT EP	0.583
	WT SP	0.999		WT SP	0.157
	ΔCOX17 EP	0.427		ΔCOX17 EP	0.064
	ΔCOX17 SP	0.850		ΔCOX17 SP	0.889
	ΔSCO1 EP	0.983		ΔSCO1 EP	1.000
	ΔSCO1 SP	0.052		ΔSCO1 SP	0.385
	ΔCOX11 EP	1.000		ΔCOX11 EP	0.433
	ΔCOX11 SP	0.385		ΔCOX11 SP	1.000
	ΔCOX4 SP	0.385		ΔCOX4 EP	0.385
	ΔCOX15 EP	0.769		ΔCOX15 EP	0.150
	ΔCOX15 SP	0.188		ΔCOX15 SP	0.861
	Rho0 EP	1.000		Rho0 EP	0.365
	Rho0 SP	0.962		Rho0 SP	0.139

ΔCOX15 EP	WT EP	0.205	ΔCOX15 SP	WT EP	0.250
	WT SP	1.000		WT SP	0.099
	ΔCOX17 EP	0.611		ΔCOX17 EP	0.077
	ΔCOX17 SP	0.376		ΔCOX17 SP	0.421
	ΔSCO1 EP	0.765		ΔSCO1 EP	0.886
	ΔSCO1 SP	0.055		ΔSCO1 SP	0.998
	ΔCOX11 EP	0.986		ΔCOX11 EP	0.193
	ΔCOX11 SP	0.150		ΔCOX11 SP	0.861
	ΔCOX4 EP	0.769		ΔCOX4 EP	0.188
	ΔCOX4 SP	0.150		ΔCOX4 SP	0.861
	ΔCOX15 SP	0.137		ΔCOX15 EP	0.137
	Rho0 EP	0.377		Rho0 EP	0.223
	Rho0 SP	0.999		Rho0 SP	0.120
Rho0 EP	WT EP	1.000	Rho0 SP	WT EP	0.586
	WT SP	0.931		WT SP	1.000
	ΔCOX17 EP	0.151		ΔCOX17 EP	0.656
	ΔCOX17 SP	0.826		ΔCOX17 SP	0.383
	ΔSCO1 EP	0.991		ΔSCO1 EP	0.838
	ΔSCO1 SP	0.067		ΔSCO1 SP	2.9E-02
	ΔCOX11 EP	0.999		ΔCOX11 EP	1.000
	ΔCOX11 SP	0.365		ΔCOX11 SP	0.139
	ΔCOX4 EP	1.000		ΔCOX4 EP	0.962
	ΔCOX4 SP	0.365		ΔCOX4 SP	0.139
	ΔCOX15 EP	0.377		ΔCOX15 EP	0.999
	ΔCOX15 SP	0.223		ΔCOX15 SP	0.120
	Rho0 SP	0.593		Rho0 EP	0.593